ผลของอนุพันธ์ของเอน เฮพทาโนอิล ไนโตร เมตา เมทอกซี อะนิไลด์ ต่อการทำงานของไมโตคอนเดรียที่แยกจากตับหนูขาว

นางสาว พรพักตร์ วงศ์ทองแถม

วิทยานิพนธ์นี้เป็นส่วนหนึ่งของการศึกษาตามหลักสูตรปริญญาเภสัชศาสตรมหาบัณฑิต
สาขาวิชาเภสัชวิทยา ภาควิชาเภสัชวิทยา
คณะเภสัชศาสตร์ จุฬาลงกรณ์มหาวิทยาลัย
ปีการศึกษา 2546

ISBN 974-17-5522-8

EFFECTS OF N-HEPTANOYL, NITRO-m-METHOXY ANILIDE DERIVATIVES ON ISOLATED RAT LIVER MITOCHONDRIAL FUNCTIONS

Miss Pornpak Wongthongtham

A Thesis Submitted in Partial Fulfillment of the Requirements
for the Degree of Master of Science in Pharmacy in Pharmacology

Department of Pharmacology
Faculty of Pharmaceutical Sciences
Chulalongkorn University

Academic Year 2003

ISBN 974-17-5522-8

Thesis Title	Effects of N-heptanoyl, nitro-*m*-methoxy anilide derivatives on isolated rat liver mitochondrial functions
By	Miss Pornpak Wongthongtham
Field of study	Pharmacology
Thesis Advisor	Assistant Professor Withaya Janthasoot

Accepted by the Faculty of Pharmaceutical Sciences, Chulalongkorn University in Partial Fulfillment of the Requirements for the Master 's Degree

..... Dean of Faculty of Pharmaceutical Sciences

(Associate Professor Boonyong Tantisira, Ph.D.)

THESIS COMMITTEE

..... Chairman

(Associate Professor Pornpen Pramyothin,Ph.D.)

..... Thesis Advisor

(Assistant Professor Withaya Janthasoot)

..... Member

(Assistant Professor Chamnan Patarapanich, Ph.D.)

..... Member

(Associate Professor Prasan Dhummaupakorn, Ph.D.)

..... Member

(Assistant Professor Pol. Lt. Col. Somsong Lawanprasert, Ph.D.)

พรพักตร์ วงศ์ทองแถม : ผลของอนุพันธ์ของเอน เฮพทาโนอิล ไนโตร เมตา เมทอกซี อะนิไลด์ ต่อการทำงานของไมโตคอนเดรียที่แยกจากตับหนูขาว (EFFECTS OF N-HEPTANOYL, NITRO-*m*-METHOXY ANILIDE DERIVATIVES ON ISOLATED RAT LIVER MITOCHONDRIAL FUNCTIONS) อาจารย์ที่ปรึกษา : ผศ. วิทยา จันทสูตร, 89 หน้า. ISBN 974-17-5522-8

จุดมุ่งหมายของการวิจัยนี้เป็นการศึกษาเบื้องต้นถึงผลของอนุพันธ์ของเอน เฮพทาโนอิล ไนโตร เมตา เมทอกซี อะนิไลด์ (CU 18-14 และ CU 18-15) ต่อการทำงานของไมโตคอนเดรียที่แยกจากตับหนูขาว พบว่าสารทั้งคู่มีผลต่อการหายใจของไมโตคอนเดรียกล่าวคือ เมื่อใช้ glutamate ร่วมกับ malate เป็นสารสับสเตรท ที่ความเข้มข้นต่ำ (1.01×10^{-6} M) ไม่มีผลรบกวนการหายใจทั้ง State 3 และ State 4 เมื่อความเข้มข้นสูงขึ้น (1.01×10^{-5} M ถึง 4.05×10^{-4} M) แสดงฤทธิ์กระตุ้นการหายใจใน State 4 และเมื่อความเข้มข้นสูงมาก (3.04×10^{-4} M ถึง 4.05×10^{-4} M) แสดงฤทธิ์ยับยั้งการหายใจทั้ง State 3 และ State 4 เมื่อใช้ succinate เป็นสารสับสเตรท พบว่าสารทั้งคู่แสดงฤทธิ์เช่นเดียวกับกรณีที่ใช้ glutamate ร่วมกับ malate เป็นสารสับสเตรท ซึ่งแสดงให้เห็นว่าสารทั้งคู่ออกฤทธิ์เป็น uncoupling agents และสารทั้งคู่ยังออกฤทธิ์ยับยั้งการหายใจที่กระตุ้นด้วยแคลเซี่ยม และ DNP ได้ นอกจากนี้ยังสามารถกระตุ้นสมรรถนะของเอนไซม์ ATPase ของไมโตคอนเดรียได้ โดยที่ CU 18-14 มีฤทธิ์กระตุ้นแรงกว่า CU 18-15 และพบว่าสารทั้งคู่สามารถออกฤทธิ์ยับยั้งเอนไซม์โมโนเอมีนออกซิเดส โดย CU 18-14 ออกฤทธิ์เด่นในการยับยั้งเอนไซม์โมโนเอมีนออกซิเดสชนิดเอ (MAO-A Inhibitor) มากกว่า CU 18-15

ภาควิชา เภสัชวิทยา ลายมือชื่อนิสิต .....

สาขาวิชา เภสัชวิทยา ลายมือชื่ออาจารย์ที่ปรึกษา.....

ปีการศึกษา 2546

4576582033 : MAJOR PHARMACOLOGY

KEY WORD : N-HEPTANOYL, NITRO-*m*-METHOXY ANILIDE / MITOCHONDRIAL FUNCTIONS

PORNPAK WONGTHONGTHAM : EFFECTS OF N-HEPTANOYL, NITRO-*m*-METHOXY ANILIDE DERIVATIVES ON ISOLATED RAT LIVER MITOCHONDRIAL FUNCTIONS. THESIS ADVISOR: ASST. PROF. WITHAYA JANTHASOOT, 89 pp. ISBN 974-17-5522-8

The purpose of this study was to investigate effects of N-heptanoyl, nitro-*m*-methoxy anilide derivatives (CU 18-14 and CU 18-15) on isolated rat liver mitochondrial functions. Effects of CU 18-14 and CU 18-15 on mitochondrial respiration with glutamate plus malate as substrates were as following: did not show any effect on State 3 and State 4 of mitochondrial respiration at low concentration (1.01×10^{-6} M), showed the stimulating effect on State 4 of mitochondrial respiration at higher concentration (at 1.01×10^{-5} M and higher) and inhibited both State 3 and State 4 of mitochondrial respiration at concentration 3.04×10^{-4} M to 4.05×10^{-4} M. The similar results was shown on mitochondrial respiration was also found using succinate was used as a substrate. These results suggested that CU 18-14 and CU 18-15 acted as an uncoupler of oxidative phosphorylation. Calcium- and DNP- stimulated respiration were inhibited by these derivatives. CU 18-14 has stronger stimulating effect on ATPase activity than CU 18-15. Furthermore, CU 18-14 and CU 18-15 inhibited both MAO-A and MAO-B activities. Cu 18-14 demonstrated a more inhibitory potency for MAO-A activity than CU 18-15.

Department PHARMACOLOGY Student's signature Pornpak Wongthongtham

Field of study PHARMACOLOGY Advisor's signature Withaya Janthasoot

Academic year 2003

ACKNOWLEDGEMENTS

I would like to express my sincere gratitude to Assistant Professor Withaya Janthasoot, my thesis advisor, for guidance and encouragement throughout this study. Special thanks are expressed to Assistant Professor Dr. Chamnan Patarapanich for providing the tested compounds and to Associate Professor Dr. Mayuree Tantisira, Head of the Department of Pharmacology, Associate Professor Dr. Pornpen Pramyothin, Associate Professor Dr. Prasan Dhummaupakorn, Assistant Professor Dr. Somsong Lawanprasert and all staff members in the Department of Pharmacology, Faculty of Pharmaceutical Sciences, Chulalongkorn University for their suggestion and guidance.

Finally, I would like to thanks my family and friends for their understanding and support.

CONTENTS

CONTENTS (CONTINUED)

CONTENTS (CONTINUED)

LIST OF TABLES

Table Page

LIST OF FIGURES

Figure Page

LIST OF FIGURES (CONTINUED)

Figure Page

LIST OF ABBREVIATIONS

ADP	=	adenosine 5'-diphosphate
ATP	=	adenosine 5'-triphosphate
ATPase	=	adenosinetriphosphatase
BSA	=	bovine serum albumin
Ca^{2+}	=	calcium ion
$CaCl_2$	=	calcium chloride
conc.	=	concentration
CoQ	=	coenzyme Q,ubiquinone
$CuSO_4$	=	copper sulfate
$^{\circ}C$	=	degree celcius
DMSO	=	dimethylsulfoxide
DNP	=	2,4-dinitrophenol
FAD	=	flavin adenine dinucleotide
$FADH_2$	=	reduced flavin adenine dinucleotide
g	=	gram
g	=	centrifugal force unit (gravity)
H^+	=	proton
HCl	=	hydrochloric acid
HEPES	=	N-2-hydroxyethylpiperazine-N'-2-ethane-sulfonic acid
H_2O_2	=	hydrogen peroxide
H_2SO_4	=	sulfuric acid
5-HT	=	5-hydroxytryptamine
IC_{50}	=	concentration causing 50% inhibition
KCl	=	potassium chloride
Kg	=	Kilogram
M	=	molar
MAO	=	monoamine oxidase
MAO-A	=	monoamine oxidase A
MAO-B	=	monoamine oxidase B

LIST OF ABBREVIATIONS (CONTINUED)

μ atoms	=	microatoms
μg	=	microgram
μl	=	microlite
μM	=	micromolar
mg	=	milligram
min	=	minute
ml	=	millilitre
mM	=	millimolar
NAD^+	=	nicotinamide adenine dinucleotide
NADH	=	reduced nicotinamide adenine dinucleotide
n atoms	=	nanoatoms
ng	=	nanogram
O	=	oxygen
Pi	=	inorganic phosphate
RCI	=	respiratory control index
RPM	=	revolution per minute
S.E.	=	standard error of mean
TCA	=	trichloroacetic acid
w/v	=	weight by volume
/	=	per
%	=	percent
[ ]	=	concentration
$\Delta\psi_m$	=	mitochondrial membrane potential
ΔpH	=	pH gradient across inner membrane
Δp	=	proton motive force

CHAPTER I

INTRODUCTION

Nowadays, there are endlessly efforts on searching new knowledge and understanding of the action of various therapeutically applied substances embrace with new data on molecular mechanism of disease.

Acyl pyridine and acyl aniline derivatives have been developed by Assistant Professor Dr. Chamnan Patarapanich and his colleagues at the Department of Pharmaceutical Chemistry, Faculty of Pharmaceutical Sciences, Chulalongkorn University since 1998. Early studies using isolated rat liver mitochondria demonstrated that N-acylaminopyridine derivatives, CU 763-16-04, CU 763-18-01, CU 763-18-02 and CU 763-18-04 (Figure 1) acted as inhibitors of site I respiratory chain with NAD^+-linked substrates, stimulated succinate respiration but did not stimulate ATPase activity (Unchittha, 2000). CU 763-16-04 inhibited calcium- stimulated respiration but not by CU 763-18-01, CU 763-18-04 and CU 763-18-02. All of these derivatives inhibited monoamine oxidase activity (Unchittha, 2000). Preliminary studies had shown that CU 18-07, CU 18-08, CU 18-09, CU 18-10, CU 18-11, CU 18-12 and CU 18-13 (Figure 2) inhibited both MAO-A and MAO-B activities with low potency (Tatiya, 2001), and acted as site I inhibitors of respiratory chain and stimulated succinate oxidation. Aniline derivatives, CU 18-09 and CU 18-10 were more potent than the others with equal concentration. These derivatives act as like uncoupler. Calcium- and DNP- stimulated respiration were inhibited by CU 18-12, CU 18-09 and CU 18-10, which showed stimulatory effects on mitochondrial ATPase activity (Hatairat, 2003).

Subsequently, in 2002, Assistant Professor Dr. Chamnan Patarapanich and his colleagues developed new N-heptanoyl, nitro-*m*-methoxy anilide derivatives, which were N-heptanoyl-3-methoxy-4-nitro anilide (CU 18-14) and N-heptanoyl-2-nitro-5-methoxy anilide (CU 18-15) (Figure 3). The purpose of this present study is to investigate effects of CU 18-14 and CU 18-15 on isolated rat liver mitochondrial functions.

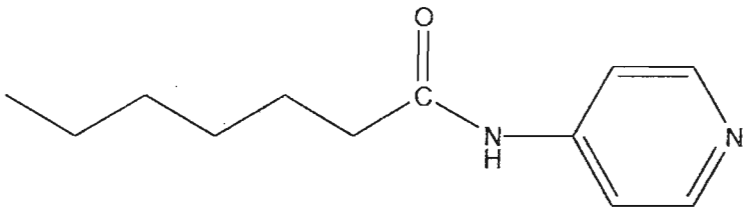

CU 763-16-04

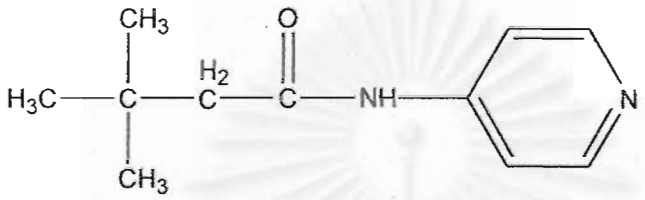

CU 763-18-01

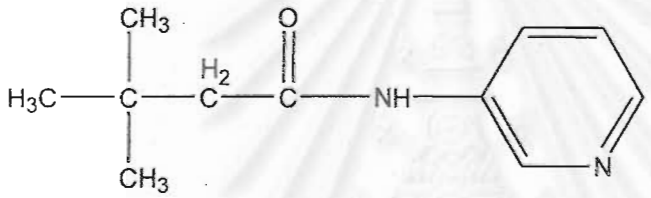

CU 763-18-02

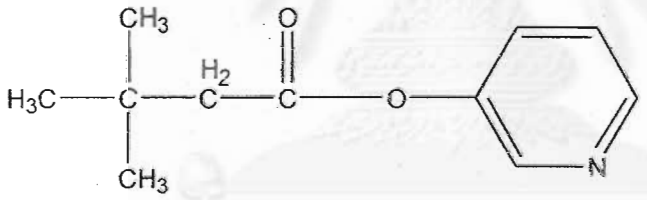

CU 763-18-04

Figure 1. Structures of CU 763-16-04, CU 763-18-01, CU 763-18-02 and CU 763-18-04

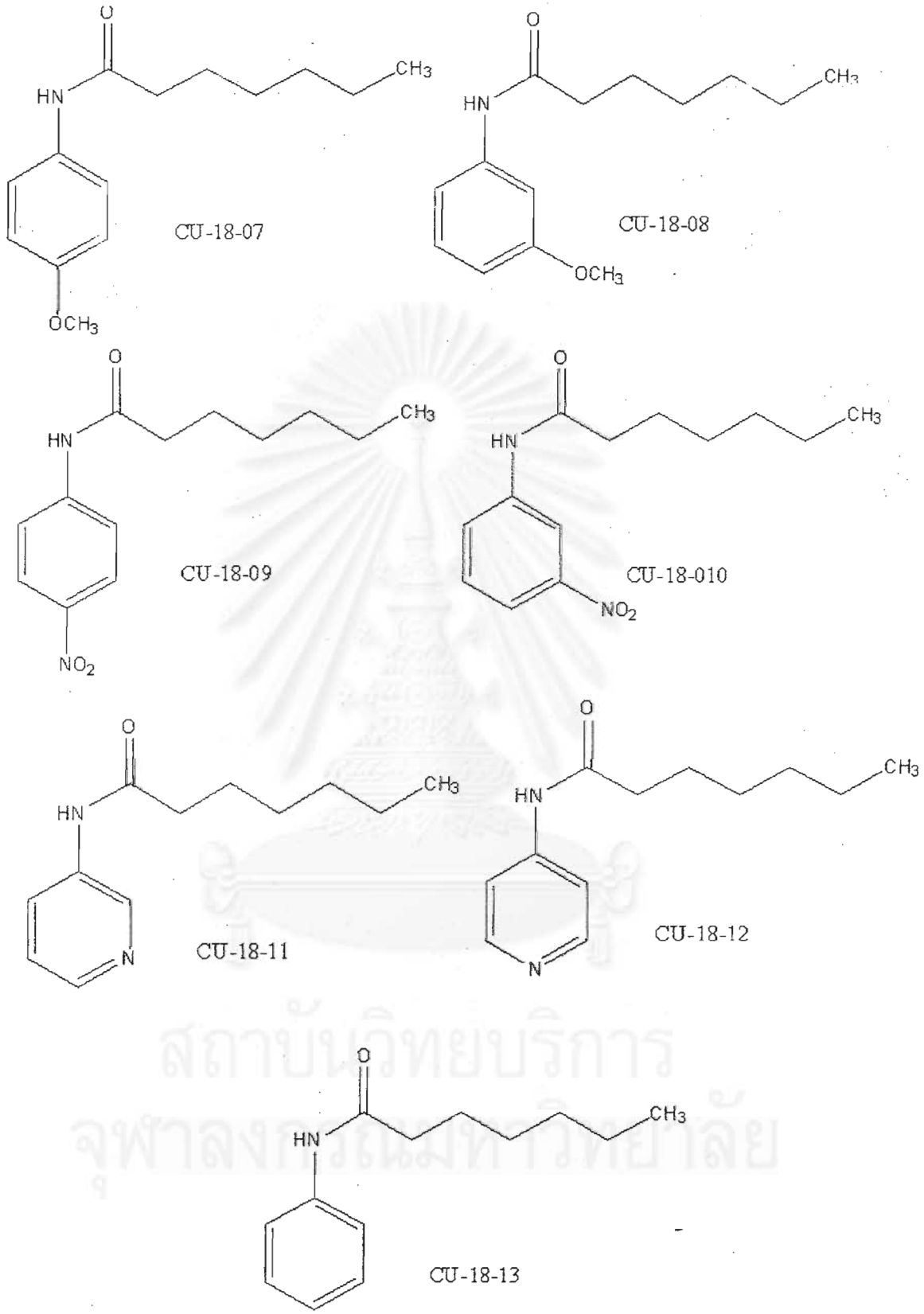

Figure 2. Structures of CU 18-07, CU 18-08, CU 18-09, CU 18-10, CU 18-11, CU 18-12 and CU 18-13

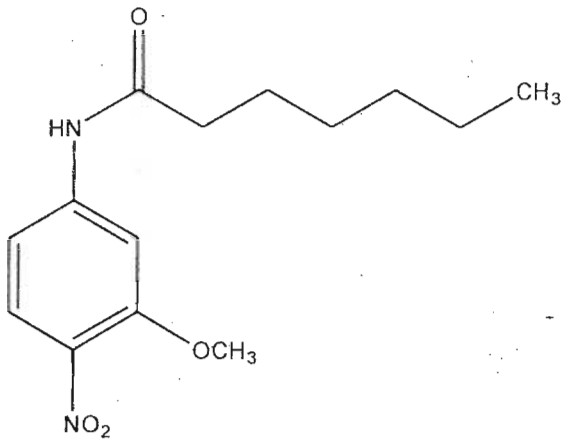

N-heptanoyl-3-methoxy-4-nitro anilide (CU 18-14)

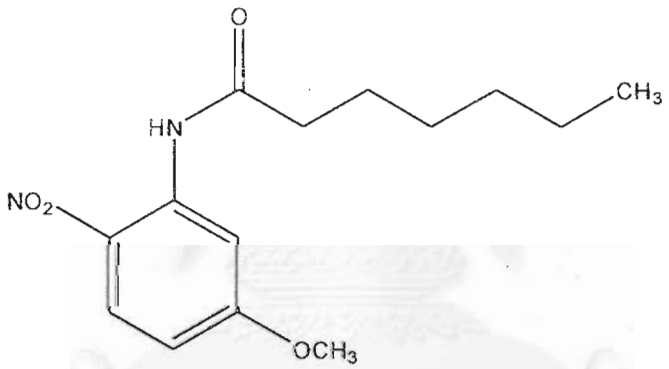

N-heptanoyl-2-nitro-5-methoxy anilide (CU 18-15)

Figure 3. Structures of N-heptanoyl, nitro-*m*-methoxy anilide derivatives (CU 18-14 and CU 18-15)

CHAPTER II

LITERATURE REVIEWS

Mitochondria, critical organelle in cytoplasm, play a central role in energy-generating processes within the cell. Apart from this important function, mitochondria are involved in such complex processes as apoptosis and cardioprotection (Green and Reed, 1998; Mootha et al., 2001; Szewczyk and Wojtczak, 2002). Mitochondria are also targets for drugs such as antidiabetic sulfonylureas, immunosuppressants, some antilipidemic agents, etc. Medically applied substances that interact with mitochondria can be divided into two groups: 1) those that are specifically designed to affect mitochondrial functions, and 2) those for which primary targets are other cellular locations and their interactions with mitochondria are secondary. In any case, identification of mitochondria as primary or secondary targets of a drug may facilitate a better understanding of its mechanism of action and open new perspectives of its application. Recognition of drugs interaction with mitochondria as secondary targets may help to understand the mechanisms of side effects and to construct new drugs in which these side effects will be eliminated or minimized. Mitochondrial functions are aimed to point to multiple pathways interconnecting mitochondrial metabolic routes with those of the rest of the cell. Pharmacological agents, which affect either intramitochondrial metabolic processes or transport pathways connecting mitochondria with the cytosol, may therefore have a considerable influence on the total cell metabolism. The classes of pharmaceuticals, which specifically interact with mitochondrial enzymes and metabolic pathways are as following (Szewczyx and Wojtczak, 2002):

1) Mitochondria in chemotherapy-induced apoptosis
2) Mitochondria and oxidative stress, aging, and degenerative diseases
3) Mitochondria ATP-regulated potassium channel: a novel effector of cardioprotection
4) Sulfonylureas and mitochondria
   - Functional effects of antidiabetic sulfonylureas on mitochondria
   - Effect of antitumor sulfonylureas on mitochondria

5) The mitochondrial benzodiazepine receptor
6) Immunosuppressant drugs and mitochondria
7) Disruption of mitochondrial functions by antiviral drugs
8) Nonsteroidal anti-inflammatory drugs and mitochondria
9) Local anesthetics and mitochondrial energy metabolism
10) Mitochondria as a pharmacological target of lipid metabolism
    - Inhibition of the transfer of 'activated' fatty acids into mitochondria and of their β-oxidation
    - L-carnitine supplementation
    - Nonesterified fatty acids as 'natural' uncouplers: role in thermogenesis and obesity control
    - The PTP closing properties of N-acylethanolamines (NAEs) (Epps et al., 1982)

Mitochondrion and mitochondrial structure

Mitochondria are organelles, found in the cytoplasm of all eukaryotic cells. Their most immediate function is to convert energy found in nutrient molecules (substrates) and store it in the high-energy phosphate bonds of adenosine triphosphate (ATP) which is then available to power cellular functions (Mayes, 2000, Alberts et al., 2002).

The shape and the number of mitochondria per cell differ widely from cell to cell. In liver and muscle cells, mitochondria are approximate ellipsoids, about 2-3 μ long and about 1 μ thick. In liver, these organelles constitute about 10-15% of total cell volume (Erecinska and Wilson, 1981).

The mitochondrion consists of four distinct subregions, shown in Figure 4, the outer membrane, the inner membrane, the intermembrane space, and the matrix, located within the inner membrane. The inner membrane is usually highly convoluted, forming a series of infoldings, known as cristae that project into the matrix (Lodish et al., 1999, Mathews et al., 2000, Alberts et al., 2002).

The outer membrane is lipid bilayer membrane, which is permeable to ions and solutes up to 14 kDa. It is rich in cholesterol and contains embedded or attached enzymes that interface the mitochondrion with the rest of the cellular metabolic network (Wallace and Starkov, 2000). The outer membrane is characterized by the presence of monoamine

oxidase, acyl-CoA synthetase, glycerolphosphate acyltransferase, monoacyl glycerolphosphate acyltransferase, and phospholipase A_2 (Mayes, 2000).

The inner membrane consists of about 70 percent protein and 30 percent lipid, making it perhaps the most protein rich of all biological membranes (Mathews et al., 2000), which is not freely permeable to ions and metabolites, but instead contains special membrane proteins that transport selected metabolites across the membrane. The permeability of the inner membrane is highly selective even towards uncharged molecular weight (greater than approximately 100 daltons) and all ionic species (Erecinska and Wilson, 1981). This feature, the protein-mediated and regulated permeability of the inner membrane, is of vital importance for the morphological and functional integrity of the mitochondrion: It is also the most common target for mitochondrial toxicants. Many foreign chemicals damage mitochondria either by increasing the permeability of the inner membrane or by inhibiting transports proteins embedded within it. The lipid composition of the inner membrane is unique in that it contains large amounts of phospholipid cardiolipin and virtually no cholesterol (Mayes, 2000; Wallace and Starkov, 2000). Whatever the compartment in which biological oxidations occur, all of these processes generate reduced electron carriers, primarily NADH. Most of this NADH is reoxidized, with concomitant ATP production, by enzymes of the respiratory chain, firmly embedded in the inner membrane (Mathews et al., 2000).

Succinate dehydrogenase is found on the inner surface of the inner mitochondrial membrane, where it transports reducing equivalents to the respiratory chain enzymes, major constituents of the inner membrane. 3-Hydroxybutyrate dehydrogenase is also bound to the matrix side of the inner mitochondrial membrane. Glycerol-3-phosphate dehydrogenase is found on the outer surface of the inner membrane, where it is suitably located to participate in the glycerophosphate shuttle (Mayes, 2000).

The intermembrane space is a much narrower space, which between the outer and inner membranes ((Erecinska and Wilson, 1981; Lodish et al., 1999; Alberts et al., 2002). Adenylyl kinase and creatine kinase are found in the intermembrane space (Mayes, 2000).

Matrix is a water-containing compartment in the inner membrane, where mitochondrial DNA and various soluble enzymes, such as those of the tricarboxylic acid cycle and the β–oxidation pathway, are located. (Wallace and Starkov, 2000)

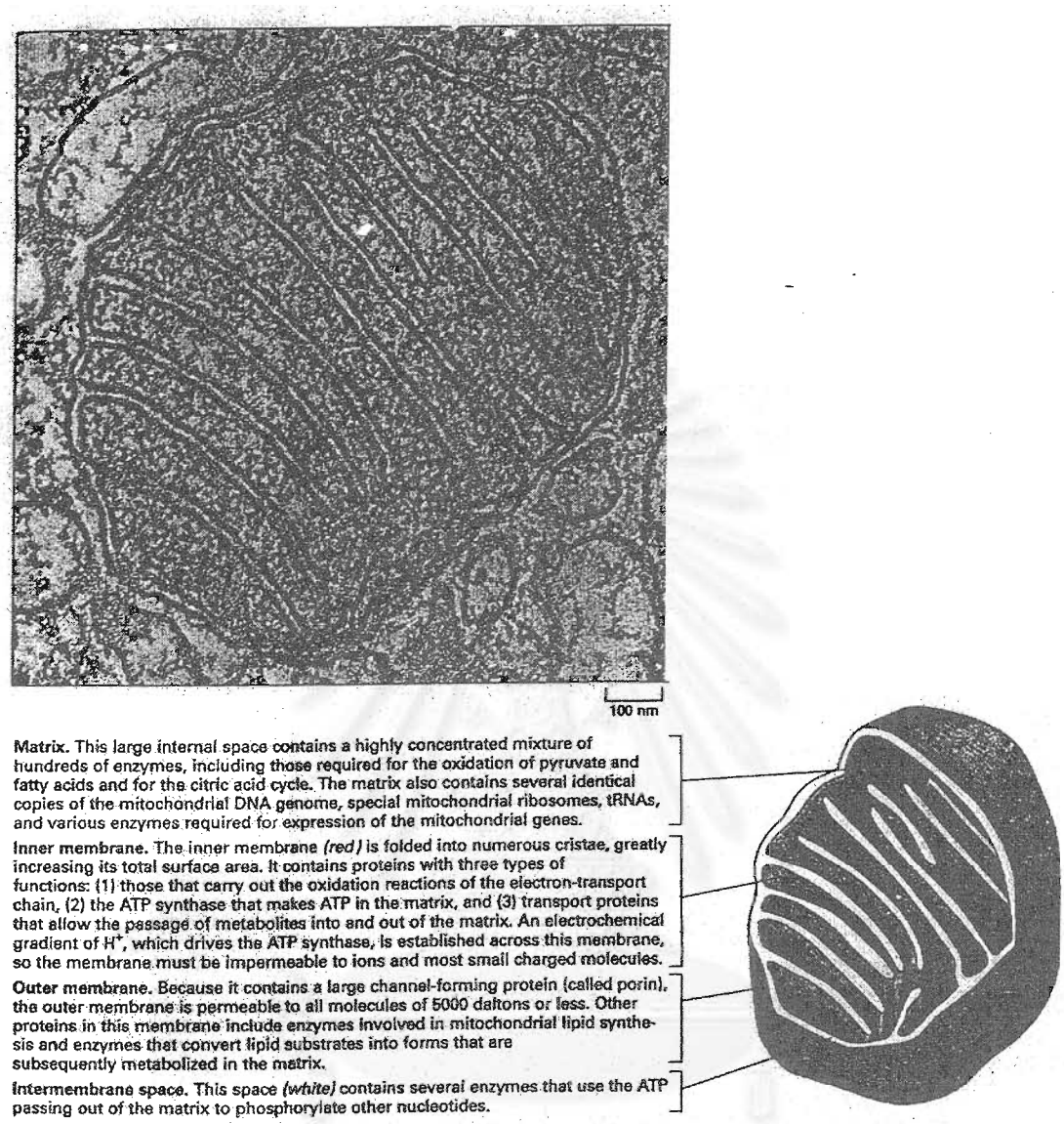

Figure 4. The general organization of a mitochondrion. In the liver, an estimated 67 % of the total mitochondrial protein is located in the matrix, 21% is located in the inner membrane, 6% in the outer membrane, and 6% in the intermembrane space. As indicated below, each of these four regions contains a special sent of proteins that mediate distinct functions (Alberts et al., 2002)

Oxidation of glucose and fatty acids to carbon dioxide

Respiration involves the oxidation of glucose and other compounds to produce energy. The complete aerobic oxidation of glucose during respiration is coupled to the synthesis of up to 36 molecules of ATP:

$$C_6H_{12}O_6 + 6O_2 + 36\ Pi + 36\ ADP + 36\ H^+ \longrightarrow 6\ CO_2 + 36\ ATP + 42\ H_2O$$

The first step in the oxidation of glucose is called glycolysis, which takes place in the cell cytosol and does not involve oxidation by O_2. During glycolysis, glucose is broken down into two molecules of pyruvate, with the concomitant conversion of 2 ADP to 2 ATP. The process of glycolysis can be regulated to meet the cell's need for ATP. One key enzyme that is regulated in ATP levels is phosphofructokinase, which is stimulated by high ADP levels and inhibited by high ATP and citrate. The next step in the oxidation of glucose involves the transport of pyruvate into mitochondria and its subsequent oxidized by O_2 to CO_2, generating 34 of the 36 ATP molecules produced during respiration (Lodish et al., 1999, Alberts et al., 2002).

Kreb's cycle/citric acid cycle

Immediately after pyruvate is transported into the mitochondrial matrix it reacts with CoA (Coenzyme A) to form acetyl CoA. Fatty acids are also converted to acetyl CoA after their conversion to fatty acyl CoA. After its synthesis, acetyl CoA is fed into a cyclic pathway alternately called the citric acid cycle, the TCA (tricarboxylic acid) cycle, or the Krebs cycle. In this cycle the acetyl group on acetyl CoA is oxidized to CO_2. Four reactions in the Krebs cycle involve the transfer of a pair of electrons from a substrate to an electron accepting coenzyme. Three of the reactions reduce the coenzyme NAD^+ to NADH, and one reduces the coenzyme FAD to $FADH_2$. In addition, a GDP is converted to GTP. The enzymes that carry out these reactions are located in the mitochondrial matrix and at the matrix surface of the inner membrane. The reduced coenzymes (NADH and $FADH_2$) generated in the citric acid cycle store the energy released in glucose oxidation, and synthesis of ATP is then coupled to the reoxidation of these compounds by O_2 in a process that involves the electron transport chain (Figure 5) (Lodish et al., 1999, Alberts et al., 2002).

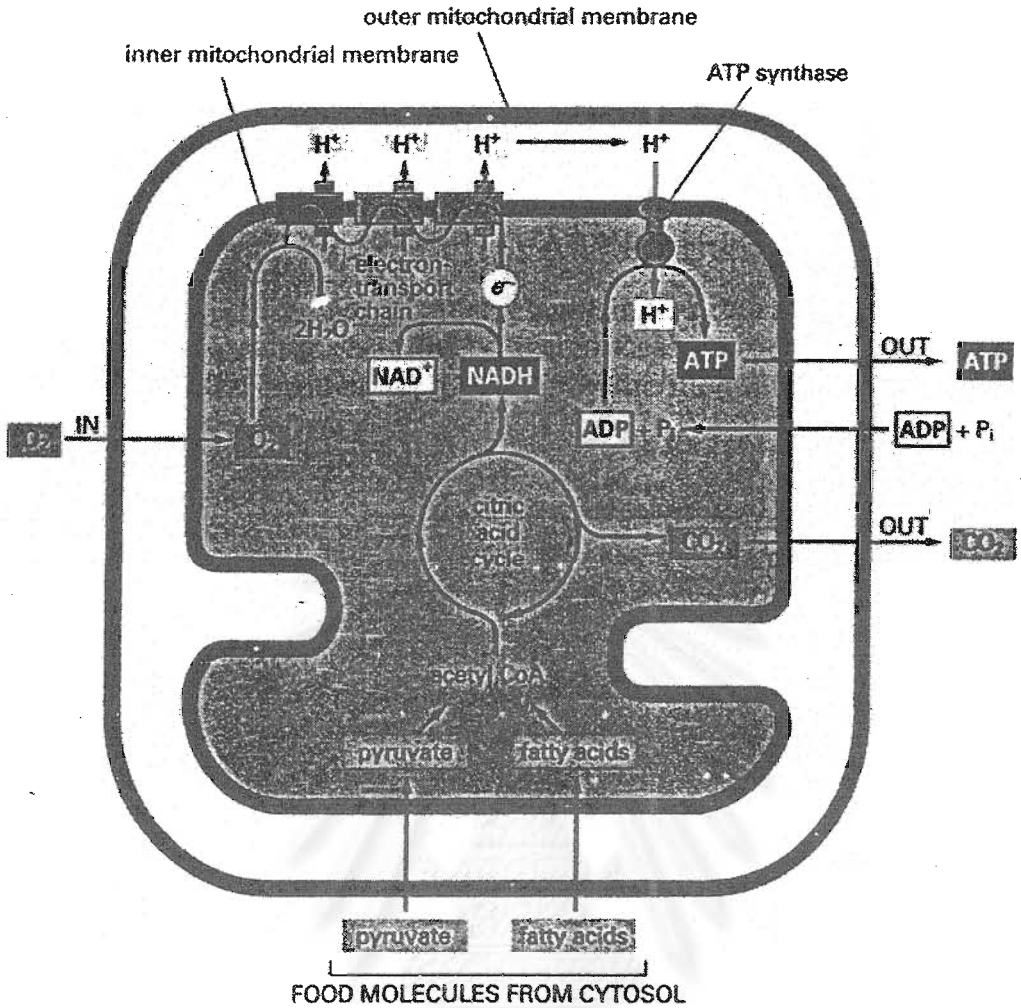

Figure 5. A summary of energy-generating metabolism in mitochondria. Pyruvate and fatty acids enter the mitochondrion (bottom) and are broken down to acetyl CoA. The acyl CoA is then metabolized by the citric acid cycle, which reduces NAD^+ to NADH (and FAD to $FADH_2$, not shown). In the process of oxidative phosphorylation, high-energy electrons from NADH (and $FADH_2$) are then passed along the electron transport chain in the inner membrane to oxygen (O_2). This electron transport generates a proton gradient across the inner membrane, which is used to drive the production of ATP by ATP synthase.

The NADH generated by glycolysis in the cytosol also passes electrons to the respiratory chain (not shown). Since NADH cannot pass across the inner mitochondrial membrane, the electron transfer from cytosolic NADH must be accomplished indirectly by means of one of several "shunttle" systems that transport another reduced compound into the mitochondrion; after being oxidized, this compound is returned to the cytosol, where it is reduced by NADH again (Alberts et al., 2002).

Electron transport chain

The most important function of electron transport chain is the production of energy for the cells. The components of the electron transport system are complexes I, II, III, and IV, plus two individual molecules, coenzyme Q and cytochrome *c*. In the electron transport chain, electrons are moved from molecules with low reduction potential (low affinity for electrons) to molecules with successively higher reduction potential (higher electron affinity) and finally to the oxygen. In respiration chain, electrons are transferred through four large protein complexes and two smaller proteins, each of which has an electron carrier group called a prosthetic group (these groups include flavins, heme, FeS, Cu, and ubiquinone). A summary of the electron transfer reactions is presented in Figure 6 and Figure 7 (Lodish et al., 1999, Alberts et al., 2002; Metzler, 2003).

The metabolic intermediates of the reactions donated electrons to specialized coenzymes, nicotinamide adenine dinucleotide (NAD^+) and flavin adenine dinucleotide (FAD), to form the energy-rich reduced coenzymes, NADH and $FADH_2$, respectively (Champe et al., 1994). The first step in the electron transport chain is the transfer of electrons from NADH to complex I (NADH-CoQ reductase complex). As an alternative first step, electrons can be transferred from $FADH_2$ to complex II (succinate-CoQ reductase complex). Complexes I and II then transfer electrons to ubiquinone (CoQ) which then transfers its electrons to carriers in complex III ($CoQH_2$–cyt *c* reductase complex). Electrons are carried between complexes III and IV (cytochrome *c* oxidase complex) by cytochrome *c*, which plays a critical role in apoptosis. In the final step cytochrome *c* oxidase donates its electrons to oxygen to create water. At various points in the electron transport chain (at complex I, III and IV), the energy released during electron transfer is used to move H^+ ions from the matrix to the intermembrane mitochondrial space, generating a gradient of protons across the inner membrane. Because complex II (succinate-CoQ reductase complex) is the only complex in the electron transport chain that does not move H^+ ions, oxidation of $FADH_2$ does not result in the movement of as many protons across the membrane, and hence produces less ATP. In summary, the energy released from the electron transport chain is used to move protons across the inner mitochondrial membrane and hence to create an electrochemical gradient that stores potential energy. The energy derived from movement of these protons back across the membrane (the proton motive force) is used to synthesize

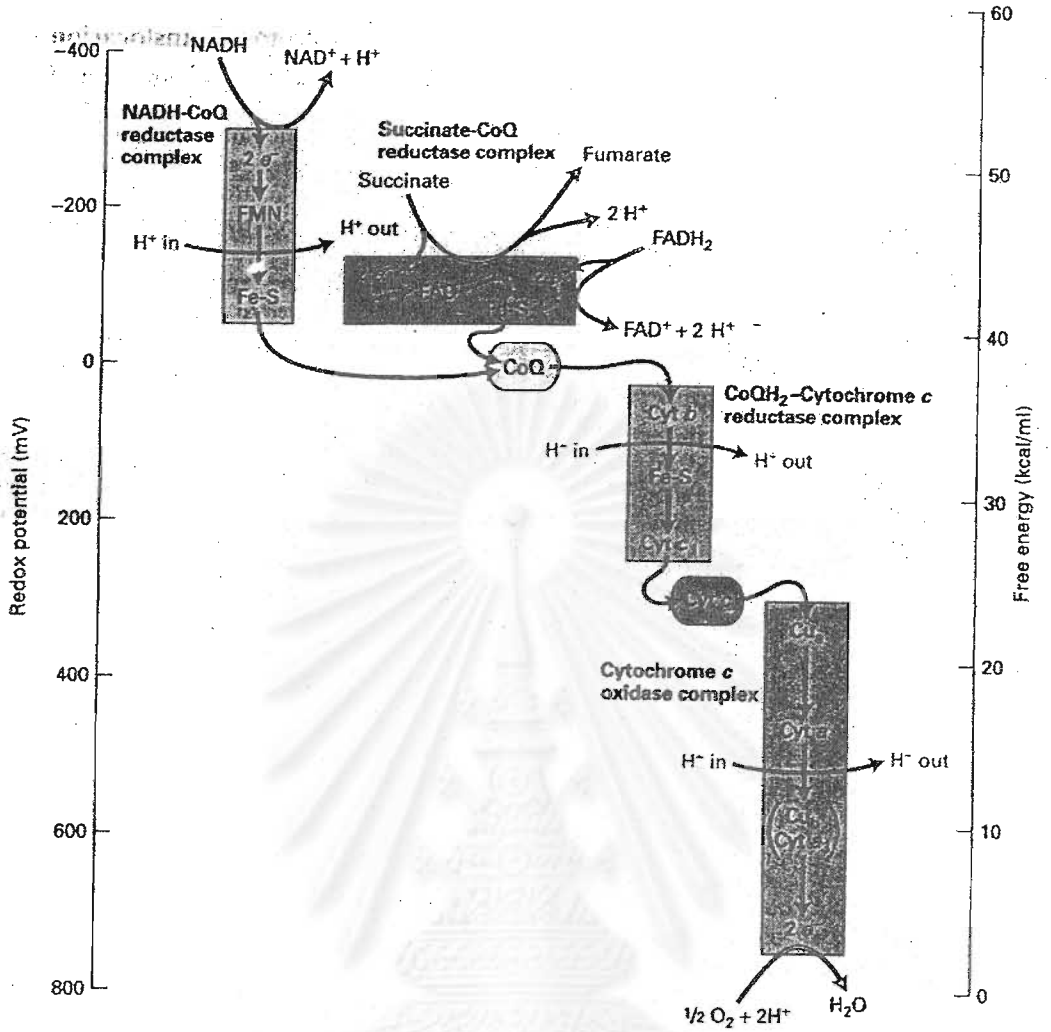

Figure 6. Stepwise flow of electrons through the electron transport chain from NADH, succinate, and $FADH_2$ to O_2. Each of the four large multiprotein complexes in the chain is located in the inner mitochondria membrane and contains several specific electron carriers. Coenzyme Q (CoQ) and cytochrome c transport electrons between the complexes. As shown by the redox scale, electrons pass in sequence from carriers with a lower reduction potential to those with a higher (more positive) potential. The free-energy scale shows the corresponding reduction in free energy as a pair of electron moves through the chain. The energy released as electrons flow through three of the complexes is sufficient to power the pumping of proton ions across the membrane, establishing a proton-motive force (Lodish et al., 1999).

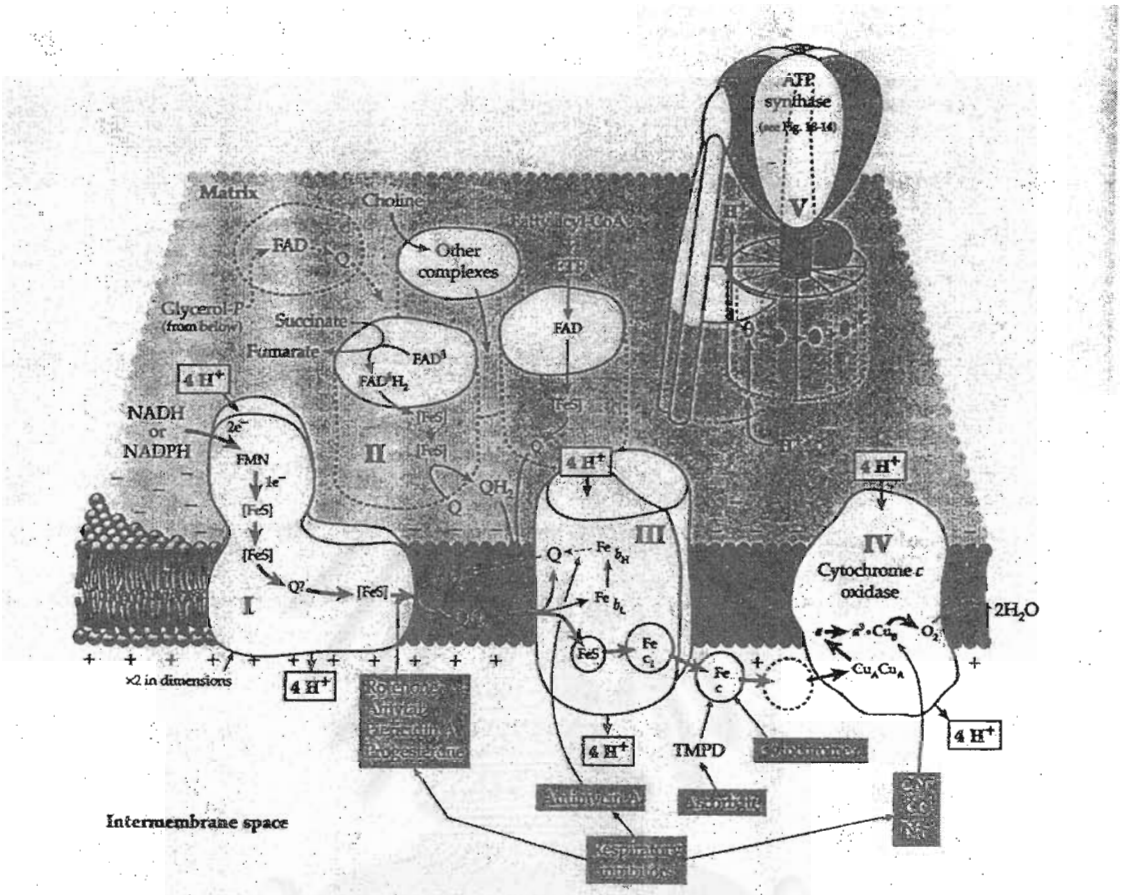

Figure 7. A current concept of the electron transport chain of mitochondria

ATP (Lodish et al., 1999). The aerobic oxidation of NADH and $FADH_2$ by the mitochondrial electron-transport chain was coupled to phosphorylation of ADP, a process called oxidative phosphorylation (Horton et al., 1993, Lodish et al., 1999, Alberts et al., 2002).

Oxidative phosphorylation

The process by which the energy stored in NADH and $FADH_2$ is used to produce ATP, called oxidative phosphorylation, can be divided into two main steps. First, high energy electrons from NADH and $FADH_2$ are passed through a series of electron carriers that make up the electron transport chain, eventually being transferred to O_2. This is the oxidation step. The energy released during electron transport is used to move protons outward from the matrix across the inner mitochondrial membrane. As a result, the energy released during electron transport is stored as a proton gradient across the membrane. In the next step, the movement of protons back across the membrane through an ATP synthesizing enzyme provides the energy used to convert ADP to ATP. This is the phosphorylation step. The importance of the proton gradient in ATP production was first proposed by Peter Mitchell in 1961 and is called the chemiosmotic hypothesis (Lodish et al., 1999, Alberts et al., 2002).

Coupling the proton motive force to ATP synthesis

In 1961, Peter Mitchell first suggested that the energy stored in an electrochemical gradient across the inner mitochondrial membrane could be coupled to ATP synthesis. The enzyme that couples the proton motive force to ATP synthesis is the F_0 F_1 ATPase or ATPase (Figure 8). Movement of protons down the electrochemical gradient through a channel between the a and c subunits of ATPase releases energy that is coupled to the rotation of the c, γ and ε subunits. This rotation causes a conformational change in the α and β subunits that promotes synthesis of ATP from ADP and Pi (Lodish et al., 1999, Alberts et al., 2002; Metzler, 2003).

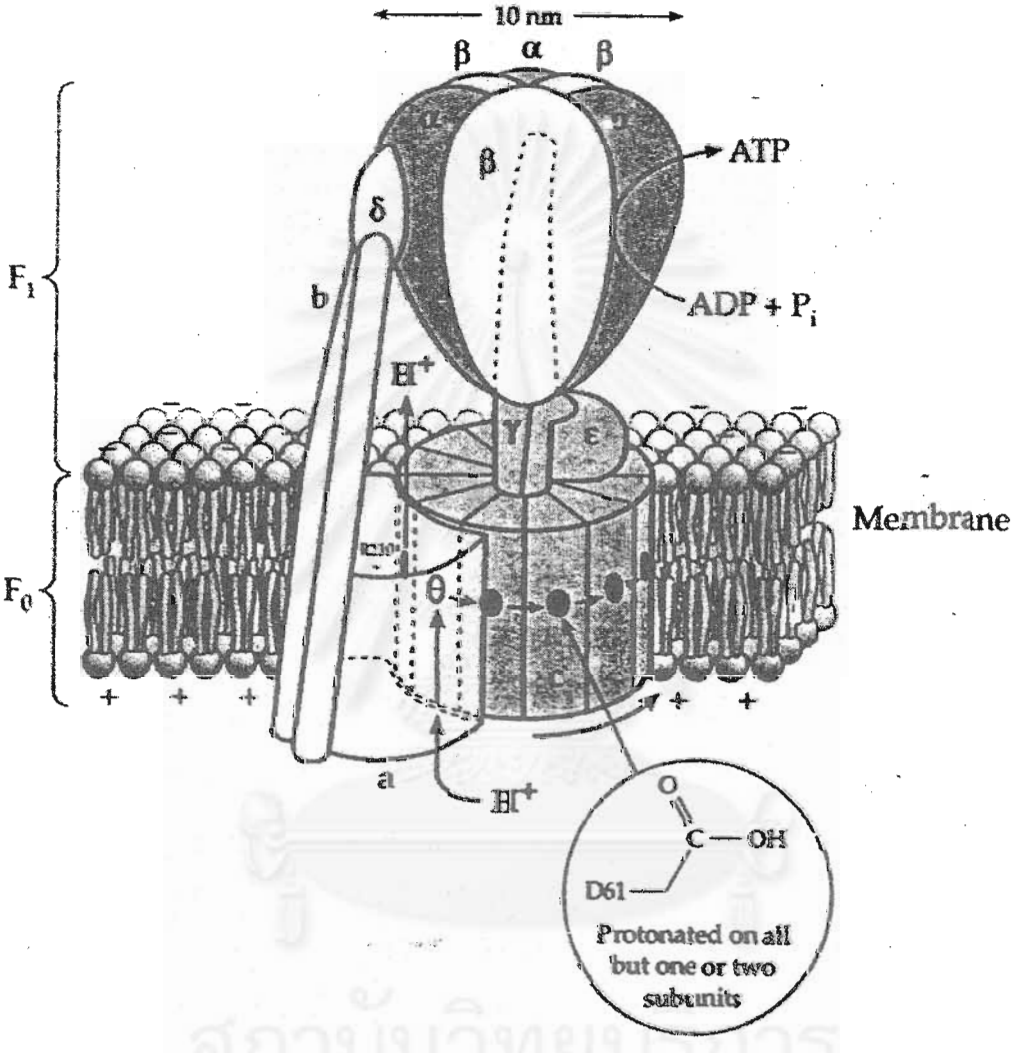

Figure 8. A model of ATP synthase (Metzler, 2003)

Inhibitors of Respiratory Chain

As mentioned above, there are three sites of energy consumption associated with the mitochondrial electron transport chain. The site of oxidative phosphorylation can be inhibited by various groups of substances, called the respiratory chain inhibitors. These inhibitors can classify into different group according to their effector, as follows (Wallace and Sarkov, 2000):

1. Inhibitors of complex I (Figure 9A)

Mitochondrial NADH: ubiquinone oxidoreductase (complex I) catalyzes the oxidation of NADH generated by NAD-linked dehydrogenase within the mitochondrial matrix. Complex I is the largest and most sophisticated enzyme of the respiration chain. It is composed of several polypeptide subunits encoded both by mitochondrial and nuclear DNA, and it contains FMN and several FeS centers. The list of inhibitors of complex I includes pesticides; neuroleptics and natural neurotoxins; antihistamic, antianginal, and antiseptic drugs; rodenticides; phenolic pollutants; fluorescent dyes; and myxobacterial and other antibiotics. All of the inhibitor can be classified into one of three categories based on their specificity toward complex I.

Group I include compounds that inhibit at the level of the NADH-flavin interaction, such as rhein. Such compounds are not specific to complex I because they also affect a variety of other dehydrogenases.

Group II is represented by quinole antagonists, which are inhibitory for both complex I and the bc_1-complex (e.g. myxothiazol and quinolone aurachins produced by *Pseudomonas aeruginosa* and *Stigmatella aurantiaca*). These compounds interfere with quinol binding and some are twice as potent as rotenone in inhibiting mammalian mitochondrial NADH: ubiquinone oxidoreductase.

Group III is specific and potent inhibitors of complex I, acting at concentrations low enough to have no effect on other respiratory chain complexes. Among this group is the classical inhibitor rotenone, which is a member of the rotenoid family of naturally occurring isoflavonoids produced by Leguminosae plants.

2. Inhibitors of complex III (Figure 9B)

Complex III (bc_1-complex, ubiquinol: cytochrome *c* oxidoreductase) oxidizes ubiquinol, reduces cytochrome *c*, and generates electrochemical proton gradient ($\Delta\mu_H+$). The

sensitivity of various species to a particular inhibitor of the bc_1-complex also varies greatly, which allows relatively safe practical application of some of these compounds as fungicides and as antimalarial, antiprotozoan, and anticancer drugs. The major inhibitors of the bc_1-complex can be classified in four groups according to the site of action and the part of electron transfer within the bc_1-complex that is blocked by a particular inhibitor.

Group I includes compounds of natural origin, such as myxothaizol, strobilurines, and oudemansins. These quinol antagonists contain a β –methoxyacrylate group that resembles part of the structure of ubiquinone. As a result, they block ubiquinol oxidation at center Q_0.

Group II inhibitors also resemble ubiquinone in that they contain a 6-hydroxyquinone fragment as common structural element. They block electron transfer between the Rieske $Fe_2 S_2$ center and cytochrome *c*1, thereby inhibiting the reduction of cytochrome b_L. This group includes undercylhydroxydioxobenzothiazole (UHDBT), undecylhydroxynaphtoquinone (UHNQ), and similar compounds.

Group III includes inhibitors acting at center Q_i. Inhibitors of center Q_i such as the antibiotics antimycin A, funiculosin, and quinolones such as heptylhydroxyquinoline-N oxide (HHQNO) are specific for the bc_1 complex, whereas naturally occurring center Q_0 inhibitors, which possess ubiquinone-like structure, are less specific and inhibit complex I as well.

3. Inhibitors of complex IV, Cytochrome *c* Oxidase (Figure 9C)

Complex IV, Cytochrome *c* Oxidase (COX) is a heme/copper terminal oxidase that uses cytochrome *c* as electron donor. It catalyzes the four-electron reduction of O_2 to water, coupled to the generation of $\Delta\mu_H+$ across the inner mitochondrial membrane in which it is embedded. All of the inhibitor can be classified into one of four categories: (a) heme-binding inhibitors that are noncompetitive with both O_2 and cytochrome *c* (e.g. azide, cyanide, and sulfide), (b) inhibitors competitive with oxygen, such as carbon monoxide (CO) and nitric oxide (NO), (c) inhibitors competitive with cytochrome *c* (polycations): and (d) noncompetitive inhibitors not affecting the heme groups, such as phosphate ions and alkaline pH.

4. Inhibitors of ATP-Synthetase (Figure 9D)

H^+-ATPase (complex V) uses the $\Delta\mu_H+$ to produce ATP from ADP and phosphate. It is major source of ATP in aerobic cells. The enzyme is reversible. Under some conditions it can hydrolyze ATP and generate $\Delta\mu_H+$. Antibiotic such as mycotoxins are the most powerful inhibitors of mitochondrial ATPase, many other compounds and classes of compounds share this same activity. Examples include naturally occurring flavonoids, a commonly used beta-adrenergic receptor antagonist propranolol, local anesthetics, the herbicide paraquat, and several pyrethroid insecticides and possible DDT and parathion, diethylstilbestrol, several cationic dyes, and organotin compounds.

Uncouplers of Oxidative Phosphorylation

Electrons can pass through the electron transport chain without generate ATP that called uncoupling of oxidative phosphorylation and a related kind of uncoupling of electron transport from ATP synthesis is brought about by various lipophillic anions called uncouplers (Erecinska and Wilson, 1981; Metzler, 2003). Additional types of uncouplers and uncoupling mechanisms are list as follows (Wallace et al., 2000).

1. Lipophillic Weak Acids: proton shuttling

The majority of compounds possessing protonophoric activity are lipophillic weak acids. Generally, structural requirements for uncoupling activity include the presence of an acid-dissociable group, bulky lipophillic groups, and a strong electron-withdrawing moiety. Proton-transporting lipophillic weak acids affect their uncoupling efficiency, such as the solubility in lipid membranes, the stability of the ionized form in the membrane, and the ability to release and bind a proton. The most representative uncouplers of this class are 2,4-Dinitrophenol (DNP) and other substituted phenols, trifluoromethylbenzimidazoles, salicylanilides, and carbonyl cyanide phenylhydrazones.

2. Other Types of Uncouplers

1) Protein-Mediated Uncoupling by Free Fatty Acids

The protonophoric action requires that fatty acids (FAs) cross the membrane in both the protonated and anionic forms. Studies over the past decade reveal that adenine nucleotide translocase, an integral protein of the inner mitochondrial membrane, is involved in the uncoupling action of long chain FFAs.

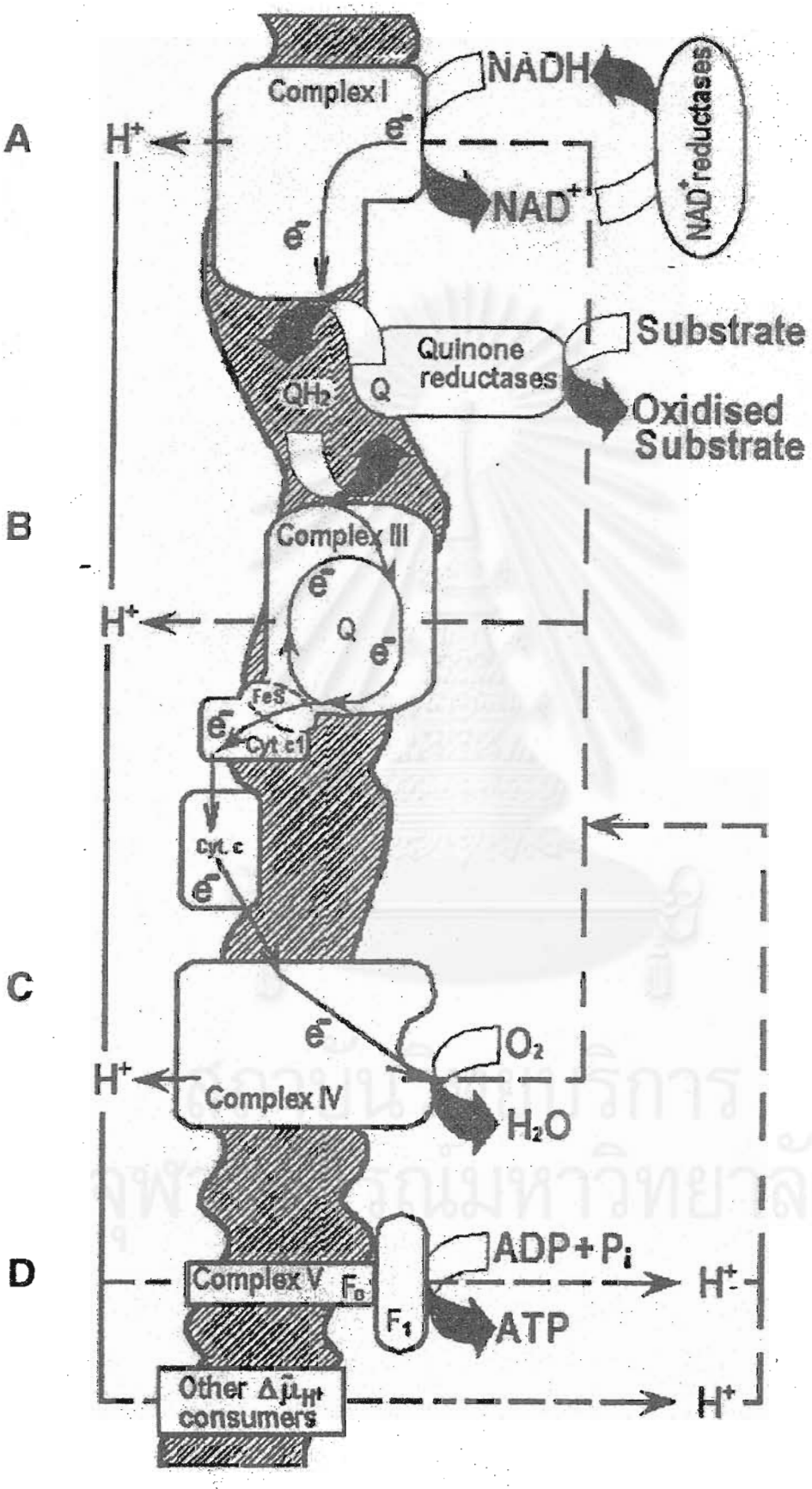

Figure 9. Inhibitors of Respiratory Chain (Wallace and Sarkov, 2000)

2) Ionophores

Ionophores are compounds of various chemical structures that are capable of transporting small ions across a lipid membrane and can be divided into two general groups based on the mechanism of ion transport: a carrier type or a channel type. Carrier-type ionophores are able to form neutral or charged lipid-soluble complexes with an ion to facilitate its electrophoretic transport (uniport) or electroneutral excharge with protons (antiport) across a hydrophobic membrane. Channel-type is typical of short amphiphillic peptides that form channels of various sizes in lipid membranes. These channels can be selective toward small ions such as protons or K^+, depending on the particular peptide, the membrane structure, and the experimental conditions.

3) Cationic Uncouplers

Several cationic compounds uncouple mitochondria by increasing membrane permeability to ions.

4) Membrane-Active Peptides

Membrane-active peptides can form channels, which are more or less selective to alkaline cations and/or protons, or they can form large pores allowing permeation of high-molecular-weight (>100 Da) solutes.

5) Alternate Electron Acceptors

Alternate electron acceptors are capable of the being reduced by an electron carrier of the respiratory complex, thus competing with a natural acceptor of this carrier. These compounds intercept electron flow and divert it toward their own reduction. Electron shunts can be both reduced and oxidized by the respiratory chain, thus allowing electrons to bypass a portion of a respiratory complex or a whole segment of respiratory chain and excluding it from energy generation.

Mitochondrial Ca^{2+} transport

While the mitochondrial outer membrane is believed to be freely permeable to ions and molecules up to 14 kDa (Mayes, 2000), the inner membrane is tightly sealed to all ions, but for the presence of specific transporters. The uptake of Ca^{2+} into the matrix is catalyzed by an electrophoretic uniporter that is driven by the membrane potential (≈180 mV, negative insides) component of the proton-motive gradient set up through proton extrusion

by the respiratory chain (McCormack et al., 1990). When a proton gradient created by coupled electron transfer or ATP hydrolysis, mitochondrial take up Ca^{2+} from the external medium. The Ca^{2+}-uptake is catalyzed by Ca^{2+} uniporter' (presumably a gated channel) in the inner membrane which exchanges Ca^{2+} for H^+ (net electrogenicity, 1+ charge) (Chakraborti et al., 1999).

When respiratory chain is inhibited, the membrane potential can be maintained by a reversal of the H^+ ATPase. Accordingly, to block mitochondrial Ca^{2+} uptake in living cells endowed with an active glycolysis, both the respiratory chain and the H^+ ATPase must be inhibited. If mitochondria accumulate of Ca^{2+} (in the presence of phosphate) they store it in the matrix as insoluble phosphate salts called 'hydroxyapatite', visible as dense granules in electron micrographs, and the release occurs very slowly (Carofoli et al., 1974; Pozzan and Rizzuto, 2000). When there is sufficient Ca^{2+} and phosphate to form this complex, mitochondria behave as perfect buffers of extramitochondrial Ca^{2+}, accumulating the cation whenever its concentration rises above the set point at which uptake and efflux balance and releasing Ca^{2+} below this value (Nicholls and Budo, 2000).

Because of accumulation of Ca^{2+} is limited, the release is fast and depends on two pathways. The first, and more efficient, exchanges Ca^{2+} for Na^+ as called 'an electroneutral $Na^+ - Ca^{2+}$ exchanger'. This in turn is driven by the exchange of Na^+ for H^+ and depends on the pH component of the proton-motive gradient (McCormack et al., 1990). The second exchanges direct Ca^{2+}-$2H^+$ exchange (Bernardi, 1999). Under steady state conditions the Ca^{2+} concentration in the matrix thus depends on a futile cycle of Ca^{2+} uptake via the uniporter and release via the antiporters, the mitochondrial Ca^{2+} cycle as shown in Figure 10 (Carafoli, 1979).

Calcium accumulation by isolated mitochondria can lower mitochondrial membrane potential ($\Delta\psi_m$) in one of three ways. First, in the absence of phosphate, the capacity of isolated mitochondria to accumulate Ca^{2+} is restricted, since the protons extruded by the respiratory chain during Ca^{2+} accumulation are no longer neutralized by phosphate uptake. The second, phosphate is also present, a net uptake of calcium phosphate occurs, which precipitates inside the mitochondria as hydroxyapatite, visible as dense granules in electron micrographs. The third mechanism is the condition of Ca^{2+} overload leading to mitochondrial swelling, loss of respiratory control, collapse of $\Delta\psi_m$, and release of matrix

Ca^{2+} caused by a permeabilization of the mitochondrial inner membrane to sucrose and other molecules up to 1.5 kDa (Nicholls and Budo, 2000).

Maintenance of low cytosolic Ca^{2+} is necessary for proper functioning of cells. Mitochondria transport Ca^{2+} (1) to regulate cytosolic Ca^{2+}, (2) to serve as a store of Ca^{2+} when its concentration in the cytosol is excessive, (3) to serve as a releasable source of activator Ca^{2+}, and (4) to regulate mitochondrial matrix Ca^{2+} and thereby control the level of activation of Ca^{2+}–sensitive metabolic enzymes (Wallace et al., 2000).

The uptake pathway for Ca^{2+} can be inhibited by physiological concentration of Mg^{2+}, which acts competitively on the kinetics of Ca^{2+} uptake. There are also two potent but nonphysiological inhibitors of mitochondrial Ca^{2+} uptake, namely the glycoprotein stain ruthenium red and lanthanide ions.

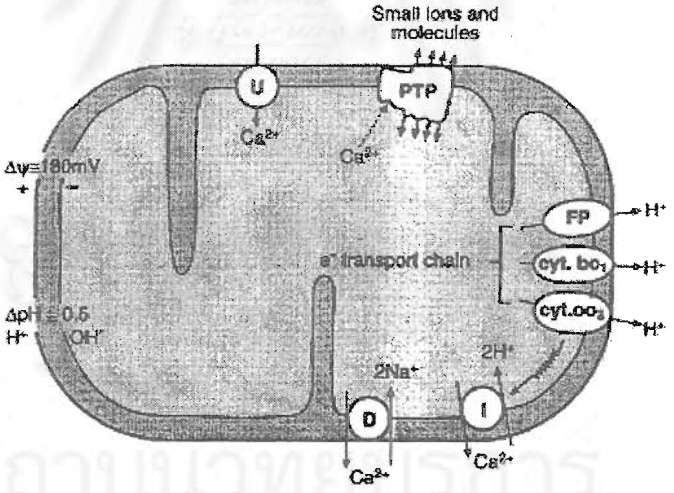

Figure 10. Ca^{2+} transport systems in mitochondria. The mitochondrial Ca^{2+} uniporter (U) facilitates the transport of Ca^{2+} in an inward direction down the electrochemical gradient of this ion. The Na^{+} independent efflux mechanism (I) is depicted here as an active Ca^{2+}–$2H^{+}$ exchanger, receiving energy from the electron-transport chain. The Na^{+}-dependent efflux mechanism (D) is depicted here as a Ca^{2+}–2 Na^{+} exchanger. A Ca^{2+} activated permeability transition pore (PTP) also is shown (Gunter, K.K., and Gunter, T.E., 1994; Chakraborti et al., 1999).

Role of monoamine oxidases on mitochondrial function

The mitochondrial monoamine oxidase that is believed to be synthesized by the endoplasmic reticulum under nuclear DNA control and later becomes attached to the outer mitochondrial membrane (Chau and Hackenbrock, 1975; Murphy, 1978). Prolonged sonication and/or detergent treatment could isolate enzyme in soluble form. The soluble form of enzyme has been showed to differ from membrane-bound enzyme in its sensitivity towards inhibitors and in the kinetic mechanism (Houslay and Tipton, 1975; 1976). It is now generally accepted that the enzyme contain 1 mole of flavin cofactor, identified as flavin-adenosine-dinucleotide (FAD), covalently bound as a prosthetic group (Tipton, 1968; Youdim and Sourkes, 1971) and consist of a mononuclear Cu (II) ion (McGuirl and Dooley, 1999).

Monoamine oxidase (MAOs, monoamine; oxygen oxidoreductase, deaminating) converts biogenic amines in the brain and peripheral tissues to their corresponding aldehydes (Shih, 1991; Thorpe et al., 1987). The enzymatic reaction requires molecular oxygen and produces aldehyde and hydrogen peroxide according to the overall equation:

$$R\text{-}CH_2\text{-}NH_2 + O_2 + H_2O \longrightarrow R\text{-}CHO + NH_3 + H_2O_2$$

Subsequently, the aldehyde intermediate is rapidly metabolized, usually by oxidation via the enzyme aldehyde dehydrogenase to the corresponding acid, or in some circumstances to the alcohol or glycol by the enzyme aldehyde reductase (Holschneider et al., 2001).

Multiple forms of monoamine oxidase

Monoamine oxidase (MAO) is now understood to exist for at least two types: MAO-A and MAO-B, which differ in substrate specificity and inhibitor sensitivity. The specificity must be reflected in the amino acid sequence and molecular structure of the active sites. The different forms of MAO are the products of two related but different genes. In human and other mammals the two genes are closely linked on the X-chromosome (Kochersperger et al., 1986; Caspi et al, 2002). MAO-A preferentially oxidizes the biogenic amine serotonin (5-HT), norepinephrine (NE), dopamine (DA). And the selective inhibitor is clorgyline. MAO-B structure preferentially oxidizes different neurotransmitters. MAO-B oxidizes phenylethylamine (PEA), benzylamine. And the selective inhibitor is deprenyl.

(Powell, 1991; Shih et al., 1999). Comparison of the sequence of the different forms with other species showed that there is a degree of similarity between the same form from different species. For example, rat and human MAO-B have approximately 90 percent of amino acid sequences identical (Powell, 1991).

The effectiveness of each isoenzyme is different. MAO-B seems to have a limited capacity to deaminate catecholamines. Individuals with a MAO-B deficiency appear to be mentally normal which has led many researchers to believe that MAO-A is the more important isoenzyme of the two. Deficiencies of MAO-A results in disturbed systemic amine metabolism, borderline mental retardation and possible cardiovascular and behavior abnormalities (Finber, 1998).

Localization and development of monoamine oxidase

The localization of MAO in rodent, cat, primate and human are varied. The distribution of MAO-A and B in brain shows that MAO-A is predominantly found in catecholaminergic neurons, and MAO-B is the form most abundant in serotonergic and histaminergic neurons and glia cells. The distribution of MAO in the periphery varies within the same organism. Some tissue (human platelet and bovine liver and kidney) mainly contains MAO-B and others (human placenta and bovine thyroid gland) predominantly contain MAO-A. In human and rodents, MAO-A is existing before MAO-B in most tissue. MAO-A is almost at adult levels at birth whereas MAO-B activity increase several-fold with aging (Yang et al., 1972; McEntire et al., 1979; Shih et al., 1999).

The ratio of MAO-A / MAO-B activity for brain was 6/4 while the ganglion it was 9/1 and they concluded that tyramine is deaminated by both MAO-A and MAO-B whereas noradrenaline (NE) is deaminated only by MAO-A, the enzyme which is most active in the ganglion. These observations are consistent with the hypothesis that a specific intraneuronal MAO plays an important role in the catabolism of NE in sympathetic nerves. In human blood platelet, only the B form of MAO is present (Goridis and Neff, 1971; McEntire et al., 1979).

Monoamine oxidases (MAO-A and MAO-B) are well known targets for antidepressant drugs and for drugs used to treat neurological disorders and diseases of aging, such as Parkinson's disease and Alzheimers disease. The MAO-B inhibitor deprenyl

is administered to increase the effectiveness of L-dopa therapy in the treatment of Parkinson's disease. Recent studies have also demonstrated that MAO-B is inhibited by compounds present in tobacco smoke, which may contribute to the addictive properties of tobacco use (Shih et al., 1999). Recent trials, have demonstrated the efficacy of MAO-A inhibitor, brofaromine and moclobemide, in the treatment of symptoms of major depression, panic and phobia (Holschneider et al., 2000).

Hypothesis

N-heptanoyl-3-methoxy-4-nitro anilide (CU 18-14) and N-heptanoyl-2-nitro-5-methoxy anilide (CU 18-15) can affect the following mitochondrial functions

1. Oxidation and phosphorylation
2. ATPase
3. Calcium stimulated respiration
4. Monoamine oxidase

Significance

Describe a benefit and harmful effect of N-heptanoyl-3-methoxy-4-nitro anilide (CU 18-14) and N-heptanoyl-2-nitro-5-methoxy anilide (CU 18-15) on mitochondria functions. The results of this study may be using for further development of new high potential compounds with fewer side effects such as monoamine oxidase inhibitors.

CHAPTER III

MATERIALS AND METHODS

1. Experimental animals

Male albino Wistar rats weighing 180-200 g were used in this study. They were purchased from the National Experimental Animal Center, Mahidol University, Salaya, Nakornprathom Province. The animals were acclimatized and fed ad libitum in animal care unit, Faculty of Pharmaceutical Sciences, Chulalongkorn University for at least one week before the experiment.

2. Chemicals

Most reagents were dissolved in ultrapure water and some were dissolved in absolute ethanol or dimethylsulfoxide (DMSO). When necessary, the pH of the solutions was adjusted with KOH and HCl.

1. Source of test compounds and reagents

1.1 Tested compounds are kindly supplied by Assist. Prof. Dr. C. Patarapanich: N-heptanoyl-3-methoxy-4-nitro anilide (CU 18-14) and N-heptanoyl-2-nitro-5-methoxy anilide (CU 18-15) (Figure 3).

1.2 Reagents

1) Reagents from Sigma Chemical Company were adenosine 5' diphosphate (ADP), adenosine 5' triphosphate (ATP), 1-amino-2-naphthol-4-sulfonic acid, ammonium molybdate, benzylamine hydrochloride, bovine serum albumin (BSA), calcium chloride ($CaCl_2$), cupric sulfate ($CuSO_4$), cytochrome *c*, dimethyl sulfoxide (DMSO), 2,4-dinitrophenol (DNP), Folin&Ciocalteu's phenol reagent, HEPES, 5-hydroxytryptamine (5-HT), L-glutamic acid, magnesium chloride ($MgCl_2$), malic acid, oligomycin, potassium chloride (KCl), potassium phosphate monobasic anhydrous (KH_2PO_4), sodium bisulfate, sodium hydroxide (NaOH), sodium phosphate dibasic anhydrous, sodium phosphate monobasic, sodium potassium tartrate, sodium sulfite,

succinic acid, sucrose, trichloroacetic acid (TCA), and tyramine hydrochloride.

2) Reagents from E. Merck, Darmstadt Company were absolute ethanol, sodium carbonate anhydrous (Na_2CO_3), sulfuric acid (H_2SO_4), hydrochloric acid (HCl), potassium hydroxide (KOH).

2. *Dissolution of tested compounds and reagents*

2.1 Tested compounds (CU 18-14 and CU 18-15) at concentrations 1.01×10^{-6}, 1.01×10^{-5}, 1.01×10^{-4}, 2.02×10^{-4}, 3.04×10^{-4}, 4.05×10^{-4} M were prepared by dissolving the compounds in DMSO.

2.2 Reagents

1) Reagents dissolved in ultrapure water were 2.5% w/v ammonium molybdate, 2 µl of 0.3 M ADP + 0.6 M Pi, 150 µl of 0.1 M ATP, 10 µl of 0.1 M benzylamine hydrochloride, 0.05 – 0.30 mg/ml BSA, 10 µl of 0.4 M $CaCl_2$, 20% w/v $C_2HCl_3O_2$, 2 - 6 µl of 50 mM DNP, 10 µl of 1 M glutamate + 1 M malate (pH 7.4), 10 µl of 0.1 M 5-HT, 40 mM HEPES buffer (pH 7.4), 92 mM KCl, 0.1 – 3.0 mM KH_2PO_4, 2 mM $MgCl_2$, 0.5 M NaOH, 15% w/v sodium bisulfite, 20% w/v sodium sulfite, 10 ml of 1% w/v sodium potassium tartrate, 10 µl of 1 M succinate (pH 7.4), 0.25 M sucrose and 10 µl of 0.1 M tyramine hydrochloride.

2) A reagent dissolved in absolute ethanol was 2 µl of 5 mg/ml oligomycin.

3) A reagent dissolved in DMSO was 2 µl of 5 mg/ml rotenone.

3. Instruments

3.1 Autopipets 20,100, 200, 1,000 and 5,000 µl (Gilson, France)

3.2 Clark's oxygen electrode

3.3 Heidolph glass homogenizer (Type SO203 RZR 2)

3.4 Hitachi high speed refrigerated centrifuged Himac CR 20 B 3, Rotor model RP 18-3

3.5 Oxygen monitor (YSI model 5300)

3.6 pH meter

3.7 Spectrophotometer (Ultrospec II)

3.8 Strip chart recorder (Gilson model N2)

3.9 UV-Visible recording spectrophotometer: Shimadzu (UV-160A)

3.10 Vortex mixer (Clay Adams, USA)

4. Experimental procedures

1. Isolation of mitochondria

Liver mitochondria were isolated from Wistar rats by the method of Hogeboom (1955) modified by Myers and Slater (1957) and Hammond and Kubo (2000).

1. Rat was cervical dislocation humanely in accordance to the method approved by the Animal Ethics Committee of the Faculty of Pharmaceutical Sciences, Chulalongkorn University.
2. An incision from groin to sternum, first separating the skin then the underline muscle and peritoneum, reveals a whole of the liver was immediately removed and chilled in ice-cold homogenizing medium (0.25 M sucrose adjusted to pH 7.4). All subsequent isolation work was performed at 0-4 ^{0}C in an ice.
3. The liver was washed frequently with ice-cold isolation medium (0.25 M sucrose adjusted to pH 7.4), cut into small pieces with surgical scissors and homogenized with Heidolph glass homogenizer.
4. The homogenate was differential centrifuged (Figure 11) with Hitachi high speed refrigerated centrifuged for 5 minutes at approximately 600 *g* (2,500 rpm) at 0-4 ^{0}C to precipitate nuclei, red blood cells, cell wall and unraptured cells.
5. The mitochondria in the supernatant were decanted and centrifuged for 10 minutes at approximately 4,500 *g* (7,000 rpm).
6. The supernatant was poured off, the pellet was resuspended in 0.25 M sucrose with the aid of Heidolph glass homogenizer and centrifuged one more time for 10 minutes at 13,000 *g* (8,000 rpm).
7. The fluffy layer was removed from the firmly packed sediment of mitochondria by gently shaking with small amounts of 0.25 M sucrose, and the residual mitochondria were again resuspended in 0.25 M sucrose with the aid of

Heidolph glass homogenizer, and kept in ice-cold for the experiments during the same day.

8. This procedure was designed to isolate intact mitochondria rather than to recover all of the mitochondria present in the liver, yielded about 20 mg of mitochondrial protein /g of liver.

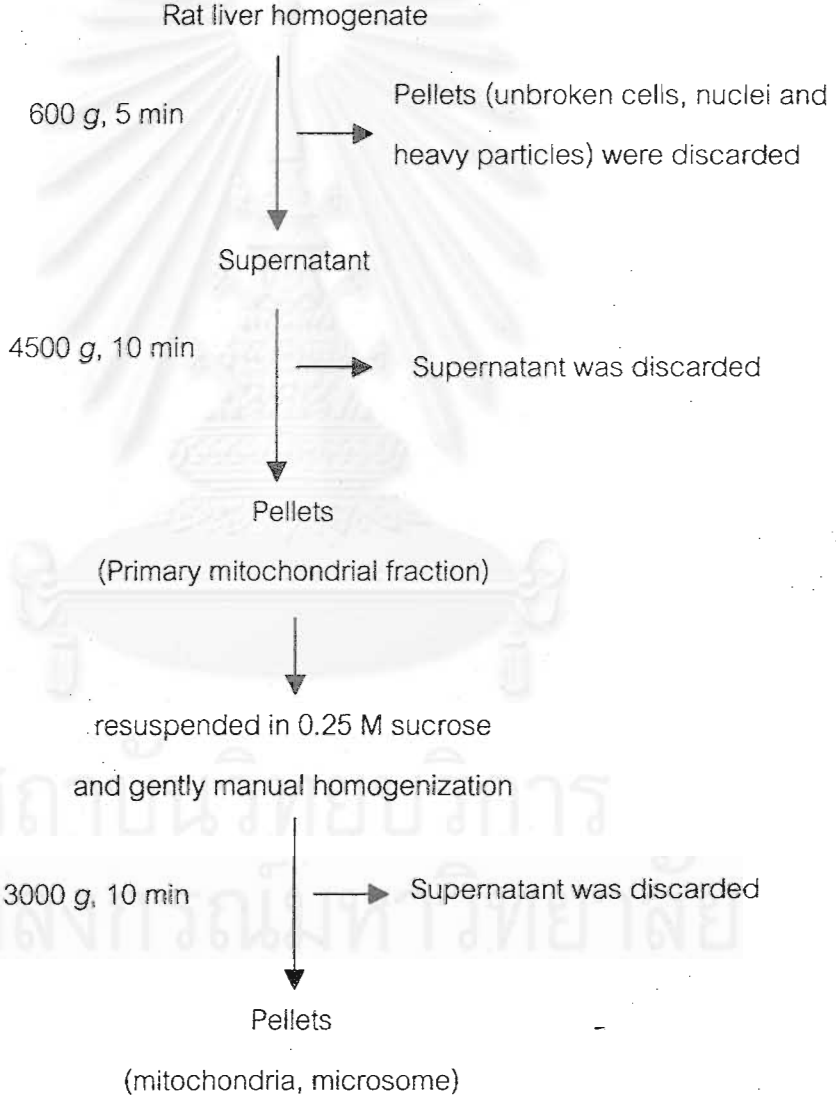

Figure 11. Schematic description of procedure for mitochondrial preparation from liver homogenate by differential centrifugation

2. Polarographic measurements of oxygen consumption

Measurement of mitochondrial respiration was a measure of the amount of oxygen consumption. Oxygen consumption measurements were performed in a Gilson reaction chamber (Figure 12) with a Clark Oxygen Electrode connected with Oxygen monitor (YSI model 5300) and Strip chart recorder. The reaction was maintained at 37°C. The chamber was about 1.7 ml in volume and consisted of the water jacket encompassed the chamber and a hollow glass stopper through which the substrates and reagents were kept at 37°C by circulating water bath. Oxygen concentrations were measured using a Clark-type polarographic electrode. A platinum cathode was set at constant voltage relative to a silver/silver chloride anode in a low volume electrolyte chamber. The electrolyte was separated from the solution to be tested by a gas-permeable Teflon membrane, which was impermeable to other components of the solutions. Oxygen diffusing through the membrane was reduced at the cathode creating an electrical current.

At the anode, silver Ag (0) was oxidized to Ag^{+}, which precipitated as AgCl. All of the oxygen in the small electrolyte solution bathing the electrodes was consumed by the reaction, creating effectively zero oxygen concentration on the electrode side of the membrane. Thus, current depends on the rate of diffusion of oxygen across the membrane, which under these conditions was proportional to the oxygen concentration on the outside of the membrane. The amount of oxygen passing through the membrane was small enough that it did not, by itself, lead to a significant change in the oxygen concentration in the measuring chamber. The current generated in the electrode was passed through a resistor and the voltage drop across the resistor was electronically amplified and the signal from the amplifier was recorded on a stripchart recorder (Gilson model N2). The tracings obtained were called "oxygraph" or "polarographic" tracings.

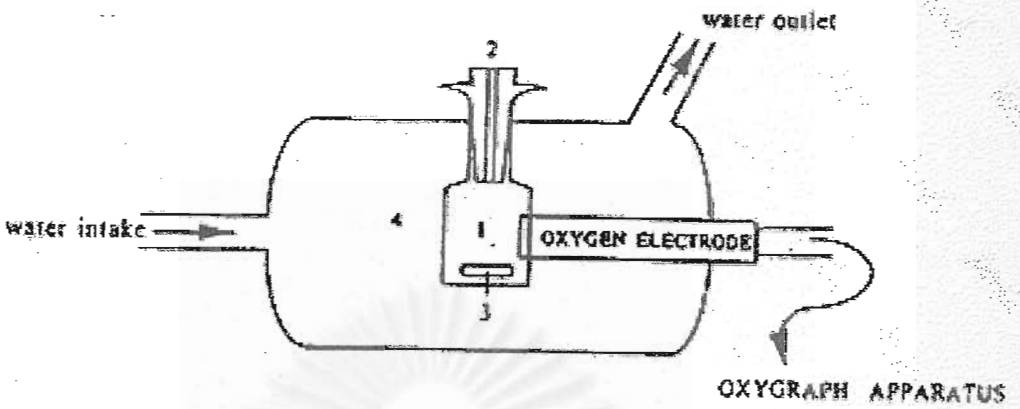

1 = reaction chamber

2 = stopper

3 = magnetic stirrer

4 = water jacket

Figure 12. Gilson reaction chamber.

The incubation medium consisted of 40 mM HEPES buffer pH 7.4, 2 mM $MgCL_2$, 92 mM KCl which is isoosmotic with the mitochondria. About 1.7 ml incubation medium and 50 µl mitochondrial suspension was incubated in the chamber with the substrates and other reagents. Mitochondria were preincubated with continuous stirring. The reaction was started by addition of 1M glutamate plus 1 M malate (pH 7.4) as substrate of complex I and substrate of complex II was 1M succinate (pH 7.4). After a slow rate of respiration had stabilized in the initial resting state, State 3 respiration was initiated by addition of ADP and inorganic phosphate (Pi). When all ADP and inorganic phosphate (Pi) has been consumed, respiration returns to a resting rate (State 4). Functional integrity of the mitochondria was measured in terms of respiratory control index (RCI), defined as the ratio of the rate of $\frac{\text{State 3}}{\text{State 4}}$.

RCI values were more than 4. Uncoupled respiration was measured after addition of the classic uncoupler of oxidative phosphorylation, DNP (Figure 13).

Experimental protocol of Polarographic measurements of oxygen consumption

1. Effect of test compounds (Cu 18-14 and Cu 18-15) on complex I of respiratory chain.

   1) Substrate of complex I of respiratory chain was 1M glutamate plus 1 M malate was added.
   2) The tested compounds (Cu 18-14 and Cu 18-15) in various concentrations were added.
   3) Adding ADP and inorganic phosphate (Pi).

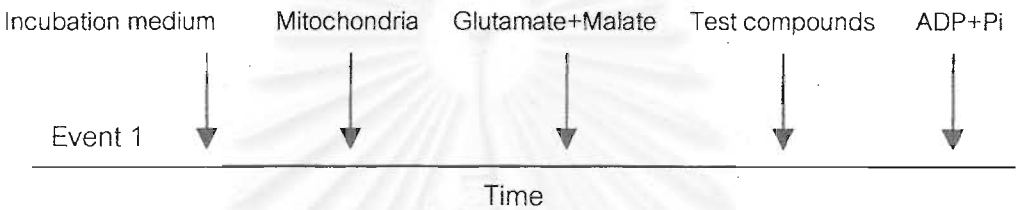

2. Effect of test compounds (Cu 18-14 and Cu 18-15) on complex II of respiratory chain.

   1) Substrate of complex II of respiratory chain was 1M succinate was added.
   2) The tested compounds (Cu 18-14 and Cu 18-15) in various concentrations were added.
   3) Adding ADP and inorganic phosphate (Pi).

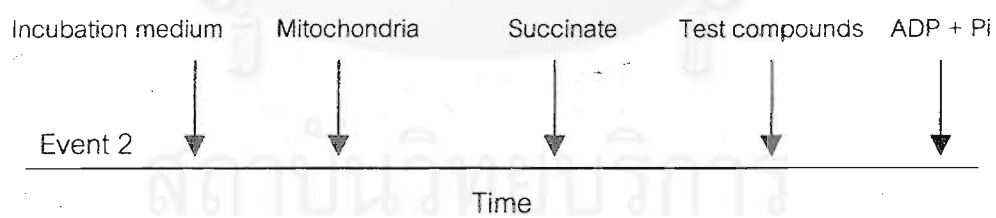

3. Effect of test compounds (Cu 18-14 and Cu 18-15) on DNP stimulated respiration.

   1) Substrate of complex I of respiratory chain was 1M glutamate plus 1 M malate was added.
   2) Adding the uncoupler, DNP.
   3) The tested compounds (Cu 18-14 and Cu 18-15) in various concentrations were added.

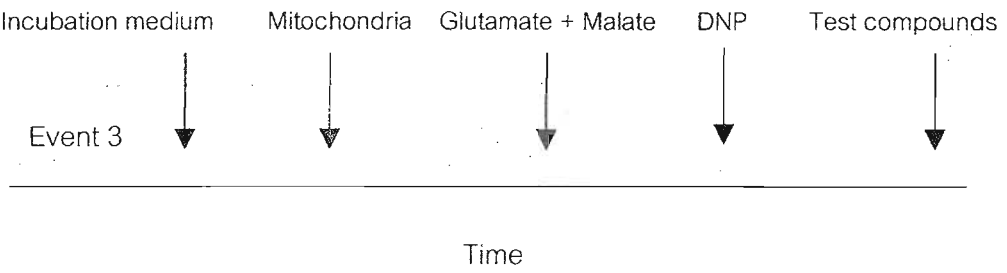

Determination of the respiratory control index (RCI)

The rate of respiration of mitochondria can be controlled by the concentration of ADP. This is because oxidation and phosphorylation are tightly coupled; i.e. oxidation cannot proceed via the respiratory chain without concomitant phosphorylation of ADP.

Chance and Williams have proposed a convention following the typical order of addition of agents during an experiment:

State 1: mitochondria alone (in the presence of Pi)

State 2: substrate added, respiration low owing to lack of ADP

State 3: a limited amount of ADP added, allowing rapid respiration

State 3u: uncoupler added, allowing rapid respiration (Chance and William, 1956)

State 4: all ADP converted to ATP, respiration slows

State 5: anoxia (Mayes, 2000; Nicholls and Ferguson, 2002).

The method used for calculating the respiratory control index (RCI) value was also described by Chance and Williams (1956).

$$RCI = \frac{\text{Rate of State 3 respiration}}{\text{Rate of State 4 respiration (after State 3)}}$$

$$\text{Or} \quad = \frac{\text{Slope of the tracing in State 3 respiration}}{\text{Slope of the tracing in State 4 respiration}}$$

Thus from figure 13:

$$RCI = \frac{Y1/X}{Y2/X} = \frac{Y1}{Y2}$$

Y1 and Y2 are the length of line Y1 and Y2 respectively.

The RCI value indicates the tightness of the coupling mechanism, that is, whether the substrate oxidation is tightly coupled to ATP synthesis. The RCI value of good intact mitochondria should be at least 4 at 37^{o}c with glutamate plus malate as substrates.

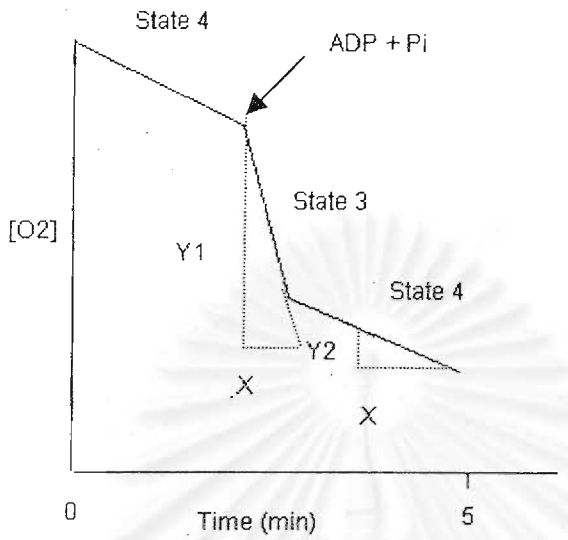

Figure 13. The oxygraph tracing for calculating the respiratory control index (RCI) values

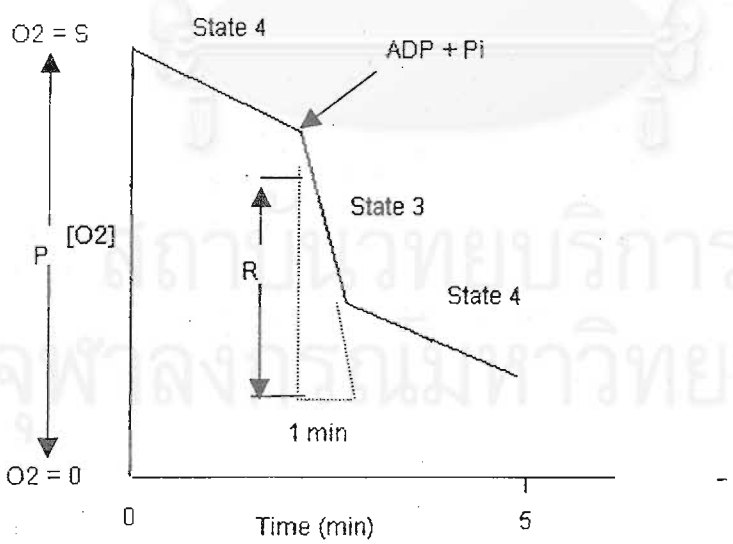

Figure 14. The oxygraph tracing for calculating the rate of oxygen consumption

Calculation of rates of oxygen consumption

Rates of oxygen consumption in various metabolic states can be calculated from oxygraph tracing as shown in figure 14.

$$\text{Method 1: rate of oxygen consumption in state 3} = \frac{R \times S}{P} \quad \text{n atom O/min}$$

$$\text{Method 2: rate of oxygen consumption in state 3} = \frac{R \times A}{P} \quad \text{n atom O/min}$$

Where R and P = the length of oxygen line R and P respectively

S = n atom oxygen initially dissolved in the reaction mixture

A = n atom oxygen dissolved in 1 ml of water

S value depends on volume of reaction mixture and temperature. For example the larger the volume and the lower the temperature, the more oxygen dissolved in the reaction mixture. S value is calculated by multiplying the amount of oxygen dissolved in 1 ml water (A) with total volume of the reaction mixture.

A value can be calculated from the following formular:

$$A = \frac{s \times p \times n \times 10^{9}}{v \times 100} \quad \text{n atom O/ml}$$

Where A = n atom oxygen dissolved in 1 ml of water

s = absorption coefficient at 37^{o}C (volume of oxygen reduced to 0^{o}Cand 760 mm, absorbed by one volume of water when the pressure of the gas itself amount to 760 mm) = 0.02373

v = volume of gas (at 0^{o}C and 760 mm) corresponding to 1 gm̄ mole = 22,400 ml

p = percentage of oxygen in atmostpheric air = 21%

n = number of atoms in a molecule of oxygen = 2

Substituting these values in the above equation, the amount of oxygen dissolved in 1 ml of water at 37 ^{o}C = 444.9 n atom O/ml.

The S value is calculated by multiplying the volume of reaction mixture (1.77 ml) with A value.

$$S = 1.77 \times A \quad \text{n atoms Oxygen}$$

Oxygen consumption rates can be divided by mitochondrial protein used in the reaction, and the unit becomes n atom O/min/mg protein.

3. ATPase activity assay

ATPase activity can be determined by measuring the total amount of inorganic phosphate (Pi) (Weinbach, 1956) or proton (Bertina et al., 1975) liberated by the hydrolysis of ATP and ADP.

$$ATP + H_2O \xleftrightarrow{\text{ATPase } (F_1\text{-}F_0\text{-ATPase})} ADP + Pi + H^+$$

In this research the former method was employed. The inorganic phosphate (Pi) liberated was quantitated by the colorimetric method of Fiske and Subbarow (1925). The mitochondrial ATPase activity was measured as described below.

1. 2.63 ml of incubation medium (40 mM HEPES buffer pH 7.4, 2 mM $MgCL_2$, 92 mM KCl adjusted to pH 7.4 which is isotonic with the mitochondria) was added to test tube which maintained at 37 °c.
2. 200 µl of mitochondrial suspension and test compounds were preincubated with continuous stirring for 1 minute.
3. Add test compounds (Cu 18-14 and Cu 18-15), DNP (uncoupler), oligomycin (ATPase inhibitor), DMSO (the blank).
4. Mitochondrial suspensions were incubated with 150 µl of 0.1 ATP that was added to the test tube and allowed to sit 10 minutes.
5. After 10 minutes incubation at 37°c, 1 ml of reaction mixture was added by 1 ml an equal volume of 20 %w/v trichloroacetic acid solution to stop the reaction.
6. Denatured proteins are removed by centrifugation at 4000 rpm for 10 minutes.

7. 1 ml of the supernatant fluid, which had the inorganic phosphate, was pipetted into 5 ml of 0.2 M sulfulic acid (H_2SO_4) solution.
8. The standard curve plots of Pi obtained from the various concentrations of potassium phosphate monobasic anhydrous (K_2HPO_4) concentrations: 0.1, 0.25, 0.50, 1.0, 1.5, 2.0, 3.0 mM/ml and ultrapure water was used as the blank.
9. 0.8 ml of 2.5 % w/v ammonium molybdate and 0.4 ml of Fiske subbarrow reducing agent were added, mixed on a Vortex mixer and allowed to stand for 10 minutes at room temperature.
10. After 10 minutes, the sample was measured the optical density at 650 ηm with a Spectrophotometer (Ultrospec II) at room temperature. Liberated inorganic phosphate was calculated from a standard curve of potassium phosphate monobasic anhydrous (K_2HPO_4).

Annotation: In the preparation of Fiske Subbarow reducing agent, some of the undissolved 1-amino-2-napthol-4-sulfonic acid was discarded by filtration and filtrate was kept, no longer than one month, in the bottle protected from light.

Experimental protocol of ATPase activity assay

1. Effect of test compounds (Cu 18-14 and Cu 18-15) on ATPase activity.
   1) The tested compounds (Cu 18-14 and Cu 18-15) in various concentrations were added.
   2) Adding ATP and allowed to stand 10 minutes.

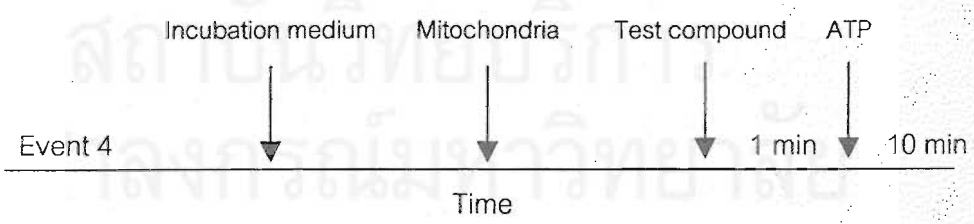

2. Effect of DNP stimulated ATPase activity.
   1) Adding the uncoupler, 50 mM DNP 10 μl and allowed sitting 1 minute.
   2) Adding ATP and allowed to stand 10 minutes.

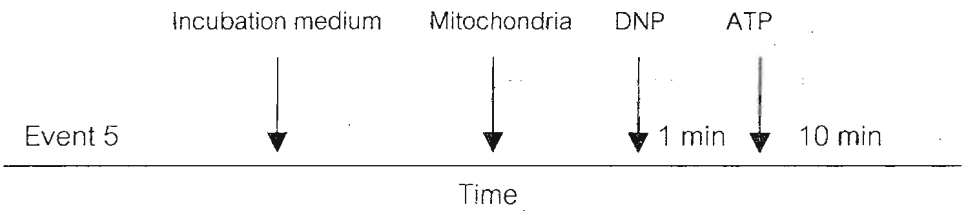

3. Effect of test compounds (Cu 18-14 and Cu 18-15) on DNP stimulated ATPase activity of mitochondria in the presence or absence of ATPase inhibitor.

    1) Adding the uncoupler, DNP.

    2) The tested compounds (Cu 18-14 and Cu 18-15) in various concentrations were added and allowed sitting 1 minute.

    3) Adding the ATPase inhibitor, oligomycin concentration was 10 μg/2 μl.

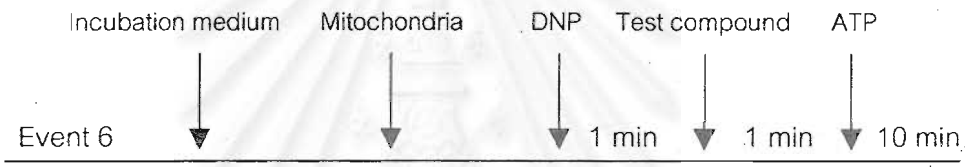

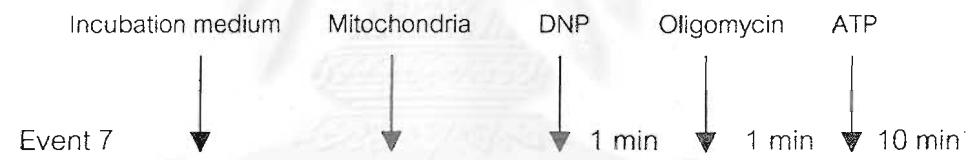

4. Effect of test compounds (Cu 18-14 and Cu 18-15) on mitochondria in the presence ATPase inhibitor.

    1) The tested compounds (Cu 18-14 and Cu 18-15) in various concentrations were added.

    2) Adding the ATPase inhibitor, oligomycin concentration was 10 μg/ 2 μl.

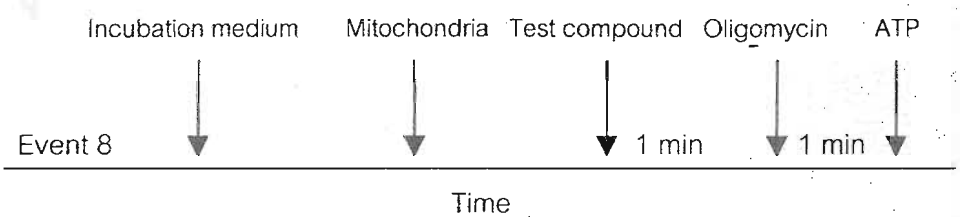

4. Calcium stimulated respiration

Calcium stimulated respiration was determined by polarography at 37 °c in a Gilson oxygraph equips with a Clark type oxygen electrode. The reaction system consisted of incubation medium (40 mM HEPES, 2 mM $MgCl_2$, 92 mM KCl, and 1 mM KH_2PO_4 adjusted to pH 7.4) and 1 M glutamate plus 1 M malate. Mitochondria were preincubated in incubation medium with continuous stirring. One minute after the addition of glutamate, 2 µl of 0.4 M $CaCl_2$ was added in order to stimulated the respiration. The increase in oxygen uptake rate was calculated n atom O/ min.

Experimental protocol of calcium stimulated respiration

Effect of test compounds (Cu 18-14 and Cu 18-15) on mitochondria with calcium stimulated respiration.

1) Substrate of complex I of respiratory chain was 1M glutamate plus 1 M malate was added.
2) The tested compounds (Cu 18-14 and Cu 18-15) in various concentrations were added.
3) Adding $CaCl_2$.

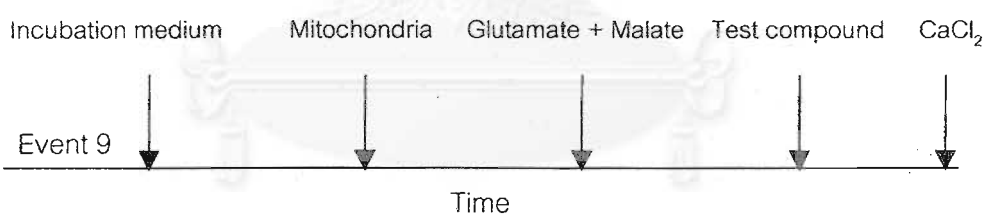

5. MAO activity

MAO activity was determined by measurements of oxygen consumption with the method of Tipton and Singer (1993). Oxygen consumption by mitochondria was measured polarographically with a Clark Oxygen Electrode connected with YSI model 5300 Biological Oxygen Monitor. Initial velocity of MAO catalyzes the oxidative of substrate was showed by oxygen consumption rate. The assay mixture consisted of potassium phosphate buffer, adjusted to pH 7.4 and mitochondria. The reaction was started by addition of MAO substrate: 100 µM tyramine HCl as a substrate for MAO-A

and B, 100 μM benzylamine HCl as a substrate for MAO-B and 100 μM 5-hydroxytryptamine as a substrate for MAO-A.

Calculation of rates of oxygen consumption

Initial velocity of MAO catalyzes the oxidative of substrate was showed by oxygen consumption rate that can be calculated from oxygraph tracing as shown in Figure 15

$$\text{Rate of oxygen consumption before the addition of substrate (X)} = \frac{Q \times S}{P} \text{ n atoms O/min}$$

$$\text{Rate of oxygen consumption after the addition of substrate (Y)} = \frac{R \times S}{P} \text{ n atoms O/min}$$

$$\text{Oxygen consumption rate in the reaction} = Y - X \text{ n atoms O/min}$$

Where Q, R and P = the length of oxygen line Q, R and P respectively

S = n atoms oxygen initially dissolved in the reaction mixture

A = n atoms oxygen dissolved in 1 ml of water

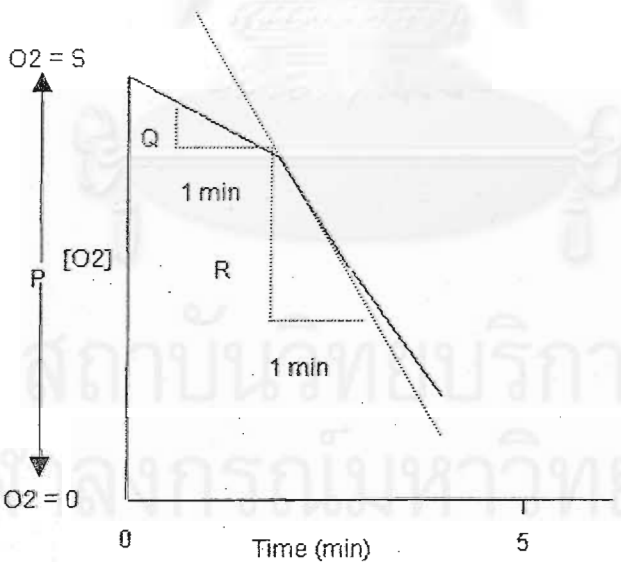

Figure 15. The oxygraph tracing illustrating the measurement of oxygen consumption for MAO activity

Experimental protocol of MAO activity

1. Effect of test compounds (Cu 18-14 and Cu 18-15) on MAO-A activity.

    1) Substrate of MAO-A was 100 μM 5-hydroxytryptamine was added.

2) The tested compounds (Cu 18-14 and Cu 18-15) in various concentrations were added.

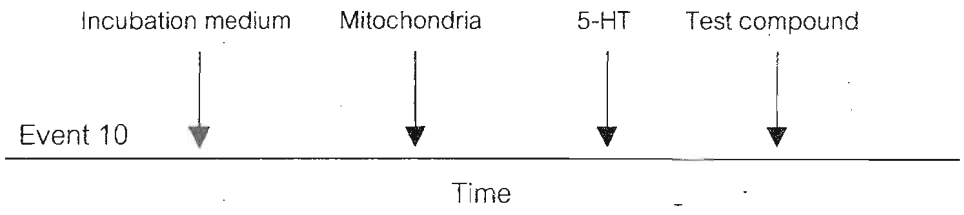

2. Effect of test compounds (Cu 18-14 and Cu 18-15) on MAO-B activity.

1) Substrate of MAO-B was 100 μM benzylamine HCl was added.

2) The tested compounds (Cu 18-14 and Cu 18-15) in various concentrations were added.

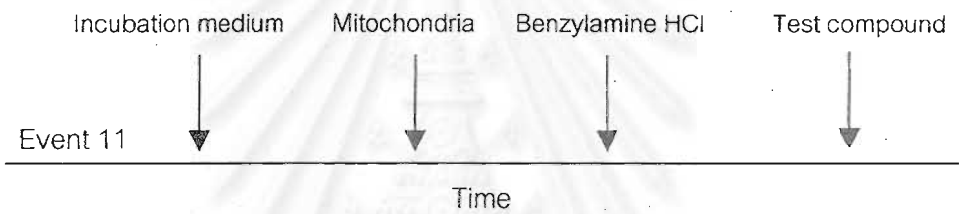

3. Effect of test compounds (Cu 18-14 and Cu 18-15) on MAO-A&B activity.

1) Substrate of MAO-A was 100 μM tyramine HCl was added.

2) The tested compounds (Cu 18-14 and Cu 18-15) in various concentrations were added.

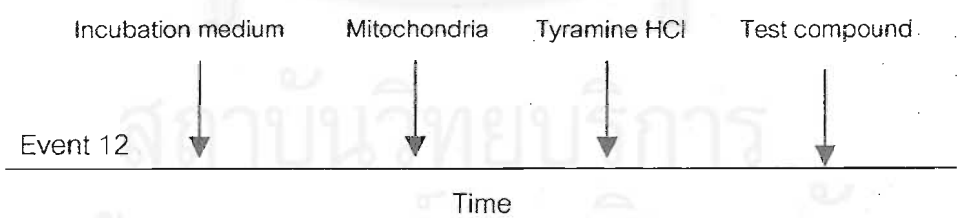

6. Protein determination

The mitochondrial protein was determined by the method of Lowry et al. (1951) as modified by Miller (1959) as following

1. Diluted of 10 μl mitochondrial suspension with 3 ml of ultrapure water (1: 300) as solution A.

2. 1 ml of alkaline copper reagent (consist of one part of 0.5% copper sulfate in 1 % potassium tartrate and 10 parts of 10% sodium carbonate in 0.5 N sodium hydroxide and discard after 1 day) was added into 1 ml aliquot of the solution A.
3. The standard protein solution was prepared from Bovine Serum Albumin (BSA) at various concentrations: 0.05, 0.10, 0.15, 0.20, -0.25 and 0.30 mg/ml and ultrapure water was used as the blank.
4. Mixed well and allowed to stand for 10 minutes or longer at room temperature as solution B.
5. 3 ml of diluted Folin & Ciocalteu's phenol reagent (1: 10) were added to solution B, mixed on a Vortex mixer and incubated in water bath at 50^{0}c for 10 minutes. The mixtures were cooled to room temperature.
6. After 30 minutes or longer, the sample was measured the optical density at 540 ηm with an UV-Visible recording spectrophotometer at room temperature and was calculated from a standard curve of BSA.

Annotation:

1) Alkaline copper reagent composed of 1 part of 0.5% $CuSo_4$ in 1% w/v of potassium tartrate and 10 parts of 10% Na_2CO_3 in 0.5 M NaOH.
2) 1:10 diluted Folin-phenol reagent was freshly prepared by diluting 1 part of concentrated Folin-Ciocalteu's Phenol reagent with 10 parts of ultrapure water

7. Data analysis

1. ANOVA test was used to evaluate statistical significance of mean differences between control and tested compound-treated group.
2. A p value of 0.05 or less was considered statistically significant.
3. The value of each condition was obtained from at least 3 experiments and given as mean ± standard error.

CHAPTER IV

RESULTS

Part I: Effects of CU 18-14 and CU 18-15 on oxidative phosphorylation of isolated rat liver mitochondria.

In this study, rat liver mitochondria preparation was suspended in an incubation medium pH 7.4 and the temperature was maintained at 37°C.

1. **Effects of CU 18-14 and CU 18-15 on mitochondrial respiration with glutamate plus malate as substrates.**

Figure 16 illustrated the control respiratory response of the isolated rat liver mitochondria and shown value of rate of oxygen consumption with glutamate plus malate as substrates on every state was n atom O/min/mg protein. In the initial rate of oxygen consumption was 0.36 n atoms O/min/mg protein. Addition of ADP causes a sudden burst of oxygen uptake as the ADP is converted into ATP. The activity respiring state is referred to as "State 3" respiration that the value of rate of oxygen consumption was 2.78 n atoms O/min/mg protein. While the slower rate after all the ADP has been phosphorylated to form ATP is referred to as "State 4" respiration that value of rate of oxygen consumption was 0.38 n atoms O/min/mg protein. The addition of an uncoupling agent, which DNP leads to a permanently high rate of respiration in the absence of ADP, until all the oxygen has been consumed which value of rate of oxygen consumption was 4.97 n atoms O/min/mg protein. Functional integrity of the mitochondria was measured in terms of respiratory control index (RCI), defined as the ratio of the rate of State 3/State 4. In Figure 16, RCI was 13.2/1.8 = 7.33 indicating the mitochondria used were the good intact ones.

The tracings demonstrating the effect of CU 18-14 on mitochondrial oxygen consumption with glutamate plus malate as substrates are shown in Figure 17, which was determined by the addition of glutamate plus malate as substrates into the reaction mixture (containing incubation medium and mitochondrial suspension) then followed by the addition of tested compounds and ADP plus Pi, respectively. The values of the rate of oxygen consumption of State 3 and State 4 were calculated from the slope of oxygraph

tracing (Table 1). In Figure 18 shown the tracings of CU 18-15 at each of concentrations with similar to determined in study of CU 18-15. The effects of state 4 respiration by CU 18-14 and CU 18-15 are presented in Figure 19.

The rate of oxygen consumption of State 3 respiration with glutamate plus malate as substrates by CU 18-14 at concentrations of 1.01×10^{-6} M and 1.01×10^{-5} M were 1.96 $\pm$ 0.20 and 1.93 $\pm$ 0.16 n atoms O/min/mg protein, respectively, but not found the rate of oxygen consumption at concentration 1.01×10^{-4} M, 2.02×10^{-4} M, 3.04×10^{-4} M and 4.05×10^{-4} M (Table 1).

The rate of oxygen consumption of State 3 respiration with glutamate plus malate as substrates by CU 18-15 at concentrations of 1.01×10^{-6} M and 1.01×10^{-5} M were 1.54 $\pm$ 0.05 and 1.29 $\pm$ 0.05 n atoms O/min/mg protein, respectively, but not found the rate of oxygen consumption at concentration 1.01×10^{-4} M, 2.02×10^{-4} M, 3.04×10^{-4} M and 4.05×10^{-4} M (Table 1).

The rate of oxygen consumption of State 4 respiration with glutamate plus malate as substrates by CU 18-14 at concentrations of 1.01×10^{-6} M, 1.01×10^{-5} M, 1.01×10^{-4} M, 2.02×10^{-4} M, 3.04×10^{-4} M and 4.05×10^{-4} M were 0.40 $\pm$ 0.03, 0.65 $\pm$ 0.06, 1.80 $\pm$ 0.32, 1.52 $\pm$ 0.09, 1.38 $\pm$ 0.09 and 0.72 $\pm$ 0.09 n atoms O/min/mg protein, respectively (Table 1).

The rate of oxygen consumption of State 4 respiration with glutamate plus malate as substrates by CU 18-15 at concentrations of 1.01×10^{-6} M, 1.01×10^{-5} M, 1.01×10^{-4} M, 2.02×10^{-4} M, 3.04×10^{-4} M and 4.05×10^{-4} M were 0.61 $\pm$ 0.04, 0.89 $\pm$ 0.05, 1.44 $\pm$ 0.39, 1.13 $\pm$ 0.34, 1.12 $\pm$ 0.10 and 1.11 $\pm$ 0.07 n atoms O/min/mg protein, respectively (Table 1).

2. **Effects of CU 18-14 and CU 18-15 on mitochondrial respiration with succinate as substrate.**

It is well know that glutamate plus malate donate electrons to mitochondrial respiratory chain via complex I. In the present study, succinate which donates electrons to CoQ via complex II was used as substrate. Figure 20 illustrates the control respiratory response of the isolated rat liver mitochondria and shown value of rate of oxygen consumption with succinate as substrates on every state was n atom O/min/mg protein. In the initial rate of oxygen consumption was 0.673 n atom O/min/mg protein and was faster

than the initial rate of mitochondrial respiration with glutamate plus malate as substrates. Addition of ADP causes a sudden burst of oxygen uptake as the ADP is converted into ATP. The activity respiring state is referred to as "State 3" respiration that the value of rate of oxygen consumption was 3.447 n atoms O/min/mg protein. While the slower rate after all the ADP has been phosphorylated to form ATP is referred to as "State 4" respiration that value of rate of oxygen consumption was 0.652 n atoms O/min/mg protein. The addition of an uncoupling agent, which DNP leads to a permanently high rate of respiration in the absence of ADP, until all the oxygen has been consumed which value of rate of oxygen consumption was 4.540 n atoms O/min/mg protein. Functional integrity of the mitochondria was measured in terms of respiratory control index (RCI), defined as the ratio of the rate of State 3/State 4. In Figure 16, RCI was 16.4/3.1 = 5.29 indicating the mitochondria used were the good intact ones.

Figure 21 and 22 are presents the tracings demonstrating the effect of CU 18-14 and CU 18-15 on mitochondrial respiration with succinate as substrate, respectively, which was determined by the addition of succinate into reaction mixture (containing incubation medium and mitochondrial suspension) then followed by the addition of tested compounds and ADP plus Pi, respectively. The value of the rate of oxygen consumption of State 3 and State 4 respiration was calculated from the slope of oxygraph tracing (Table 2).

The rate of oxygen consumption of State 3 respiration with succinate as substrate by CU 18-14 at concentrations of 1.01×10^{-6} M and 1.01×10^{-5} M were 0.49 ± 0.11 and 0.50 ± 0.07 n atoms O/min/mg protein, respectively, but not found the rate of oxygen consumption at concentration 1.01×10^{-4} M, 2.02×10^{-4} M, 3.04×10^{-4} M and 4.05×10^{-4} M (Table 2).

The rate of oxygen consumption of State 3 respiration with succinate as substrate by CU 18-15 at concentrations of 1.01×10^{-6} M and 1.01×10^{-5} M were 0.82 ± 0.05 and 0.82 ± 0.13 n atoms O/min/mg protein, respectively, but not found the rate of oxygen consumption at concentration 1.01×10^{-4} M, 2.02×10^{-4} M, 3.04×10^{-4} M and 4.05×10^{-4} M (Table 2).

The rate of oxygen consumption of State 4 respiration with succinate as substrate by CU 18-14 at concentrations of 1.01×10^{-6} M, 1.01×10^{-5} M, 1.01×10^{-4} M, 2.02×10^{-4} M, 3.04×10^{-4} M and 4.05×10^{-4} M were 1.66 ± 0.57, 1.50 ± 0.29, 1.79 ± 0.48, 1.18 ± 0.52, 0.76 ± 0.34 and 0.69 ± 0.26 n atoms O/min/mg protein, respectively (Table 2).

The rate of oxygen consumption of State 4 respiration with succinate as substrate by CU 18-15 at concentrations of $1.01x10^{-6}$ M, $1.01x10^{-5}$ M, $1.01x10^{-4}$ M, $2.02x10^{-4}$ M, $3.04x10^{-4}$ M and $4.05x10^{-4}$ M were 3.18 ± 0.18, 3.16 ± 0.01, 1.20 ± 0.34, 1.08 ± 0.54, 0.83 ± 0.39 and 0.60 ± 0.21 n atoms O/min/mg protein, respectively (Table 2).

3. **Effects of CU 18-14 and CU 18-15 on DNP stimulated mitochondrial respiration with glutamate plus malate as substrates.**

The rate of oxygen consumption of DNP stimulated mitochondrial respiration with glutamate plus malate as substrate was studied by the addition of DNP and then followed by the addition of tested compounds. The effect of tested compounds on DNP stimulated respiration was referred to as State 3u respiration which was calculated from the slope of the oxygraph tracing (Figure 24 and 25) and expressed as percent inhibition (see Table 3 and Figure 26). In this result was the percent inhibition of State 3u respiration by CU 18-14 at concentrations of $1.01x10^{-6}$ M, $1.01x10^{-5}$ M, $1.01x10^{-4}$ M, $2.02x10^{-4}$ M, $3.04x10^{-4}$ M and $4.05x10^{-4}$ M were 7.16 ± 3.15, 22.14 ± 3.19, 78.14 ± 7.90, 91.81 ± 2.24, 93.84 ± 1.35 and 94.15 ± 1.46, respectively as shown in Table 3.

The percent inhibition of DNP stimulated mitochondrial respiration with glutamate plus malate as substrates by CU 18-15 at concentrations of $1.01x10^{-6}$ M, $1.01x10^{-5}$ M, $1.01x10^{-4}$ M, $3.04x10^{-4}$ M and $4.05x10^{-4}$ M respectively, were 12.76 ± 9.66, 44.46 ± 5.76, 78.01 ± 1.07, 88.95 ± 1.39, 94.27 ± 1.23 and 94.89 ± 0.24, respectively as shown in Table 3.

The IC_{50} values in the DNP stimulated respiration of CU 18-14 and CU 18-15 were 2.15×10^{-5} M and 1.32×10^{-5} M respectively (Table 4).

Part II: Effects of CU 18-14 and CU 18-15 on ATPase activity of isolated rat liver mitochondria.

The ATPase reaction is generally believed to represent the reversed process of the ATPase reaction. Agents which inhibit ATP synthesis, for example oligomycin, depress the uncoupler induced ATPase activity. The ATPase activity was expressed in according to inorganic phosphate (Pi) liberated concentration from ATP hydrolysis at 10 minutes. The effect of tested compounds on mitochondrial ATPase activity of isolated rat liver mitochondria is shown in Table 5.

In Figure 27 the present of DMSO, the control ATPase activity was very low, which Pi liberated was 4.98 ± 0.19 μmoles/mg protein/10 min. When 0.1 mM DNP was added the ATPase activity greatly increased significantly which Pi liberated was 52.08 ± 8.60 μ moles/mg protein/10 min. In this study the concentration of tested compounds was studied at $1.01x10^{-4}$ M and $3.04x10^{-4}$ M.

The Pi liberated concentration in the addition of CU 18-14 at concentrations of $1.01x10^{-4}$ M and $3.04x10^{-4}$ M were 14.44 ± 2.93 and 44.13 ± 3.13, respectively. When in addition of $3.04x10^{-4}$ M CU 18-14 and then followed by the addition of oligomycin was found that the Pi liberated concentration was 6.33 ± 0.10 (Table 5).

As a result of the Pi liberated concentration in the addition of CU 18-15 at concentrations of $1.01x10^{-4}$ M and $3.04x10^{-4}$ M were 8.36 ± 1.34 and 16.12 ± 1.50, respectively. When in addition of $3.04x10^{-4}$ M CU 18-15 after 1minute then followed by the addition of oligomycin was found that the Pi liberated concentration was 4.89 ± 0.11 (Table 5).

Part III: Effects of CU 18-14 and CU 18-15 on calcium stimulated respiration by isolated rat liver mitochondria.

Another the function of mitochondria is the ability in accumulating calcium ions. When electron from oxidation substrate transfer and moving along electron transport chain or ATP hydrolysis generates a proton gradient, mitochondrial take up Ca^{+2} from the external medium. As a consequence in addition of Ca^{+2} to a suspension of energized mitochondria results in the stimulation of respiration, the extrusion of protons and the uptake of Ca^{+2} into the mitochondria (Chakraborti et al., 1999). The Effect of CU 18-14 and CU 18-15 on calcium stimulated respiration with glutamate plus malate as substrates are shown in Figure 28, which were determined by the addition of tested compounds into the reaction mixture (containing incubation medium and mitochondrial suspension) then followed by the addition of $CaCl_2$. The result was showed in oxygraph tracing and expressed as the rate of oxygen consumption. The rate of oxygen consumption of mitochondria after the addition of CU 18-14 at concentrations of $1.01x10^{-6}$ M, $1.01x10^{-5}$ M, $1.01x10^{-4}$ M, $3.04x10^{-4}$ M and $4.05x10^{-4}$ M respectively, were 2.78 ± 0.37, 2.32 ± 0.37, 2.34 ± 0.27, 0.98 ± 0.22, 0.32 ± 0.08 and 0.31 ± 0.08 n atoms O/min/mg protein, respectively as shown in Table 6.

The rate of oxygen consumption of CU 18-15 at concentrations of $1.01x10^{-6}$ M, $1.01x10^{-5}$ M, $1.01x10^{-4}$ M, $3.04x10^{-4}$ M and $4.05x10^{-4}$ M respectively, were 2.80 ± 0.22, 2.39 ± 0.24, 1.18 ± 0.19, 0.67 ± 0.15, 0.43 ± 0.06 and 0.39 ± 0.05 n atoms O/min/mg protein, respectively as shown in Table 6.

Part IV: Effects of CU 18-14 and CU 18-15 on monoamine oxidase activity of isolated rat liver mitochondria.

The inhibitory effect of tested compounds on MAO activity towards different MAO substrate were studied by using 100 μM of tyramine (as a non-selective MAO substrate), 100 μM of 5-HT (as a selective MAO-A substrate) and 100 μM of benzylamine (as a selective MAO-B substrate). The concentrations of tested compounds were varied from $1.01x10^{-6}$ M to $4.05x10^{-4}$ M. MAO inhibitory effect of tested compounds were determined by the addition of tested compounds into reaction mixture (containing phosphate buffer and mitochondrial suspension) then followed by the addition of MAO substrate. The degree of inhibition of MAO substrate oxidation deamination was expressed as percent MAO activity inhibition (see Table 7). As shown in Figure 29 and 30, both of CU 18-14 and CU 18-15 inhibited the oxidative deamination of tyramine, benzylamine and 5-HT and were concentration-dependent.

The percent MAO activity inhibition on tyramine as substrate of CU 18-14 at concentrations of $1.01x10^{-6}$ M, $1.01x10^{-5}$ M, $1.01x10^{-4}$ M, $3.04x10^{-4}$ M and $4.05x10^{-4}$ M respectively, were 31.67 ± 0.14, 42.39 ± 6.38, 56.13 ± 9.71, 74.17 ± 5.83, 95.56 ± 4.44 and 95.83 ± 4.17, respectively (Table 7).

The percent MAO activity inhibition on 5-HT as substrate of CU 18-14 at concentrations of $1.01x10^{-6}$ M, $1.01x10^{-5}$ M, $1.01x10^{-4}$ M, $3.04x10^{-4}$ M and $4.05x10^{-4}$ M respectively, were 74.09 ± 5.64, 74.28 ± 6.38, 90.89 ± 2.37, 89.62 ± 3.37, 98.78 ± 3.61 and 99.07 ± 0.93, respectively (Table 7).

The percent MAO activity inhibition on benzylamine as substrate of CU 18-14 at concentrations of $1.01x10^{-6}$ M, $1.01x10^{-5}$ M, $1.01x10^{-4}$ M, $3.04x10^{-4}$ M and $4.05x10^{-4}$ M respectively, were 57.12 ± 5.88, 59.74 ± 7.11, 73.07 ± 4.99, 99.04 ± 0.96, 100 ± 0.00 and 100 ± 0.00, respectively (Table 7).

The percent MAO activity inhibition on tyramine as substrate of CU 18-15 at concentrations of $1.01x10^{-6}$ M, $1.01x10^{-5}$ M, $1.01x10^{-4}$ M, $3.04x10^{-4}$ M and $4.05x10^{-4}$ M respectively, were 30.52 ± 1.77, 40.43 ± 2.20, 70.45 ± 7.64, 72.15 ± 0.36, 78.89 ± 9.53 and 90.48 ± 1.66, respectively (Table 7).

The percent MAO activity inhibition on 5-HT as substrate of CU 18-15 at concentrations of $1.01x10^{-6}$ M, $1.01x10^{-5}$ M, $1.01x10^{-4}$ M, $3.04x10^{-4}$ M and $4.05x10^{-4}$ M respectively, were 68.01 ± 8.11, 68.27 ± 7.11, 82.95 ± 7.64, 90.36 ± 6.74, 96.88 ± 3.13 and 99.38 ± 4.61, respectively (Table 7).

The percent MAO activity inhibition on benzylamine as substrate of CU 18-15 at concentrations of $1.01x10^{-6}$ M, $1.01x10^{-5}$ M, $1.01x10^{-4}$ M, $3.04x10^{-4}$ M and $4.05x10^{-4}$ M respectively, were 66.97 ± 5.82, 68.37 ± 7.56, 88.70 ± 7.19, 100 ± 0.00, 100 ± 0.00 and 100 ± 0.00, respectively (Table 7).

In this study, it was found that the IC_{50} on tyramine, 5-HT and benzylamine as substrates of CU 18-14 were $9.66x10^{-6}$ M, $6.30x10^{-7}$ M and $1.44x10^{-2}$ M, respectively and of CU 18-15 were $1.18x10^{-5}$ M, $2.60x10^{-4}$ M and $7.96x10^{-3}$ M, respectively (Table 8).

Control respiratory response with glutamate plus malate on isolated rat liver mitochondria.

Figure 16.

The oxygraph tracing demonstrating the control respiratory response with glutamate plus malate as substrates on isolated rat liver mitochondria. The reaction composed of 37.50 mM HEPES buffer pH 7.4, 1.88 mM $MgCl_2$, 86.25 mM KCl, 5.21 mM glutamate + 5.21 mM malate, 0.31 mM ADP + 0.62 mM Pi, 0.05 mM DNP, 13.02 mM sucrose and 50 μl of mitochondrial suspension, and maintained at 37^0c. The total volume was 1.77 ml and the average protein concentration of the reaction was 13.30 mg/ml. Every State was calculated as n atom O/min/mg protein.

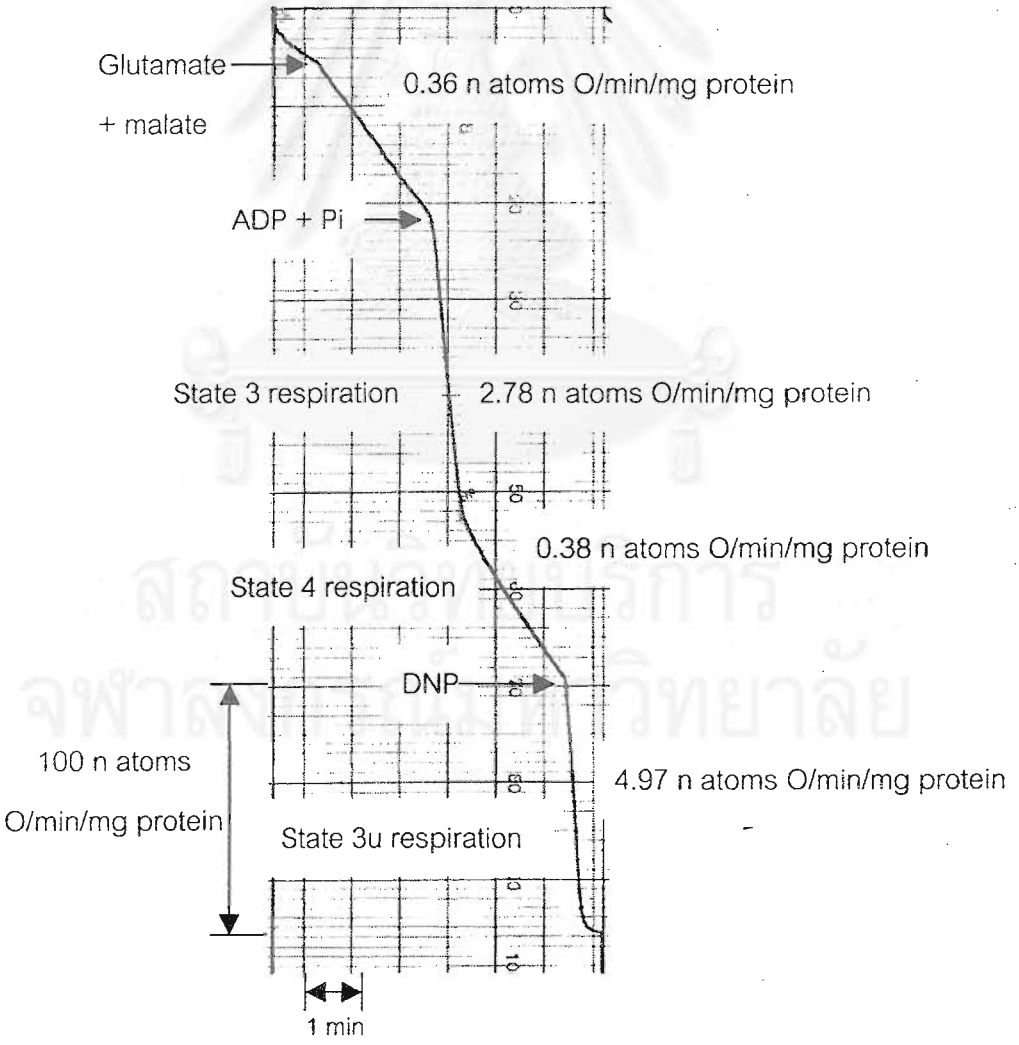

Effect of mitochondrial respiration with glutamate plus malate as substrates by CU 18-14

Figure 17.

The oxygraph tracings demonstrating the effect of CU 18-14 at concentration 1.01 $\times 10^{-6}$ M to 4.05 $\times 10^{-4}$ M on mitochondrial oxygen consumption with glutamate plus malate as substrates. Every State was calculated as n atom O/min/mg protein. The reaction composed of 37.50 mM HEPES buffer pH 7.4, 1.88 mM $MgCl_2$, 86.25 mM KCl, 5.21 mM glutamate + 5.21 mM malate, 0.31 mM ADP + 0.62 mM Pi, 13.02 mM sucrose and 50 µl of mitochondrial suspension, and maintained at 37^0c. The total volume was 1.77 ml and the average protein concentration of the reaction was 13.30 mg/ml.

Annotation: A was oxygraph tracing of CU 18-14 at concentration 1.01 $\times 10^{-6}$ M

B was oxygraph tracing of CU 18-14 at concentration 1.01 $\times 10^{-5}$ M

C was oxygraph tracing of CU 18-14 at concentration 1.01 $\times 10^{-4}$ M

D was oxygraph tracing of CU 18-14 at concentration 2.02 $\times 10^{-4}$ M

E was oxygraph tracing of CU 18-14 at concentration 3.04 $\times 10^{-4}$ M

F was oxygraph tracing of CU 18-14 at concentration 4.05 $\times 10^{-4}$ M

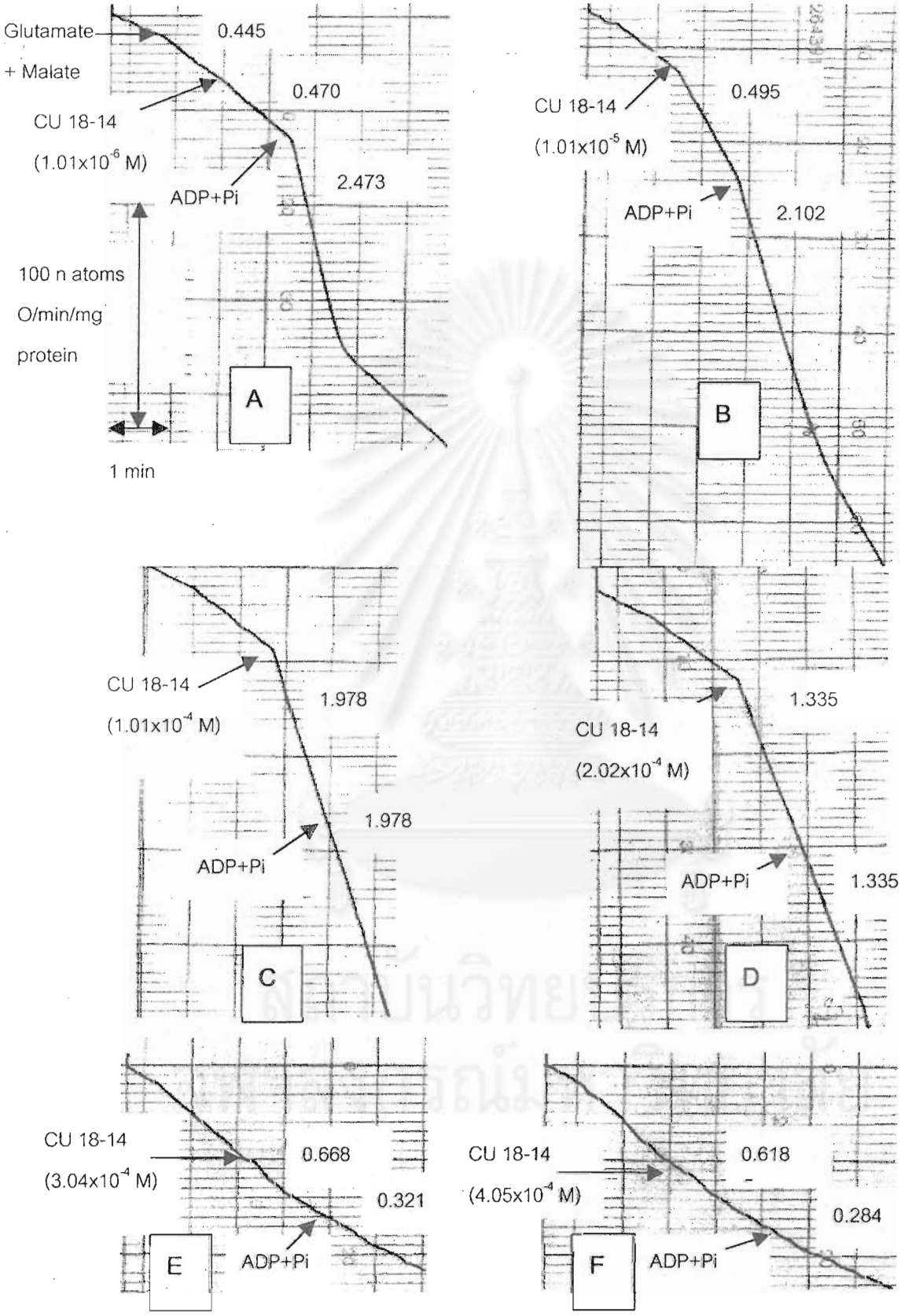

Figure 17. The oxygraph tracing demonstrating the effect of CU 18-14 on mitochondrial oxygen consumption with glutamate plus malate as substrates

Effect of mitochondrial respiration with glutamate plus malate as substrates by CU 18-15

Figure 18.

The oxygraph tracings demonstrating the effect of CU 18-15 at concentration 1.01×10^{-6} M to 4.05×10^{-4} M on mitochondrial oxygen consumption with glutamate plus malate as substrates. Every State was calculated as n atom O/min/mg protein. The reaction composed of 37.50 mM HEPES buffer pH 7.4, 1.88 mM $MgCl_2$, 86.25 mM KCl, 5.21 mM glutamate + 5.21 mM malate, 0.31 mM ADP + 0.62 mM Pi, 13.02 mM sucrose and 50 µl of mitochondrial suspension, and maintained at 37^0c. The total volume was 1.77 ml and the average protein concentration of the reaction was 13.87 mg/ml.

Annotation: A was oxygraph tracing of CU 18-15 at concentration 1.01×10^{-6} M

B was oxygraph tracing of CU 18-15 at concentration 1.01×10^{-5} M

C was oxygraph tracing of CU 18-15 at concentration 1.01×10^{-4} M

D was oxygraph tracing of CU 18-15 at concentration 2.02×10^{-4} M

E was oxygraph tracing of CU 18-15 at concentration 3.04×10^{-4} M

F was oxygraph tracing of CU 18-15 at concentration 4.05×10^{-4} M

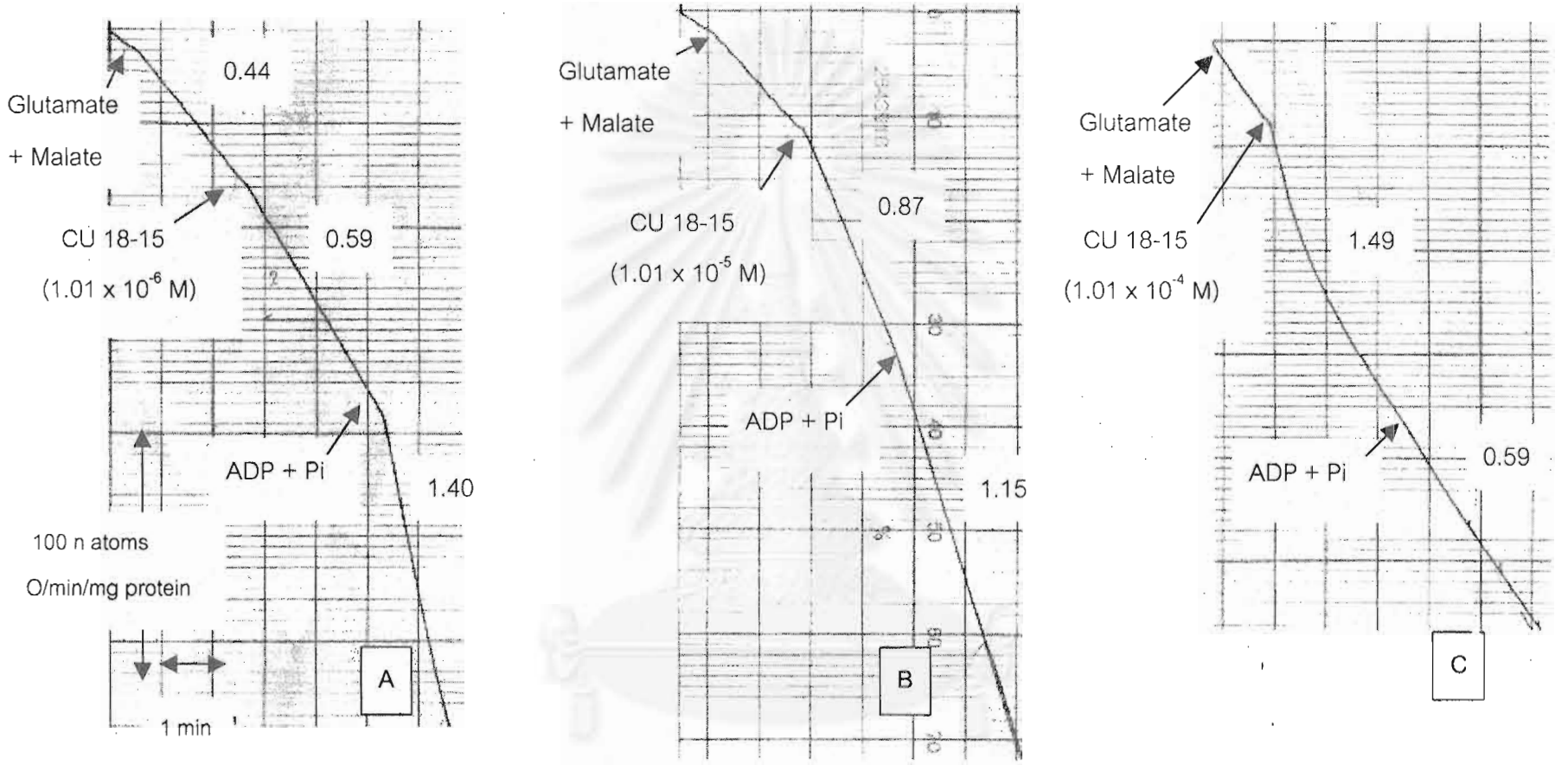

Figure 18. The oxygraph tracing demonstrating the effect of CU 18-15 on mitochondrial oxygen consumption with glutamate plus malate as substrates.

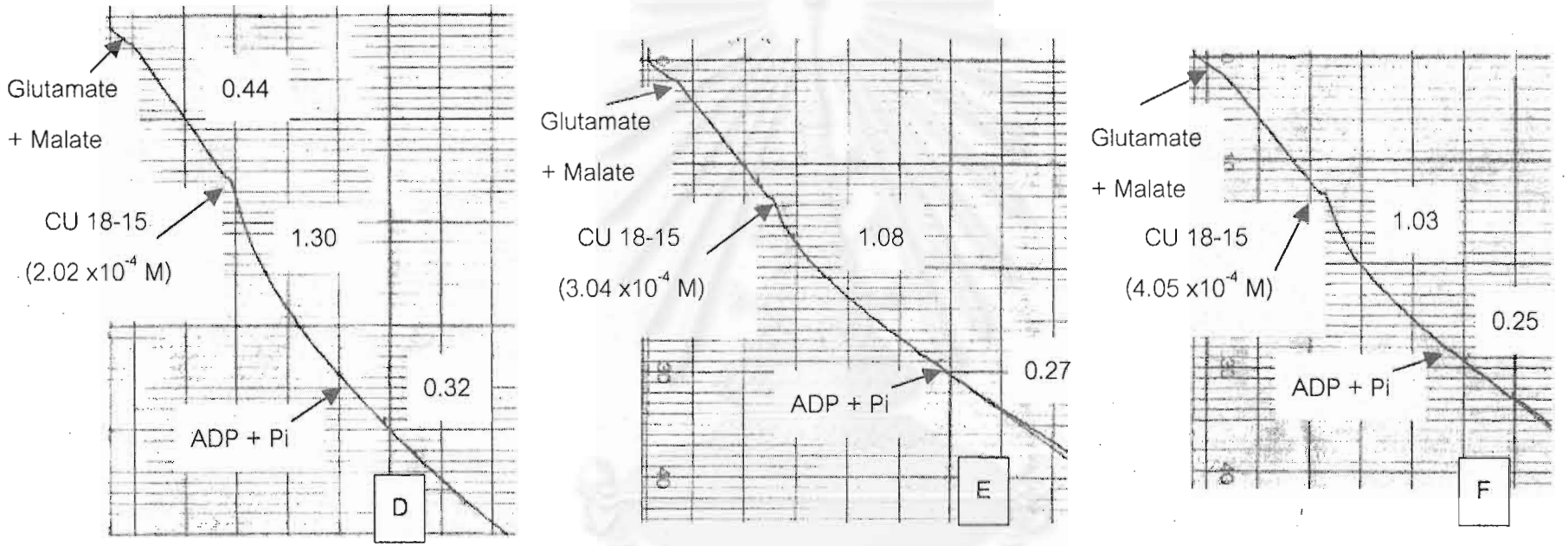

Figure 18 (continued). The oxygraph tracing demonstrating the effect of CU 18-15 on mitochondrial oxygen consumption with glutamate plus malate as substrates.

Figure 19.

The rate of oxygen consumption of State 4 respiration by CU 18-14 and CU 18-15 with glutamate plus malate as substrates on isolated rat liver mitochondria. The reaction composed of 37.50 mM HEPES buffer pH 7.4, 1.88 mM $MgCl_2$, 86.25 mM KCl, 5.21 mM glutamate + 5.21 mM malate, 0.31 mM ADP + 0.62 mM Pi, 13.02 mM sucrose and 50 µl of mitochondrial suspension, and maintained at 37^0c. Control group using 10 µl of DMSO. The total reaction was 1.77 ml and the average protein concentration of the reaction by CU 18-14 and CU 18-15 was 13.30 and 13.87 mg/ml, respectively. Each point was the mean ± S.E. of n = 4.

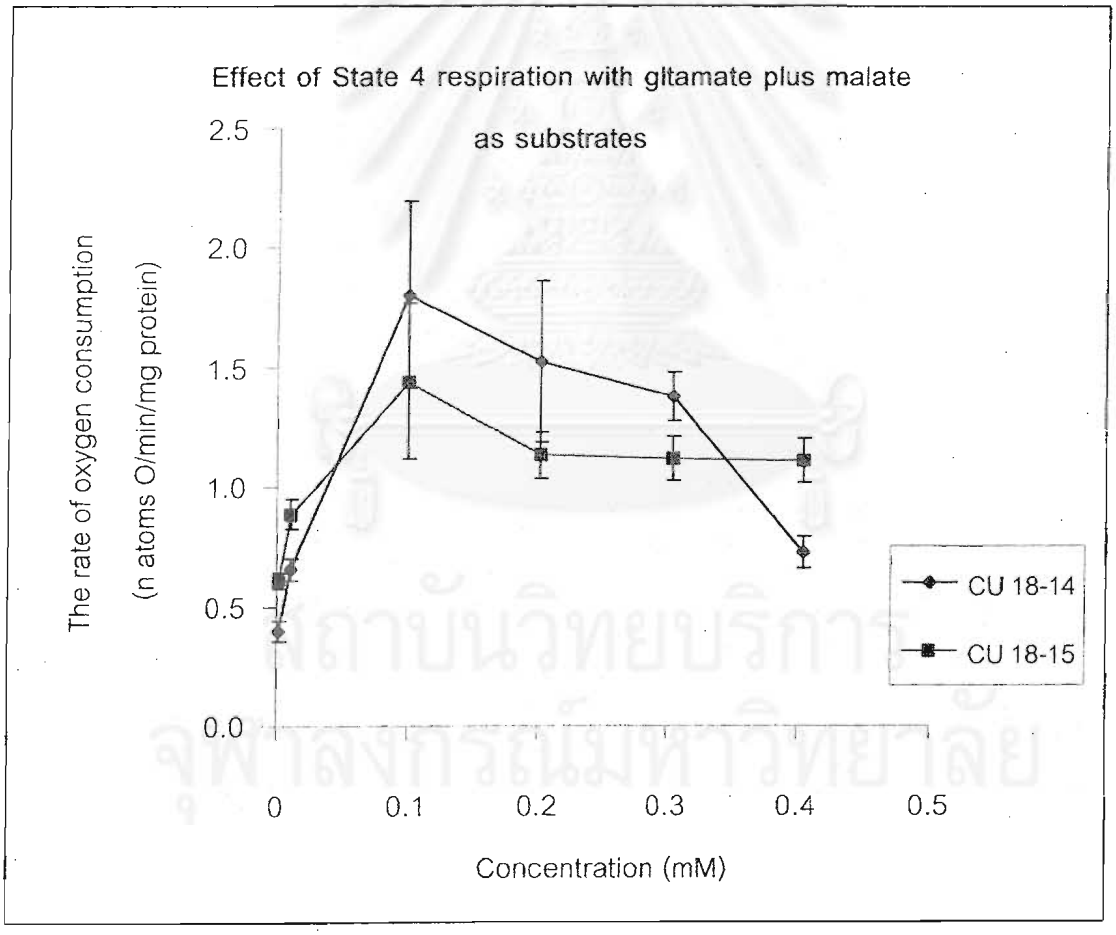

Table 1.

The rate of oxygen consumption of State 3 and State 4 respiration with glutamate plus malate as substrates on isolated rat liver mitochondria by CU 18-14 and CU 18-15. Each value was mean ± S.E. of n = 4.

Concentration of compounds (Molar)	The rate of Oxygen Consumption (n atom O/min/mg protein)			
	State 3 respiration		State 4 respiration	
	CU 18-14	CU 18-15	CU 18-14	CU 18-15
1.01×10^{-6}	1.96±0.20	1.54±0.05	0.40 ± 0.03	0.61 ± 0.04
1.01×10^{-5}	1.93±0.16	1.29±0.05	0.65 ± 0.06	0.89 ± 0.05
1.01×10^{-4}	Not found	Not found	1.80 ± 0.32	1.44 ± 0.39
2.02×10^{-4}	Not found	Not found	1.52 ± 0.09	1.13 ± 0.34
3.04×10^{-4}	Not found	Not found	1.38 ± 0.09	1.12 ± 0.10
4.05×10^{-4}	Not found	Not found	0.72 ± 0.09	1.11 ± 0.07

Control respiratory response with succinate on isolated rat liver mitochondria.

Figure 20.

The oxygraph tracing demonstrating the control respiratory response with succinate as substrates on isolated rat liver mitochondria. The reaction composed of 37.50 mM HEPES buffer pH 7.4, 1.88 mM $MgCl_2$, 86.25 mM KCl, 5.21 mM succinate, 0.31 mM ADP + 0.62 mM Pi, 13.02 mM sucrose and 50 µl of mitochondrial suspension, and maintained at 37^0c. The total volume was 1.77 ml and the average protein concentration of the reaction was 20.45 mg/ml. Every State was calculated as n atom O/min/mg protein.

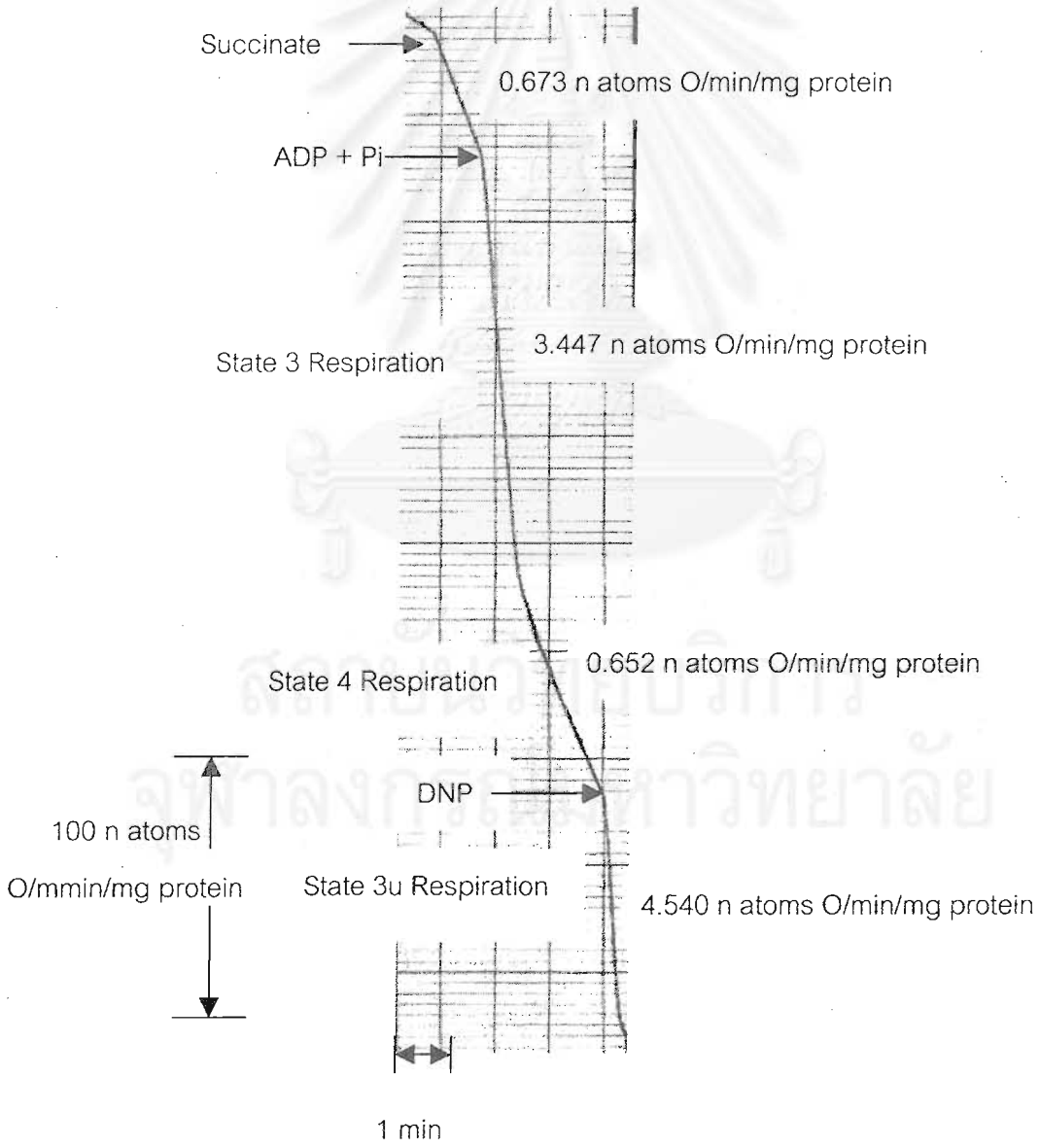

Effect of mitochondrial respiration with succinate as substrate by CU 18-14

Figure 21.

The oxygraph tracings demonstrating the effect of CU 18-14 at concentration 1.01×10^{-6} M to 4.05×10^{-4} M on mitochondrial oxygen consumption with succinate as substrate. Every State was calculated as n atom O/min/mg protein. The reaction composed of 37.50 mM HEPES buffer pH 7.4, 1.88 mM $MgCl_2$, 86.25 mM KCl, 5.21 mM succinate, 0.31 mM ADP + 0.62 mM Pi, 13.02 mM sucrose and 50 µl of mitochondrial suspension, and maintained at 37^0c. The total volume was 1.77 ml and the average protein concentration of the reaction was 20.45 mg/ml.

Annotation: A was oxygraph tracing of CU 18-14 at concentration 1.01×10^{-6} M

B was oxygraph tracing of CU 18-14 at concentration 1.01×10^{-5} M

C was oxygraph tracing of CU 18-14 at concentration 1.01×10^{-4} M

D was oxygraph tracing of CU 18-14 at concentration 2.02×10^{-4} M

E was oxygraph tracing of CU 18-14 at concentration 3.04×10^{-4} M

F was oxygraph tracing of CU 18-14 at concentration 4.05×10^{-4} M

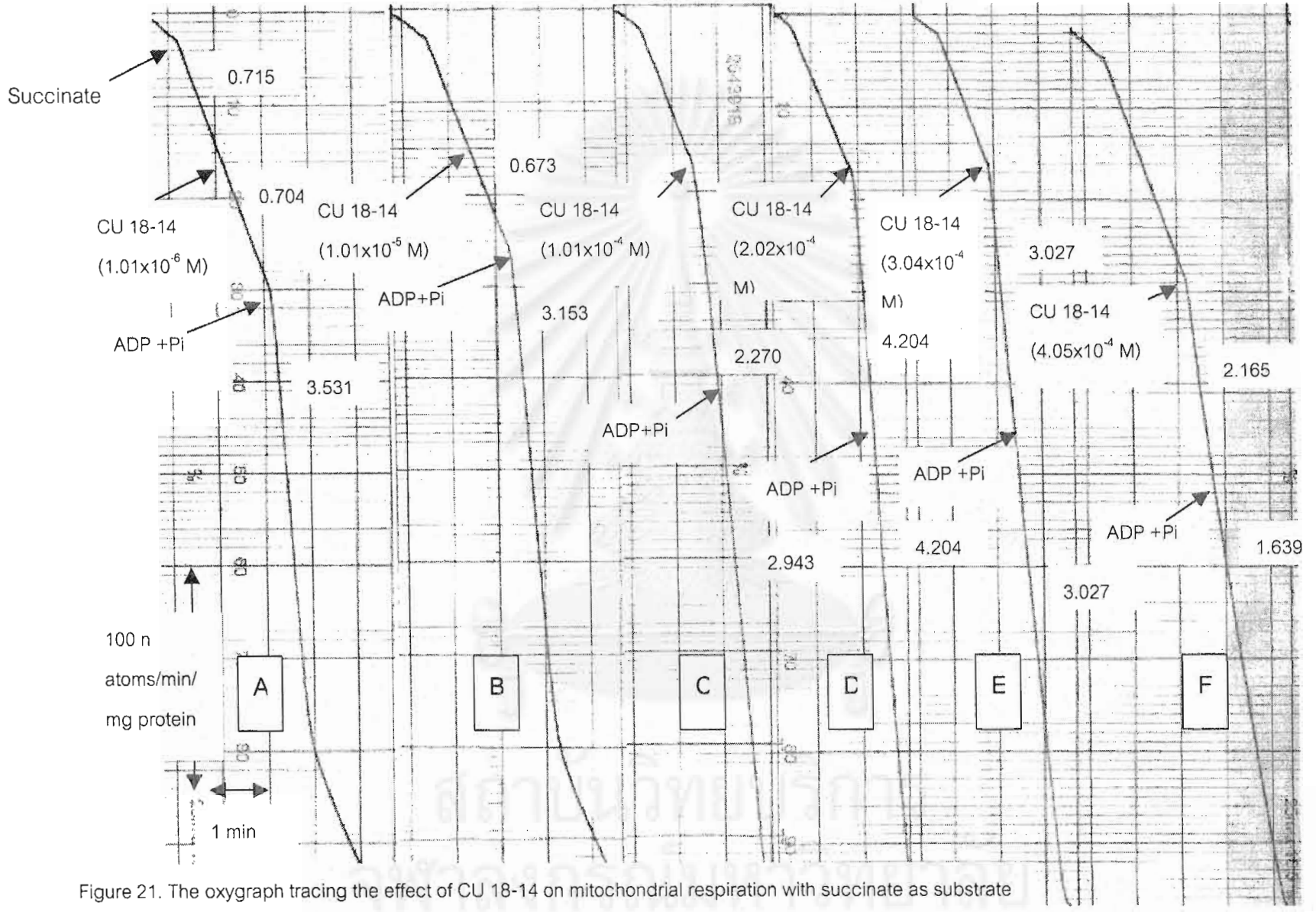

Figure 21. The oxygraph tracing the effect of CU 18-14 on mitochondrial respiration with succinate as substrate

Effect of mitochondrial respiration with succinate as substrate by CU 18-15

Figure 22.

The oxygraph tracings demonstrating the effect of CU 18-15 at concentration 1.01×10^{-6} M to 4.05×10^{-4} M on mitochondrial oxygen consumption with succinate as substrate. Every State was calculated as n atom O/min/mg protein. The reaction composed of 37.50 mM HEPES buffer pH 7.4, 1.88 mM $MgCl_2$, 86.25 mM KCl, 5.21 mM succinate, 0.31 mM ADP + 0.62 mM Pi, 13.02 mM sucrose and 50 µl of mitochondrial suspension, and maintained at 37^0C. The total volume was 1.77 ml and the average protein concentration of the reaction was 15.40 mg/ml.

Annotation: A was oxygraph tracing of CU 18-15 at concentration 1.01×10^{-6} M

B was oxygraph tracing of CU 18-15 at concentration 1.01×10^{-5} M

C was oxygraph tracing of CU 18-15 at concentration 1.01×10^{-4} M

D was oxygraph tracing of CU 18-15 at concentration 2.02×10^{-4} M

E was oxygraph tracing of CU 18-15 at concentration 3.04×10^{-4} M

F was oxygraph tracing of CU 18-15 at concentration 4.05×10^{-4} M

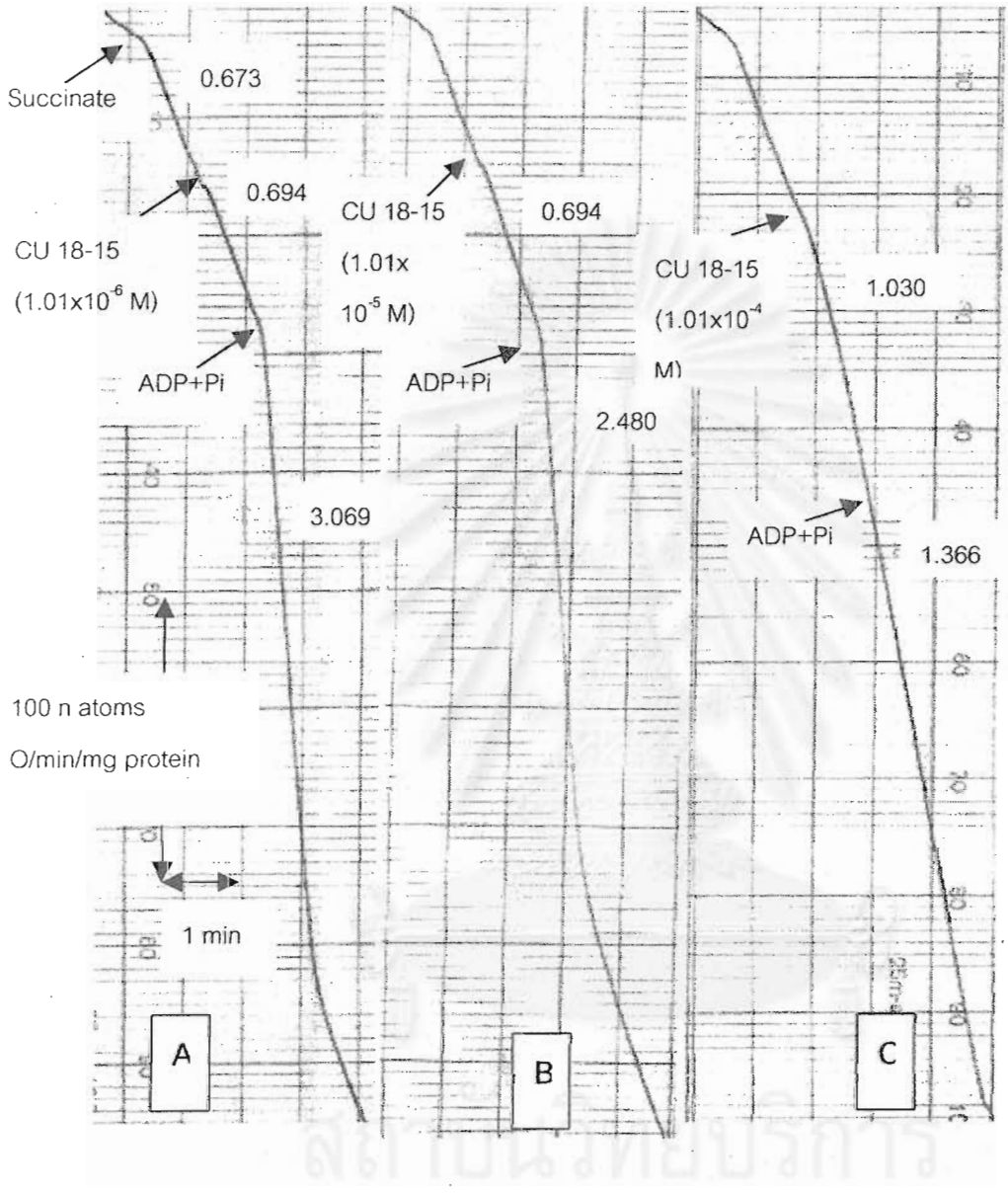

Figure 22. The oxygraph tracing the effect of CU 18-15 on mitochondrial respiration with succinate as substrate

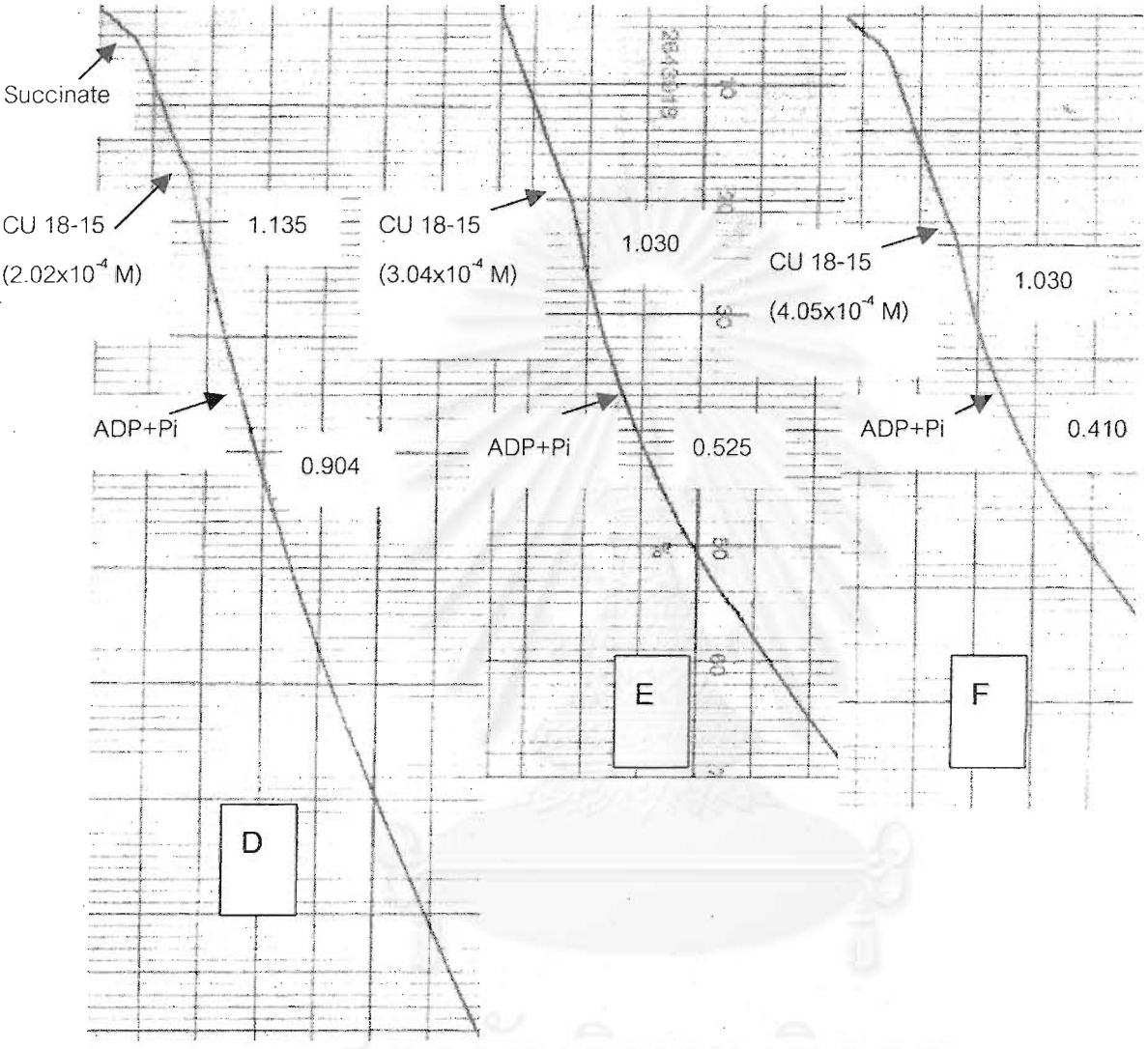

Figure 22 (continued). The oxygraph tracing the effect of CU 18-15 on mitochondrial respiration with succinate as substrate

Effect of mitochondrial respiration with succinate as substrate by CU 18-14 and CU 18-15

Figure 23.

The rate of oxygen consumption of State 4 respiration by CU 18-14 and CU 18-15 with succinate as substrate on isolated rat liver mitochondria. The reaction composed of 37.50 mM HEPES buffer pH 7.4, 1.88 mM $MgCl_2$, 86.25 mM KCl, 5.21 mM succinate, 0.31 mM ADP + 0.62 mM Pi, 13.02 mM sucrose and 50 µl of mitochondrial suspension, and maintained at 37^0C. Control group using 10 µl of DMSO. The total volume was 1.77 ml and the average protein concentration of the reaction by CU 18-14 and CU 18-15 was 20.45 and 15.40 mg/ml, respectively. Each point was the mean ± S.E. of n = 4.

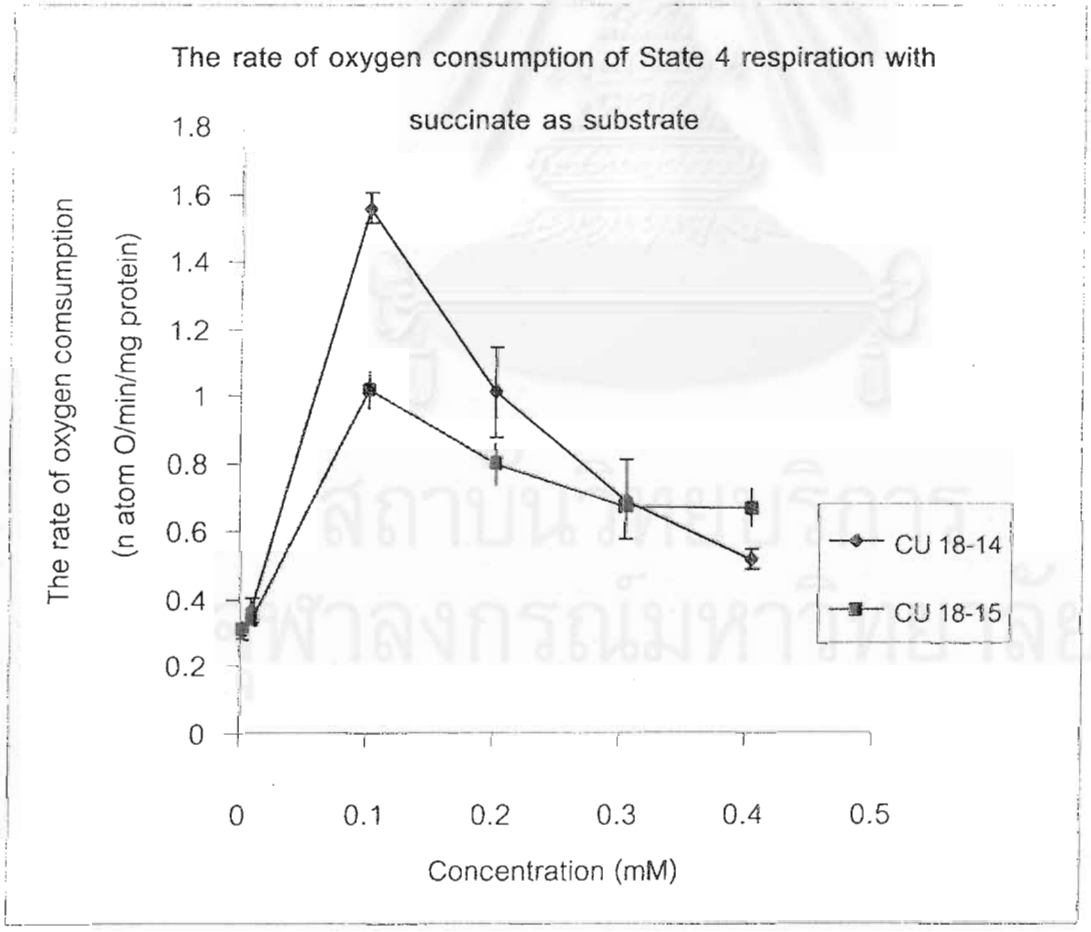

Table 2.

The rate of oxygen consumption of State 3 and State 4 respiration with succinate as substrate on isolated rat liver mitochondria by CU 18-14 and CU 18-15 (range 1.01×10^{-6} M to 4.05×10^{-4} M). Each value was the mean $\pm$ S.E. of n = 4.

Concentration of compounds (Molar)	The rate of Oxygen Consumption (n atom O/min/mg protein)			
	State 3 respiration		State 4 respiration	
	CU 18-14	CU 18-15	CU 18-14	CU 18-15
1.01×10^{-6}	0.49 ± 0.11	0.82 ± 0.05	1.66 ± 0.57	3.18 ± 0.18
1.01×10^{-5}	0.50 ± 0.07	0.82 ± 0.13	1.50 ± 0.29	3.16 ± 0.01
1.01×10^{-4}	Not found	Not found	1.79 ± 0.48	1.20 ± 0.34
2.02×10^{-4}	Not found	Not found	1.18 ± 0.52	1.08 ± 0.54
3.04×10^{-4}	Not found	Not found	0.76 ± 0.34	0.83 ± 0.39
4.05×10^{-4}	Not found	Not found	0.69 ± 0.26	0.60 ± 0.21

Effect of DNP stimulated respiration by CU 18-14

Figure 24.

The oxygraph tracings demonstrating the effect of CU 18-14 at concentration 1.01×10^{-6} M to 4.05×10^{-4} M on mitochondrial oxygen consumption with glutamate plus malate as substrates. Every State was calculated as n atom O/min/mg protein. The reaction composed of 37.50 mM HEPES buffer pH 7.4, 1.88 mM $MgCl_2$, 86.25 mM KCl, 5.21 mM glutamate + 5.21 mM malate, 0.05 mM DNP, 13.02 mM sucrose and 50 µl of mitochondrial suspension, and maintained at 37^0C. The total volume was 1.77 ml and the average protein concentration of the reaction was 15.93 mg/ml.

Annotation: A was oxygraph tracing of CU 18-15 at concentration 1.01×10^{-6} M

B was oxygraph tracing of CU 18-15 at concentration 1.01×10^{-5} M

C was oxygraph tracing of CU 18-15 at concentration 1.01×10^{-4} M

D was oxygraph tracing of CU 18-15 at concentration 2.02×10^{-4} M

E was oxygraph tracing of CU 18-15 at concentration 3.04×10^{-4} M

F was oxygraph tracing of CU 18-15 at concentration 4.05×10^{-4} M

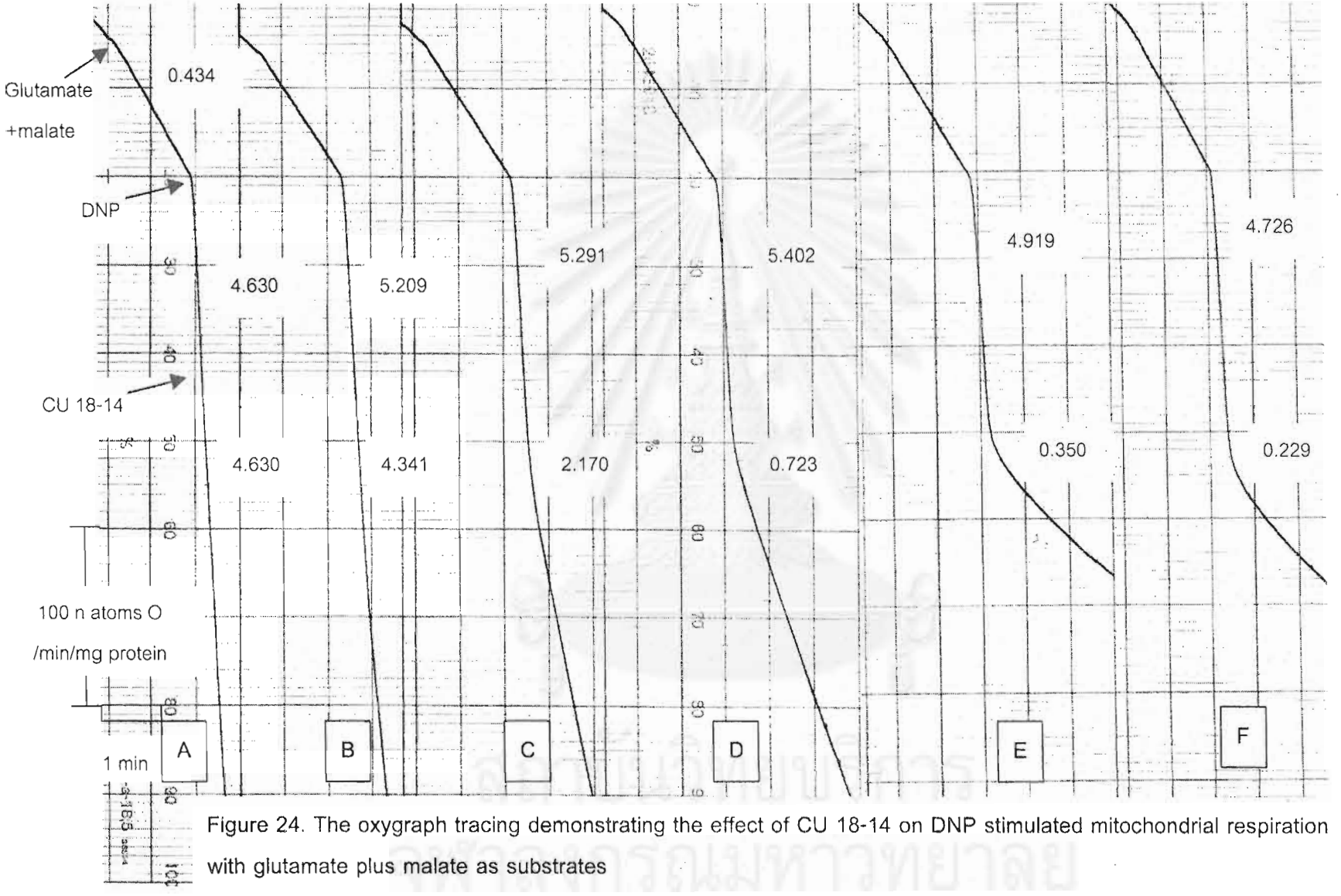

Figure 24. The oxygraph tracing demonstrating the effect of CU 18-14 on DNP stimulated mitochondrial respiration with glutamate plus malate as substrates

Effect of DNP stimulated respiration by CU 18-15

Figure 25.

The oxygraph tracings demonstrating the effect of CU 18-15 at concentration $1.01x10^{-6}$ M to $4.05x10^{-4}$ M on mitochondrial oxygen consumption with glutamate plus malate as substrates. Every State was calculated as n atom O/min/mg protein. The reaction composed of 37.50 mM HEPES buffer pH 7.4, 1.88 mM $MgCl_2$, 86.25 mM KCl, 5.21 mM glutamate + 5.21 mM malate, 0.05 mM DNP, 13.02 mM sucrose and 50 µl of mitochondrial suspension, and maintained at 37^0c. The total volume chamber was 1.77 ml and the average protein concentration of the reaction was 16.34 mg/ml.

Annotation: A was oxygraph tracing of CU 18-15 at concentration 1.01×10^{-6} M

B was oxygraph tracing of CU 18-15 at concentration 1.01×10^{-5} M

C was oxygraph tracing of CU 18-15 at concentration 1.01×10^{-4} M

D was oxygraph tracing of CU 18-15 at concentration 2.02×10^{-4} M

E was oxygraph tracing of CU 18-15 at concentration 3.04×10^{-4} M

F was oxygraph tracing of CU 18-15 at concentration 4.05×10^{-4} M

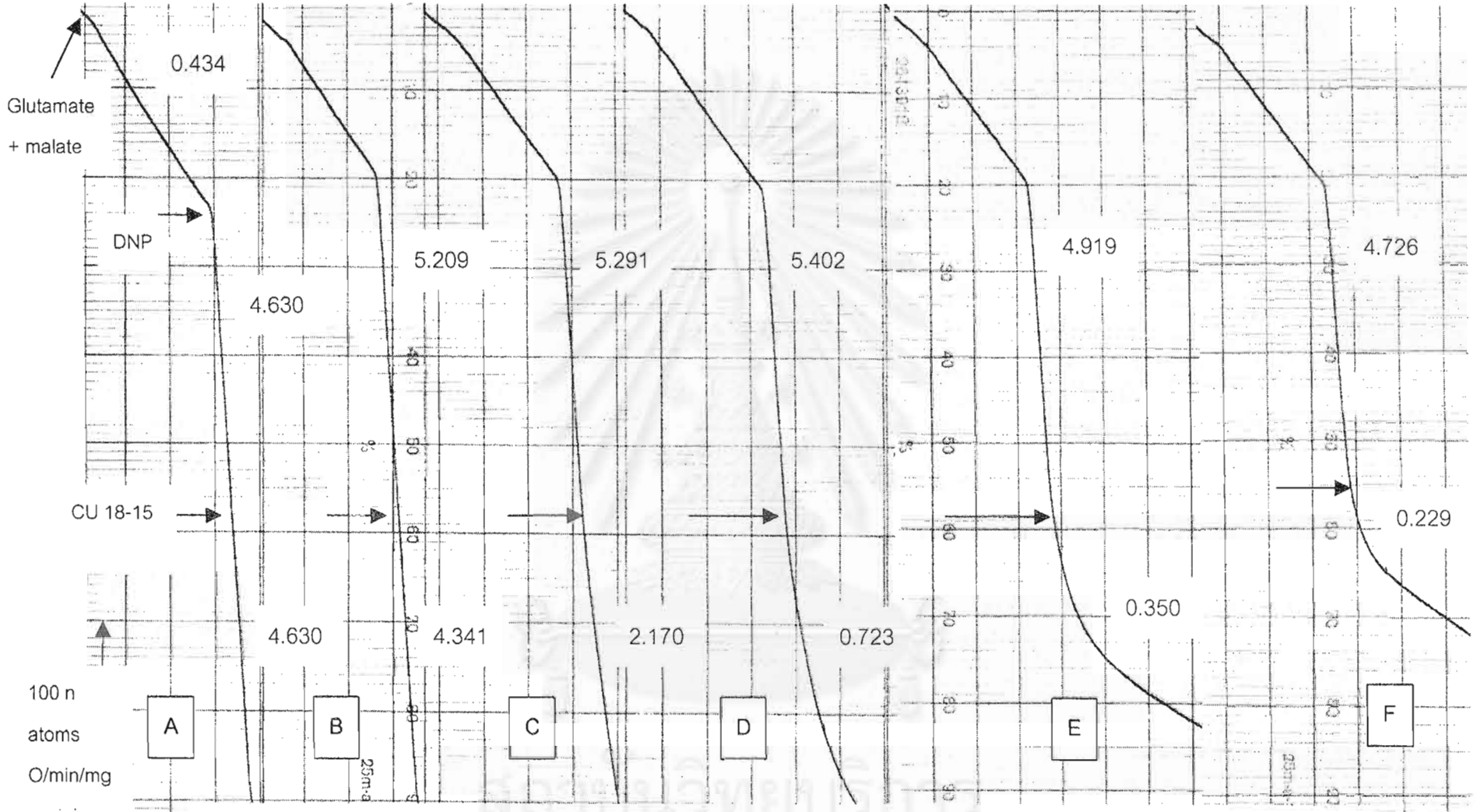

Figure 25. The oxygraph tracing demonstrating the effect of CU 18-15 on DNP stimulated mitochondrial respiration with glutamate plus malate as substrates

Figure 26.

The inhibition of State 3u respiration by Cu 18-14 and CU 18-15 with glutamate plus malate as substrates on isolated rat liver mitochondria. The reaction composed of 37.50 mM HEPES buffer pH 7.4, 1.88 mM $MgCl_2$, 86.25 mM KCl, 5.21 mM glutamate + 5.21 mM malate, 0.05 mM DNP, 13.02 mM sucrose and 50 µl of mitochondrial suspension, and maintained at 37°C. Control group using 10 µl of DMSO. The total volume was 1.77 ml and the average protein concentration of the reaction was 16.34 mg/ml. Each point was the mean ± S.E. of n = 4.

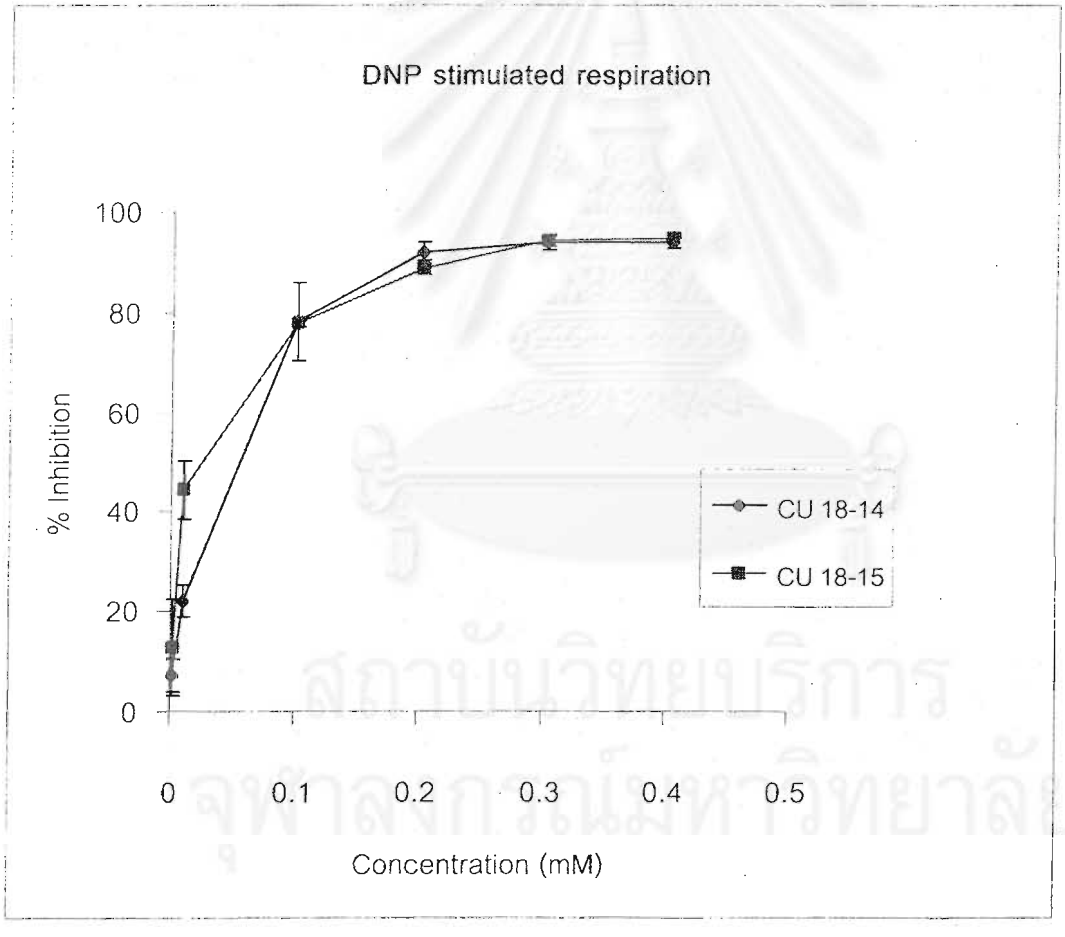

Table 3.

The inhibition of State 3u respiration by Cu 18-14 and CU 18-15 with glutamate plus malate as substrates on isolated rat liver mitochondria (n=4).

Concentration of compounds (Molar)	% Inhibition of State 3u respiration (mean ± S.E)	
	CU 18-14	CU 18-15
1.01×10^{-6}	7.16 ± 3.15	12.76 ± 9.66
1.01×10^{-5}	22.14 ± 3.19	44.46 ± 5.76
1.01×10^{-4}	78.14 ± 7.90	78.01 ± 1.07
2.02×10^{-4}	91.81 ± 2.24	88.95 ± 1.39
3.04×10^{-4}	93.84 ± 1.35	94.27 ± 1.23
4.05×10^{-4}	94.15 ± 1.46	94.89 ± 0.24

Table 4.

Concentrations causing 50% inhibition (IC_{50}) in the rate of DNP stimulated respiration with glutamate plus malate as substrate by CU 18-14 and CU 18-15 (n=4).

Tested Compounds	IC_{50} (Molar)
CU 18-14	2.15×10^{-5}
CU 18-15	1.32×10^{-5}

Effects of CU 18-14 and CU 18-15 on ATPase activity.

Figure 27.

Effects of CU 18-14 and CU 18-15 on ATPase activity of isolated rat liver mitochondria. Composition of reaction system: 37.70 mM buffer pH 7.4, 1.88 mM $MgCl_2$, 0.1 mM DNP, 10μg oligomycin, 13.02 mM sucrose and 150 μl of mitochondrial suspension, and maintained at 37^0C. Control group using 10 μl of DMSO. The total reaction was 2.98 ml. The average mitochondrial protein was 17.31 mg/ml. In the present studies the mitochondria were preincubated with tested compounds for 1 minute before ATP were added. The reaction mixtures were further incubated for 10 minutes after ATP addition. Each point represented a mean ± S.E. of n = 4.

Each bar represented (A) DMSO

(B) DNP

(C) DNP +Oligomycin

(D) CU 18-14 at concentration 1.01×10^{-4} M

(E) CU 18-14 at concentration 3.04×10^{-4} M

(F) CU 18-14 at concentration 3.04×10^{-4} M + Oligomycin

(G) CU 18-15 at concentration 1.01×10^{-4} M

(H) CU 18-15 at concentration 3.04×10^{-4} M

(I) CU 18-15 at concentration 3.04×10^{-4} M + Oligomycin

* p value < 0.05 compared with DMSO

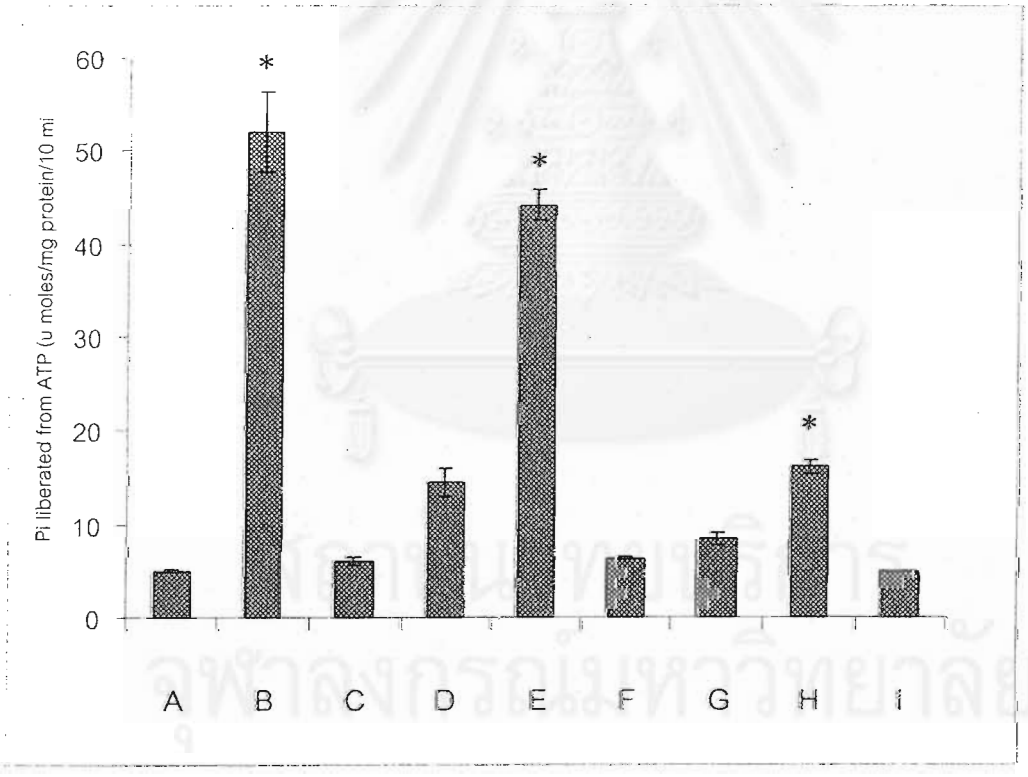

Table 5.

Effects of CU 18-14 and CU 18-15 on ATPase activity of isolated rat liver mitochondria. Pi liberated concentration from ATP by CU 18-14 and CU 18-15. Each value represented a mean ± S.E. (n = 4).

* p value < 0.05 compared with DMSO

Compounds	Pi liberate (μmoles/mg protein/ 10 min)
DMSO	4.98 ± 0.19
DNP	52.0773 ± 8.60 *
DNP + Oligomycin	6.04 ± 0.69
CU 18-14 (1.01×10^{-4} M)	14.44 ± 2.93
CU 18-14 (3.04×10^{-4} M)	44.13 ± 3.13 *
CU 18-14 (3.04×10^{-4} M) + Oligomycin	6.33 ± 0.10
CU 18-15 (1.01×10^{-4} M)	8.36 ± 1.34
CU 18-15 (3.04×10^{-4} M)	16.12 ± 1.50 *
CU 18-15 (3.04×10^{-4} M) + Oligomycin	4.89 ± 0.11

Effects of CU 18-14 on calcium stimulated respiration.

Figure 28.

Effects of CU 18-14 on calcium stimulated respiration by isolated rat liver mitochondria with glutamate plus malate as substrates. The reaction composed of 37.50 mM HEPES buffer pH 7.4, 1.88 mM $MgCl_2$, 86.25 mM KCl, 5.21 mM glutamate + 5.21 mM malate, 0.42 mM $CaCl_2$, 13.02 mM sucrose and 50 µl of mitochondrial suspension, and maintained at 37^0C. The total volume chamber was 1.77 ml and the average protein concentration of the reaction was 18.17 mg/ml. Each point was the mean ± S.E. of n = 4.

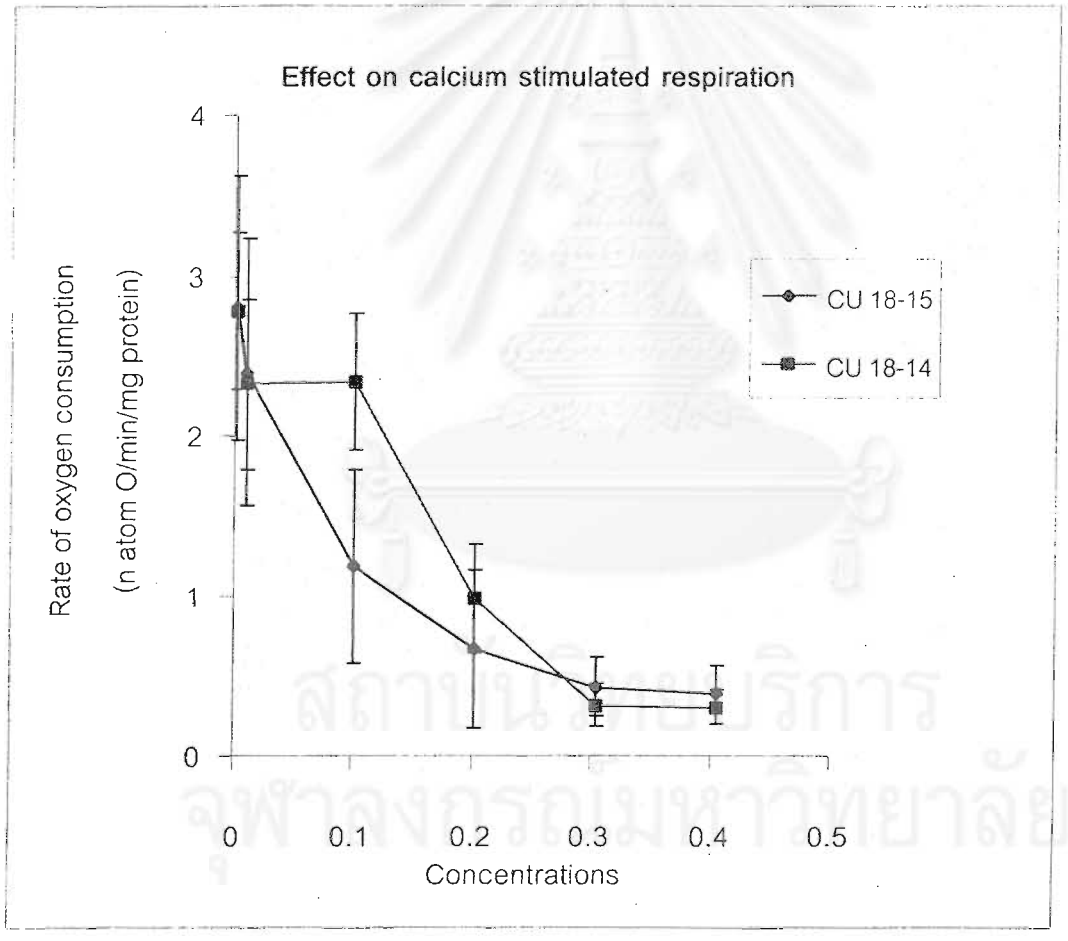

Table 6.

The rate of Oxygen Consumption of CU 18-14 and CU 18-15 on calcium stimulated respiration by isolated rat liver mitochondria with glutamate plus malate as substrates. Each value represented a mean ± S.E. of n = 4.

Concentration (mM)	Rate of Oxygen Consumption (n atoms O/min/mg protein)	
	CU 18-14	CU 18-15
$CaCl_2$	2.80 ± 0.15	
$1.01x10^{-6}$	2.78 ± 0.37	2.80 ± 0.22
$1.01x10^{-5}$	2.32 ± 0.37	2.39 ± 0.24
$1.01x10^{-4}$	2.34 ± 0.27	1.18 ± 0.19
$2.02x10^{-4}$	0.98 ± 0.22	0.67 ± 0.15
$3.04x10^{-4}$	0.32 ± 0.08	0.43 ± 0.06
$4.05x10^{-4}$	0.31 ± 0.08	0.39 ± 0.05

Effect of CU 18-14 on monoamine oxidase activity.

Figure 29.

The inhibition of rat liver mitochondria MAO by CU 18-14 towards 100 μM tyramine, 100 μM 5-HTand 100 μM benzylamine as substrate. The reaction composed of 1.77 ml of phosphate buffer pH 7.4 and 50 μl of mitochondrial suspension, and maintained at 37°C. The average protein concentration of the reaction using tyramine, 5-HTand benzylamine was 24.89, 27.69 and 31.81 mg/ml respectively. Each point was the mean ± S.E. of n = 4.

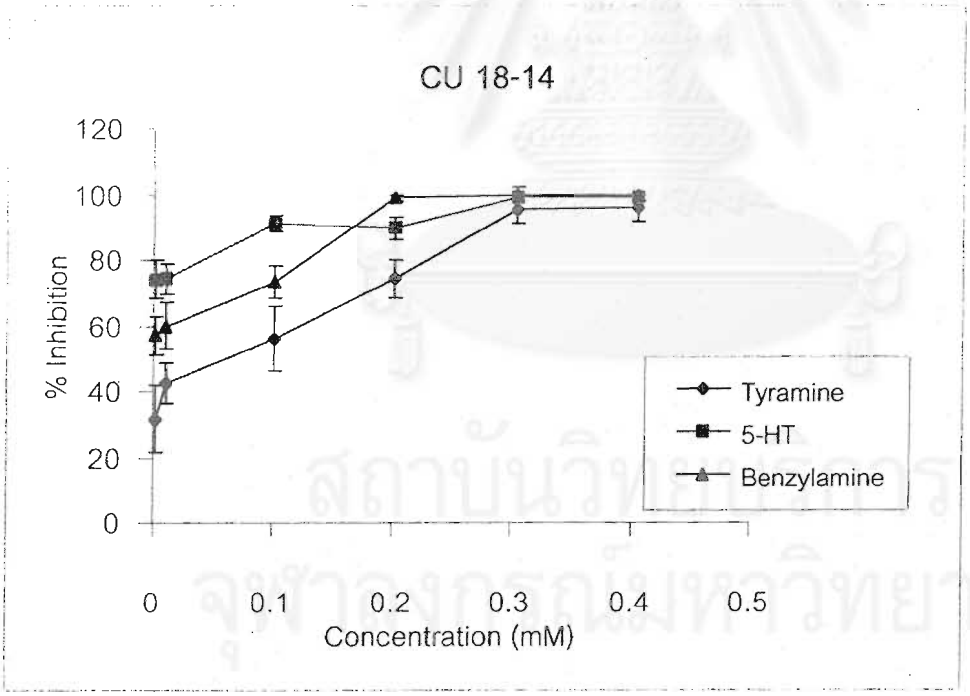

Effect of CU 18-15 on monoamine oxidase activity.

Figure 30.

The inhibition of rat liver mitochondria MAO by CU 18-15 towards 100 μM tyramine, 100 μM 5-HTand 100 μM benzylamine as substrate. The reaction composed of 1.77 ml of phosphate buffer pH 7.4 and 50 μl of mitochondrial suspension, and maintained at 37^{0}C. The average protein concentration of the reaction using tyramine, 5-HTand benzylamine was 16.44, 27.49 and 35.31 mg/ml respectively. Each point was the mean ± S.E. of n = 4.

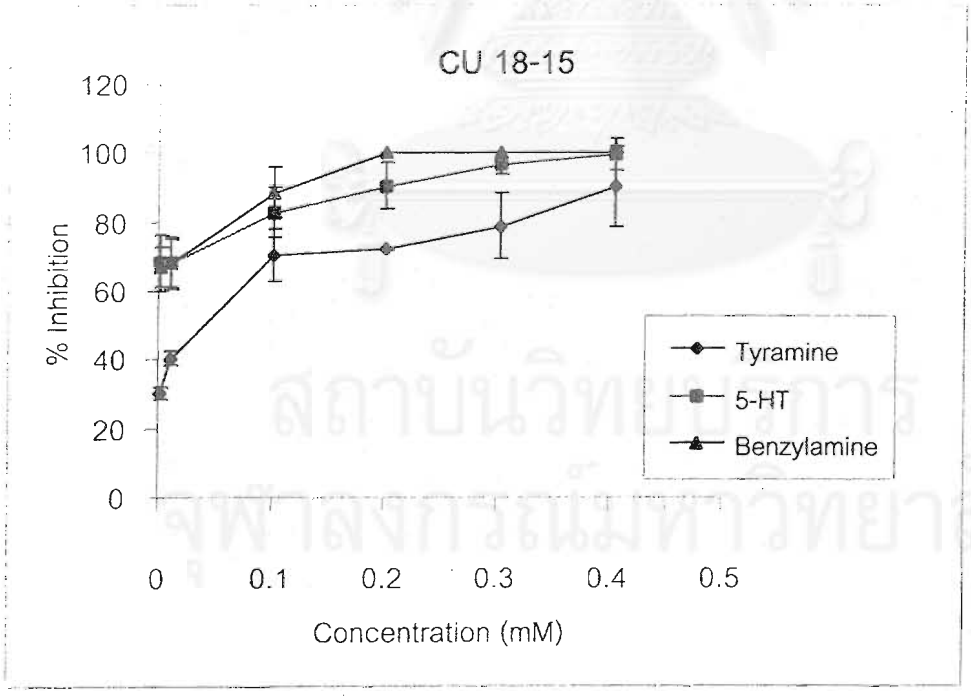

Table 7.

The percent inhibition of MAO activity by CU 18-14 and CU 18-15. Each value represented a mean ± S.E. of n = 4.

Concentration. (Molar)	% Inhibition (mean ± S.E)					
	CU 18-14			CU 18-15		
	Tyramine	5-HT	Benzylamine	Tyramine	5-HT	Benzylamine
1.01×10^{-6}	31.67±10.14	74.09 ± 5.64	57.12 ± 5.88	30.52 ± 1.77	68.01 ± 8.11	66.97 ± 5.82
1.01×10^{-5}	42.39 ± 6.38	74.28 ± 4.73	59.74 ± 7.11	40.43 ± 2.20	68.27 ± 7.11	68.37 ± 7.56
1.01×10^{-4}	56.13 ± 9.71	90.89 ± 2.37	73.07 ± 4.99	70.45 ± 7.64	82.95 ± 7.64	88.70 ± 7.19
2.02×10^{-4}	74.17 ± 5.83	89.62 ± 3.37	99.04 ± 0.96	72.15 ± 0.36	90.36 ± 6.74	100.00 ± 0.00
3.04×10^{-4}	95.56 ± 4.44	98.78 ± 3.61	100.00 ± 0.00	78.89 ± 9.53	96.88 ± 3.13	100.00 ± 0.00
4.05×10^{-4}	95.83 ± 4.17	99.07 ± 0.93	100.00 ± 0.00	90.48±11.66	99.38 ± 4.61	100.00 ± 0.00

Table 8.

Concentrations causing 50% inhibition (IC_{50}) in the rate of MAO activity by CU 18-14 and CU 18-15 (n=4).

Tested compounds And MAOIs	Tyramine as substrate IC_{50} (M)	5-HT as substrate IC_{50} (M)	Benzylamine as substrate IC_{50} (M)	Ratio MAO-A (IC_{50}) MAO-B (IC_{50})
CU 18-14	9.66×10^{-6}	6.30×10^{-7}	1.44×10^{-2}	4.38×10^{-5}
CU 18-15	1.18×10^{-5}	2.60×10^{-4}	7.96×10^{-3}	3.27×10^{-2}

CHAPTER V

DISCUSSION

The purpose of this study was to identify the effects of new N-heptanoyl, nitro-*m*-methoxy anilide derivatives, which are N-heptanoyl-3-methoxy-4-nitro anilide (CU 18-14) and N-heptanoyl-2-nitro-5-methoxy anilide (CU 18-15), on isolated rat liver mitochondrial functions. The findings were divided into four major parts.

Part I: Effects of CU 18-14 and CU 18-15 on oxidative phosphorylation of isolated rat liver mitochondria.

The effect of CU 18-14 and CU 18-15 on isolated rat liver mitochondrial respiration were investigated with glutamate plus malate as substrates. Both CU 18-14 and CU 18-15 showed the uncoupling effect by stimulating State 4 respiration, but at higher concentration (more than 3.04×10^{-4} M), the compounds inhibited both State 3 and State 4 respiration (Figure 19 and Table1).

When using succinate as substrate similar result was obtained as shown in Figure 23 and Table 4. These results suggested that CU 18-14 and CU 18-15 acted as uncoupling agents like DNP, which is the classical uncoupler (Wallace et al., 2000).

CU 18-14 and CU 18-15 were found to inhibit DNP stimulated respiration in a concentration manner (Figure 25), and the IC_{50} by CU 18-14 (2.15×10^{-5} M) was close to Cu 18-15 (1.32×10^{-5} M) (Table 6). The detail of mechanism of uncoupling effects and the interaction with DNP need further investigation.

Part II: Effects of CU 18-14 and CU 18-15 on ATPase activity of isolated rat liver mitochondria.

In the present study the effect of CU 18-14 and CU 18-15 on ATPase activity of isolated rat liver mitochondria was expressed in according to inorganic phosphate liberated from ATP hydrolysis. The classical uncoupler, DNP, stimulated mitochondrial ATPase activity that produced Pi from ATP hydrolysis (Cambell, 1995; Lehninger et al., 2000; Garrett and Grisham, 2002). CU 18-14 and CU 18-15 showed stimulation effect on ATPase

activity with different potency. CU 18-14 had stronger effect on ATPase stimulation than CU 18-15, however, both compounds might have a weak stimulation on mitochondrial ATPase, especially CU 18-15 (Figure 27 and Table 7).

Furthermore, both stimulation effect of DNP were inhibited by oligomycin, which inhibited mitochondrial ATPase induced by uncoupler or detergents (Lardy, 1981). Effect of activated ATPase activity by high concentration of CU 18-14 and CU 18-15 were also inhibited by oligomycin, which were similar to DNP. These showed that DNP and tested compounds might have similar mechanism on stimulation of ATPase activity.

Part III: Effects of CU 18-14 and CU 18-15 on calcium stimulated respiration of isolated rat liver mitochondria.

The result of the present study that both of CU 18-14 and CU 18-15 could slow the calcium stimulated respiration of isolated rat liver mitochondria (Figure 28 and Table 8). Mitochondria calcium transport is driven by membrane potential (McCormack et al., 1990). This may be partly explained by the uncoupling effect and stimulation of mitochondrial ATPase to collapse membrane potential of the inner membrane. The inhibition of calcium transport into mitochondria may cause increasing the calcium in cytoplasm. The consequence effect may lead to changes in the cellular activity.

Part IV: Effects of CU 18-14 and CU 18-15 on monoamine oxidase activity of isolated rat liver mitochondria.

The inhibitory potencies of these derivatives on MAO activity using different kinds of substrate were studied. There are at least two types of MAO isoenzyme, MAO-A and MAO-B (Johnston, 1968). MAO-A and MAO-B oxidized tyramine whereas 5-HT and benzylamine are selectively oxidized by MAO-A and MAO-B, respectively (Neff and Yang, 1974). Both CU 18-14 and CU 18-15 showed the inhibitory effect on MAO activity in Table 9. However, the comparison of the concentration causing 50% inhibitory ratio of substrate for MAO-A and MAO-B, the ratio of IC_{50} for 5-HT/ IC_{50} for benzylamine of CU 18-14 is 4.38×10^{-5} and CU 18-15 is 3.27×10^{-2} (Table 10). This indicated that CU 18-14 is preferred to inhibit MAO-A more than MAO-B.

Regarding to structure-activity relationship, the molecular structures of N-heptanoyl-3-methoxy-4-nitro anilide (CU 18-14) was similar to N-heptanoyl-2-nitro-5-methoxy anilide (CU 18-15), but were different in the position of nitro group ($-NO_2$) substitution on aniline ring, which link to meta-methoxy group ($m-OCH_3$). CU 18-14 has para-nitro group ($p-NO_2$) and CU 18-15 has orthro-nitro group ($o-NO_2$). Hence the effect on mitochondria function of CU 18-14 and CU 18-15 were different regarding to the MAO inhibitory effect. CU 18-14 is preferred to inhibit MAO-A more than MAO-B.

From the results of N-heptanoyl, nitro-*m*-methoxy anilide derivatives, CU 18-14 and CU 18-15 showed that both compounds are mitochondrial uncoupler. However, CU 18-14 showed more selective MAO-A than MAO-B and the IC_{50} for MAO-A is low concentration (6.30×10^{-7} M). This result is particular interesting for further investigation on its antidepressant effect. The chemical modification and other detail information of these compounds regarding toxicity and other pharmacological action are needed for further investigation.

CHAPTER VI

CONCLUSIONS

N-heptanoyl-3-methoxy-4-nitro anilide (CU 18-14) and N-heptanoyl-2-nitro-5-methoxy anilide (CU 18-15) affected the following mitochondrial functions

1. CU 18-14 and CU 18-15 acted as the uncoupling agents on oxidative phosphorylation of isolated rat liver mitochondria and CU 18-14 stimulated State 4 respiration more than CU 18-15.
2. CU 18-14 and CU 18-15 inhibited DNP stimulated respiration of isolated rat liver mitochondria with a similar potency.
3. CU 18-14 and CU 18-15 stimulated ATPase activity of isolated rat liver mitochondria similar to DNP and the effect was inhibited by oligomycin. CU 18-14 had stronger stimulation effects on ATPase than CU 18-15.
4. CU 18-14 and CU 18-15 slowed the calcium stimulated respiration of isolated rat liver mitochondria
5. CU 18-14 and CU 18-15 inhibited both MAO-A and MAO-B activity. CU 18-14 more preferentially inhibited MAO-A than did CU 18-15.

Results from this study demonstrated that CU 18-14 and CU 18-15 affected mitochondrial function, especially oxidative phophorylation via the uncoupling effects. This may be accounted as on adverse effect of these compounds on cellular activity and integrity due to the deprivation of ATP. However, the selective inhibitory effects of CU 18-14 on monoamine oxidase type A was an advantageous characteristic which was potentially developed to be a new antidepressant.

REFERENCES

Alberts, B., Johnson, A., Lewis, J., Raff, M., Roberts, K., and Walter, P. 2002. Energy Conversion: Mitochondria and Chloroplasts. Molecular Biology of The Cell. 4th ed. pp. 767-829.

Bernardi, P. 1999. Mitochondrial transport of cations: channels, exchangers and permeability transition. Physiol. Rev. 79: 1127-1155.

Bertina, R.M., and Slater, E.C. 1975. The effect of phosphate and electron transport on the carbonyl cyanide m-chlorophenylhydrazone-induced ATPase of rat liver mitochondria. Biochem. Biophys. Acta. 376: 492-504.

Cambell, M.K. 1995. Electron transport and oxidative phosphorylation. Biochemistry. 3rd ed. New York: Wiley-Liss: 391-417.

Carafoli, E. 1979. The Ca^{2+} cycle of mitochondria. FEBS Lett. 104: 1-5.

Carafoli, E., Tiozzo, R., Lugli, G., Crovetti, F., Kratzing, C. 1974. The release of calcium from heart mitochondria by sodium. J. Mol. Cell. Cardiol. 6: 361-371.

Chakraborti, T., Das, S., Mondal, M., Roychoudhury, S., Chakraborti, S. 1999. Oxidant, Mitochondria and Calcium: An Overview. Cell. Signal. 11/2: 77-85.

Chance, E., and Williams, G.R. 1956. The respiratory chain and oxidative phosphorylation. Adv. Enzymology. 17: 65-134.

Chau, R.M., and Hackenbrock, C.R. 1975. Localization of monoamine oxidase on the outer and inner surfaces of the outer membrane of rat liver mitochondria. J. Cell. Biol. 67: 63a.

Epps, D.E., Palmer. J.W.,Schmid, H.M.O., and Pfeiffer D.R. 1982. Inhibition of permeability-dependent Ca2+ release from mitochondria by N-acylethanolamines, a class of lipids synthesized in ischemic heart tissue. J. Biol. Chem. 257: 1383-1391.

Erecinska, M., and Wilson, D.F. 1981. The mitochondrion and its functions. Inhibitors of mitochondrial functions. 1-17. Pergamon Press.

Fiske, O.H., and Subbarow, Y. 1925. The colorimetric determination of phosphorus. J. Biol. Chem. 66: 375-400.

Goridis, C., and Neff, N.H. 1971. Monoamine oxidase in sympathetic nerves: a transmitter specific enzyme type. Br. J. Pharmacol. 43: 814-818.

Garrett, R.H., and Grisham, C.M. 2002. Electron transport and oxidative phosphorylation. Principles of Biochemistry with a Human Focus. Philadelphia: Harcourt College: 519-551.

Green, D.R., and Reed J.C., 1998. Mitochondria and Apoptosis. Science. 281: 1309-1312.

Hammond, D.G., and Kubo, I. 2000. Alkanols inhibit respiration of intact mitochondria and display cutoff similar to that measured in vivo. JPET. 293: 822-828.

Hatairat Keansen. 2002. Effect of acylaminopyridine and acylaniline derivatives on respiratory chain function of isolated rat liver mitochondria. Master's Thesis, Department of Pharmacology, Faculty of Pharmaceutical Sciences, Chulalongkorn University.

Heytler, P.G. 1981. Uncouplers of Oxidative Phosphorylation. Inhibitors of mitochondrial functions. 119-210. Pergamon Press.

Hogeboom, G.H. 1955. Fractionation of cell components of animal tissues. In S.P. Colowick, and N.O. Kaplan (eds.), Methods in enzymology. Vol. I, pp. 16-19. New York: Academic Press.

Holschneider, D.P., Chen, K., Seif, I., and Shih, J.C. 2001. Biochemical, behavioral, physiologic, and neurodevelopmental changes in mice deficient in monoamine A or B. Brain Res.Bull. 56(5): 453-462.

Holschneider, D.P., Shih, M.D., and Shih, J.C. 2000. Monoamine Oxidase: Basic and Clinical Perspectives. Neuropsychopharmacology: The fifth generation of progress.1-19.

Houslay, M.D., and Tipton, K.F. 1975. Amine competition for oxidation by rat liver mitochondrial monoamine oxidase. Biochem. Pharmacol. 24: 627-631.

Houslay, M.D., Tipton, K.F., and Youdim, M.B.H. 1976. Minireview: Multiple forms of monoamine oxidase: Fact and artifact.. Life Sci. 19: 467-478.

Jeevaratnam, K., 2000. Inhibition of Ca^{2+}-ATPase and perturbation in Ca^{2+} homeostasis in rat liver on administration of methyl isocyanate. Indian Journal of Pharmacology. 32:120-125.

Johnston, J.P. 1968. Some observations upon a new inhibitor of monoamine oxidase in brain tissue, Biochem. Pharmacol. 17: 1285-1297.

Kochersperger, L.M., Parker, E.L., Siciliano, M., Darington, G.J., and Denny, R.M. 1986. Assignment of genes for human monoamine oxidase A and B to the X-chromosome. J. Neurosci. Res. 16: 601-616.

Lardy, H.A. 1981. Antibiotic inhibitors of mitochondrial energy transfer. Inhibitors of mitochondrial functions. 187-189. Pergamon Press.

Lehninger, A.L., Nelson, D.L., and Cox, M.M. 2000. Oxidative phosphorylation and photophosphorylation. Principles of Biochemistry. 3rd ed. : 659-721.

Lodish, H., Berk, A., Zipursky, S.L., Matsudaira, P., Baltimore, D., and Darnell, J. 1999. Cellular Energetics: Glycolysis, Aerobic Oxidation, and Photosynthesis. Molecular Cell Biology. 4th ed. 616-674. New York: W. H. Freeman and Company.

Lowry, O.H., Rosebrough, N.J., Farr, A.L., and Randall, R.J. 1951. Protein measurement with Folin phenol reagent. J. Biol. Chem. 193: 265-275.

Mathews, C.K., Holde, K.E., and Ahern, K.G. 2000. Electron Transport, Oxidative Phosphorulation, and Oxygen metabolism. Biochemistry. 3rd ed. 522-557. An Imprint of Addison Wesley Longman, Inc.

Mayers P.A. 2000. The Respiration Chain and Oxidative Phosphorylation. Harper's Biochemistry. 25 ed. 137-148.

McCormack, J.G., Halestrap. A.P., and Denton, R.M. 1990. Role of calcium ions in regulation of mammalian intramitochondrial metabolism. Pharmacol. Rev. 20/2: 391-425.

McEntire, J.E., Buchok, S.J., and Parpermaster, B.W. 1979. Determination of platelet monoamine oxidase activity in human platelet-rich plasma. Biochem. Pharmacol. 28: 2345-2347.

McGuirl, M.A., and Dooley, D.M. 1999. Copper-containing oxidase. Current Opinion in Chemical Biology. 3: 138-144.

Metzler, D.E. 2003. Electron Transport, Oxidative Phosphorylation, and Hydroxylation. Biochemistry: The Chemical Reactions of Living Cells. 2nd ed. 2 vol. 1013-1075. Academic Press.

Murphy, D.L. 1978. Commentary: Substrate-selective monoamine oxidase inhibitor, tissue, species and functional differences. Biochem. Pharmacol. 27: 1889-1893.

Miller, G.L. 1959. Protein determination for large numbers of samples. Anal. Chem. 31: 964.

Mootha, V.K., Wei, M.C., Buttle, K.F., Scorrano, L., Mannella, C.A. and Korsmeyer, S.J. 2001. A reversible component of mitochondrial respiratory dysfunction in apoptosis can be rescued by exogenous cytochrome *c*. European Molecular Biology Organization. 20 vols. 4: 661-671.

Myers, D.K., and Slater, E.C. 1957. The enzyme hydrolysis of adenosine triphosphate by liver mitochondria I. Activities at difference pH value. Biochem. J. 67: 558-572.

Neff, N.H., and Yang, H.Y. 1974. Minireview: Another look at the monoamine oxidase and the monoamine inhibitor drugs. Life Sci. 14: 2061-2074.

Nicholls, D.G., and Budo, S.L. 2000. Mitochondria and Neuronal Survival. Physiol. Rev. 80/1: 315-360.

Nicholls, D.G., and Ferguson, S.J. 2002. The chemiosmotic proton circuit. Bioenergetic 3: 57-87. Academic Press.

Powell, J.F. 1991. Molecular biological studies of monoamine oxidase: Functional significance. Pharmacol. Rev. 24(2): 331-348.

Pozzan, T.,Rizzuto, R., Volpe, P., and Meldoesi, J. 1994. Molecular and cellular physiology of intracellular Ca^{2+} stores. Physiol. Rev. 74/3. 595-636.

Pozzan, T., and Rizzuto, R. 2000. The renaissance of mitochondrial calcium transport. Eur. J. Biochem. 267, 5269-5273.

Shih, J.C., Chen, K., and Ridd, M.J. 1999. Monoamine oxidase: From genes to behavior. Annu. Rev. Neurosci. 22: 197-217.

Szewczyk, A., Wojtczak, L. 2002. Mitochondria as a Pharmacological Target. Pharmacological review. 54: 101-127.

Tatiya Thanomdee. 2001. Effect of Acylaminopyridine derivatives and Acylaniline derivatives on monoamine oxidase activity in isolated rat liver mitochondria. Master's Thesis, Department of Pharmacology, Faculty of Pharmaceutical Sciences, Chulalongkorn University.

Tipton, K.F., and Singer, T.P. 1993. Commentary: The radiochemical assay for monoamine oxidase activity. Problems and pitfalls. Biochem. Pharmacol. 46: 1311-1316.

Tipton, K.F. 1968. The prosthetic groups of pig brain mitochondrial monoamine oxidase. Biochem. Biophys. Acta. 159: 451-459.

Unchittha Tipayavongvijit. 2000. Effect of N-acylaminopyridine on monoamine oxidase activity and respiratory chain of rat liver mitochondria. Master's Thesis, Department of Pharmacology, Faculty of Pharmaceutical Sciences, Chulalongkorn University.

Wallace, K.B. and Starkov, A.A. 2000. Mitochondrial Targetss of Drug Toxicity. Annual Review of Pharmacology and Toxicology. 40: 353-388.

Weinbach, E.C. 1956. Pentachlorophenol and mitochondrial adenosine triphosphate. J. Biol. Chem. 221: 609-618.

Yang, H.Y.T., Goridis, C., and Neff, N.H. 1972. Properties of monoamine oxidase in sympathetic nerve and pineal gland. J. Neurochem. 19: 1241-1250.

Youdim, M.B.H., and Sourkes, T.L. 1971. Rat liver monoamine oxidase, a flavin containing enzyme. Biochem. J. 121: 20p.

VITAE

Miss Pornpak Wongthongtham was born in Bangkok on March 15, 1972. She received her Bachelor Degree in Pharmacy from Faculty of Pharmaceutical Sciences, Prince of Songkhanakarin University in 1996 and has been a pharmacist in Swangarom hospital, Uthaithanee for four years. And then in 2000 she was transferred to Bangyai hospital, Nonthaburi. In 2002, she came to study for the Degree of Master of Science in Pharmacology, Faculty of Pharmaceutical Sciences, Chulalongkorn University.